APPLICATIONS OF CAPILLARY ELECTROPHORESIS

by

HUA (ANGELA) WU

A dissertation submitted to the Graduate Faculty in Chemistry in partial fulfillment of the requirements for the degree of Doctor of Philosophy, The City University of New York

2002

UMI Number: 3063897

ProQuest Information and Learning Company
300 North Zeeb Road
P.O. Box 1346
Ann Arbor, MI 48106-1346

This manuscript has been read and accepted by the Graduate Faculty in Chemistry in satisfaction of the dissertation requirement for the degree of Doctor of Philosophy.

11 June 02
Date

David C. Locke
David C. Locke Chair of Examining Committee

6/28/02
Date

Gerald Koeppl
Gerald Koeppl Executive Officer

Arthur D. Baker
Arthur D. Baker Supervisory Committee

Ronald Birke
Ronald Birke Supervisory Committee

THE CITY UNIVERSITY OF NEW YORK

Abstract

Applications of Capillary Electrophoresis

by

Hua (Angela) Wu

Advisor: Professor David C. Locke

Part I. Determination of Capsaicins in *capsicum annuum* fruits using micellar electrokinetic capillary chromatography

A simple, rapid method for the quantitative determination of capsaicins using micellar electrokinetic capillary chromatography (MECC) was optimized, validated, and applied to several varieties of Capsicum fruits. Capsaicins are extracted using acetonitrile (ACN). The injection sample was prepared by diluting the extraction or standard stock solution in 10mM sodium dodecyl sulfate (SDS) aqueous solution. The best working

condition includes a background electrolyte (BGE) containing 40mM SDS, 20mM Tris buffer, and 10% ACN (v/v) at pH 9.0; an UV detector at 280nm, and a 70cm x 50μm (50cm effective length) fused silica capillary operated at 30kV and 30°C.

Part II. Study of DNA-Ruthenium(II) complex binding using capillary zone electrophoresis

Capillary zone electrophoresis (CZE) was utilized in this study to investigate the binding of a group of Ruthenium(II)- α-diimine complexes to calf thymus DNA. The chiral complexes were resolved due to their differential interaction with DNA in the separation medium. Buffer composition was optimized in terms of DNA concentration and salt concentration. The CZE enantioseparation with DNA as the chiral selector allowed a rapid screening for both stereoselectivities and relative binding constants with DNA. The actual binding constants were determined using a frontal analysis method.

Part III. Evaluation of association constant between basic enantiomers and sulfated-β-cyclodextrin using a counter-current partial filling technique

Enantioseparations based on a counter-current mode were obtained as the analytes passed through the zone of BGE containing sulfated cyclodextrin, which moved towards the injection end and interacted with it transiently and differentially. The aim of this study was to evaluate association constants using the linearity between the apparent migration time and the partial filling fraction according to a proposed theoretical model. The experimental results showed that the apparent migration time does not change linearly with the partial filling fraction. The nonlinearity was explained by field strength effect.

Dedicated to

My beloved daughter Annabel J. Wang

for her 1st birthday

and

My beloved husband Quan Wang

for our 10th marriage anniversary

ACKNOWLEDGEMENTS

This thesis owes much to many individuals.

First, my most sincere appreciation goes to my research mentor Dr. David C. Locke who provided inspiration and invaluable guidance in all phases of my graduate career. I developed a lot confidence, independence and maturity during my study in his research group. At least I won't burst into tears that easily now.

I would also like to acknowledge my thesis committee members Dr. A. David Baker and Dr. Ronald Birke for their careful reading and invaluable advice of this research.

Special thanks are expressed to Dr. Thomas Strekas, Dr. A. David Baker and Dr. Oma Morgan for their generosity in supplying the ruthenium samples and helpful discussions of the project.

I am very grateful to Dr. Hoe-Sup Byun for his crystal clear answering of my so many organic questions.

It is with particular pleasure to thank my lab mate Dr. Ralf Dolfinger for rescuing my instrument so many times and his great sense of humor.

My gratitude is also extended to Dr. Biao Liu and Dr. Sharon Lall for their friendship and unselfish help in many ways.

I remember with love and gratitude the pleasant conversations with Ms. Alice Brickman, Ms. Jeanne Deutsch and Ms. Diane Adebowale.

Many thanks to Mr. Robert Wurman, Mr. Randy Smith, Mr. Joe Badalamenti and Ms. Janine Beukelaer for their always providing the chemicals and supplies in an efficient manner.

Finally, I would like to give my heartiest appreciation to my husband and my family for their continued love, belief and support through these years.

Once again, thanks to all the people whose help and encouragements have made this work possible.

TABLE OF CONTENTS

Page

References

TABLE OF FIGURES

Part I **Page**

Part II

Part III

LIST OF TABLES

Part I **Page**

Part II

Part I

Determination of Capsaicins in *Capsicum annum* Fruits using Micellar Electrokinetic Capillary Chromatography

INTRODUCTION

The pungency of *Capsicum annuum* fruits is attributed to capsaicinoids, acid amides of vanillylamine and C_9-C_{11} branched chain fatty acids. Five naturally occurring analogs have been reported. Capsaicin (CAP) and dihydrocapsaicin (DHC) generally comprise 90% or more of the total capsaicinoid content. Interest in capsaicins is based on their toxicity, effects on the nervous system, and nutritional and therapeutic benetifs at low doses [1,2].

Conventional organoleptic [3] and spectrophotometric methods [4-6], and TLC [7,8] are limited in that they can quantitate only total capsaicinoids. Modern GC [9,10] and reversed phase HPLC methods with electrochemical [12], GC/MS [13], or UV [14-22] detection, are more convenient and reliable. Capsaicinoids are usually extracted from the fruit using ethanol or acetone, although supercritical fluid CO_2 has been successfully applied [16,19]. To eliminate interferences in the chromatogram and column contaimination, solid phase extraction (SPE) is often used [14,16,18,20,22] as sample clean-up procedure to remove extraneous substances from the crude pepper extracts. MECC with an electrochemical detector was used by Khaled et al. [23] to separate CAP, DHC, and piperine, but no application to capsicum fruits was made.

Laskaridou-Monnerville [24] developed a MECC method using SPE cleanup for application to three varieties of *Capsicum frutescens*, a tropical fruit.

The purpose of this study was to develop a simple, rapid, validated method for the determination of capsaicins in Capsicum fruits using CE. The capsaicins were solvent-extracted from various fruits and the extracts analyzed using micellar electrokinetic capillary chromatography (MECC). The method was optimized with respect to surfactant concentration, buffer composition and concentration, organic modifier, and sample matrix. Method validation was carried out in terms of precision, linearity, limits of detection and quantitation, accuracy, and ruggedness.

EXPERIMENTAL

2.1. Apparatus

An Applied Biosystems 270-HT capillary electrophoresis system (Perkin-Elmer Corp., Norwalk, CT, USA) equipped with an autosampler, a UV detector set at 280 nm, and a forced-air thermostat at 30 °C was used. Instrument control and data handling were conducted using PE Nelson Turbochrom 4.1.1 software. Samples were introduced by applying a 13 mm Hg vacuum to the outlet buffer beaker for 1.0 sec. The HPLC consisted of two Waters M-45 pumps controlled with a Waters 680 Gradient Controller, a Waters WISP 710B autosampler, an Hitachi Model 100-40 UV spectrophotometer with a flow cell, a Hewlett-Packard 3396 Series Integrator, and a Zorbax C8 column, 5 μm, 15 cm x 4.6 mm i.d.

2.2. Chemicals

"Natural" capsaicin, a 65/35 mixture of capsaicin/dihydrocapsaicin extracted from a natural product, was obtained from Aldrich (Milwaukee, WI, USA). Single component capsaicin (97.6% stated purity), dihydrocapsaicin (93.2%), N-vanillyl-n-nonamide and Trisma base (tris[hydroxymethyl] aminomethane) were purchased from Sigma (St. Louis, MO, USA). HPLC grade ACN, SDS, and acetic acid were obtained

from Fisher Scientific (Springfield, NJ, USA). The electro-osmotic flow (EOF) marker was mesityl oxide, injected as a 0.1% solution in BGE. The micelle marker was Sudan III, 50 ppm solution in BGE. Water was glass distilled and further purified using a Milli-Q system (Millipore, Bedford, MA, USA).

Figure 1. Structures of capsaicin, dihydrocapsaicin and internal standard

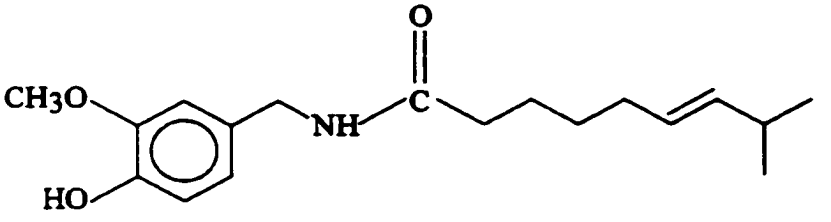

Capsaicin

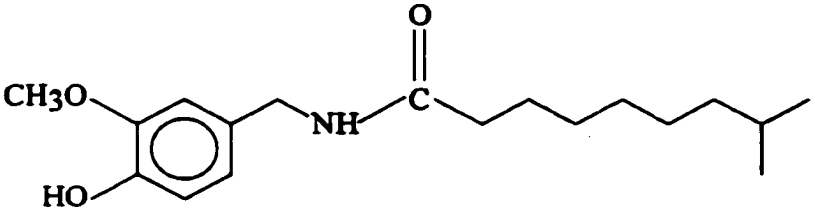

Dihydrocapsaicin

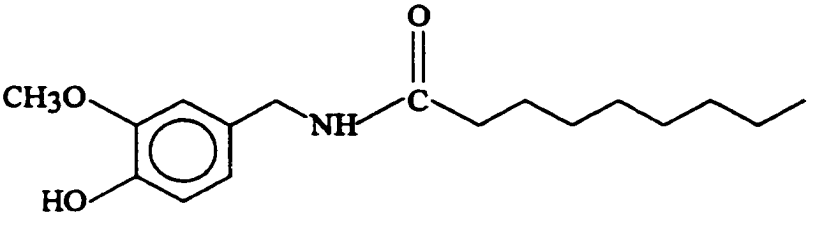

N-vanillyl-n-nonamide

2.3. Solutions

Running buffer (BGE) was prepared daily from 100 mM Tris buffer stock solution (pH 9.00), 100 mM SDS stock solution, and ACN. It was degassed ultrasonically and filtered through a 0.2 μm Millipore filter. For method development and validation, a 25 ppm (total) solution of the natural capsaicin was used as the standard. For HPLC quantitation, pure capsaicin and dihydrocapsaicin at 50 ppm each were used as an external standard since the N-vanillyl-n-nonamide was not resolved from capsaicin. Prior to injection, each sample solution was filtered through a 0.2 μm Millipore filter.

2.4. Capillary preparation

Fused silica capillary tubing (50 μm i.d. x 360 μm o.d.) was purchased from Polymicro Technologies (Phoenix, AZ, USA). Newly cut capillaries were flushed with 1 M NaOH for 1 hr. followed by flushing overnight with 0.1 M NaOH. Before use, the capillary was rinsed with H_2O for 3 min. and BGE for 10 min. 30 kV voltage was then applied for 20 min. If necessary, the BGE rinse and voltage application were repeated until a flat baseline was obtained. Between sample runs the capillary was flushed with BGE for 3 min. At the end of the day the capillary was rinsed

with H_2O for 5 min., 0.1 M NaOH for 10 min, and was left filled with 0.1 M NaOH overnight.

2.5. Extraction of samples

Dried and fresh chili peppers and a green bell pepper were purchased locally. Fresh peppers were washed and the stems, seeds and placenta removed. The remaining portions were cut into small pieces and air-dried to constant weight. Dried peppers were finely chopped in a Waring blender. Approximately 8 g of each subsample was accurately weighed into a 250 mL Erlenmeyer flask and 25 mL of ACN added. The mixture was stirred magnetically for 1 hr and then suction-filtered through Whatman No. 52 filter paper. The filter and solids were rinsed with ACN. The filtrate and rinsings were transferred to a 50 mL round bottom flask and rotary-evaporated under reduced pressure at ≈ 50 °C to dryness. The residue was taken up in 2.0 mL ACN. The extract solutions were stored at 4 °C until ready for analysis. Prior to injection into the CE, 100 μL aliquots were spiked with 50 ppm of internal standard and diluted to 1.0 mL with 10 mM SDS.

RESULTS AND DISCUSSION

3.1. Method development

3.1.1. Buffer constituents

Initially a phosphate buffer was evaluated but it produced capillary equilibration problems and consequent poor reproducibility of migration time. Replacement with the less conductive zwitterionic Tris buffer gave a much better behaved system.

3.1.2. SDS and Tris concentrations

Since capsaicinoids are neutral species, to be separable by CE an ionic surfactant in the BGE is required. Although CAP and DHC were separable even at 2.5 mM SDS (below its CMC, 8.2 mM), the peaks were excessively broadened. As the SDS concentration was increased stepwise from 10 to 100 mM, the peak heights maximized between 40 and 60 mM. The peaks became broad above 60 mM as a result of increased Joule heating as the higher SDS concentrations increased the ionic strength. Since Tris has low conductivity, its concentration over the range from 10 mM to 40 mM had little effect on the MECC separation, although the peaks were more symmetrical at the higher Tris concentrations.

3.1.3. Organic modifier

ACN in the BGE affects the EOF, BGE viscosity, and the formation

of micelles, all of which influence the MECC separation As the ACN concentration is increased from 1 to 40% (v/v), the retention factors, k', of CAP and DHC maximize at about 10%. The selectivity factor, k'_{DHC}/k'_{CAP}, maximizes at about 19%. Since a good separation was obtained at 10% ACN with a more stable baseline and current than at 19%, the lower concentration was adopted as optimum.

3.1.4. Sample matrix

The peak height and peak shape and the separation are affected by the concentrations of ACN and SDS, but not that of Tris, in the solvent used to dissolve the sample. Systematic variation of showed the optimum solvent composition to be 10mM SDS.

3.1.5. Capillary flushing

Rather than the conventional between-run rinse cycle of water NaOH-water-BGE, a simple 3 minute rinse with BGE was found to provide better reproducibility of migration time and peak area.

3.2. Method Validation

3.2.1. Precision

The "natural" capsaicin sample was used to prepare a 50 μg (total

capsaicins)/mL in the above sample solvent. To determine the within-day reproducibility, the sample was analyzed in triplicate every hour for 10 hours using the optimized method. The RSD's of the migration times were 0.74% for CAP and 0.86% for DHC, and the RSD's of the peak areas were 2.88% and 2.87%, respectively. The day-to-day reproducibility was assessed by analyzing the sample in triplicate once a day for 7 days, using the same capillary. The RSD's of the migration times were 2.2% for CAP and DHC. The RSD's of the peak areas were 5.9% and 7.2%, respectively. The column-to-column reproducibility was determined by cutting 6 identical capillaries from the same lot. These were conditioned, equilibrated, and tested as above. Based on duplicate injections of a standard sample on each capillary, the RSD's of the migration times were 4.0% for CAP and 4.6% for DHC. The RSD's of the peak areas were 3.0% and 4.7%, respectively.

3.2.2. Linearity

Solutions of the pure CAP in the optimized sample solvent were prepared at concentrations ranging from 10 μg /mL to 1500 μg /mL. The sensitivity plot of relative peak area vs. concentration injected for duplicate injections was linear (R^2 = 0.9980) up to about 700 ppm capsaicin. For

sample concentrations > 700 ppm, the peaks began to tail and linearity was lost.

3.2.3. Limits of detection (LOD)

The LOD, taken to be the concentration of sample injected producing a signal-to-noise ratio of 3, was found to be 7 ppm.

3.2.4. Accuracy

Portions of the jalapeno pepper extract were spiked with pure CAP and DHC at 25 ppm, 50 ppm, and 100 ppm. To each was added an internal standard, N- vanillyl-n-nonamide, at a concentration of 50 ppm. These were analyzed in duplicate. The average recovery of capsaicin was 106%, and that of dihydrocapsaicin 107%.

3.2.5. Ruggedness

For the capsaicin peak, a change in pH from 9.0 to 8.8 caused a 3.1% decrease in migration time; from 9.0 to 9.2 caused a 3.6% increase. A 10% decrease in SDS concentration from 40 mM to 36 mM resulted in a 4.8% increase in migration time; a 10% increase reduced migration time by 5.8%. Reducing Tris concentration from 20 mM to 18 mM produced a 2.0% decrease in migration time; an increase to 22 mM caused a 0.9% increase. The migration time with 9% ACN was 5.4% less than at 10% ACN; 11% ACN produced a 0.3% decrease. An increase in the separation

temperature from 30°C to 35°C (16.7%) caused an 8.8% decrease in migration time. The corrected capsaicin peak area was not affected by any of these changes except wavelength.

3.3. Application of the Method

The method was applied to 6 dried chili peppers and 3 fresh hot peppers. A typical electropherogram is shown in Figure 2 for the Chipotle sample. Quantitative results for the samples are given in Table 1 along with the Scoville heat index calculated according to the AOAC method [18]. It is well known that the capsaicinoid content of any particular variety of chili peppers can vary widely, depending on growing conditions such as soil and weather [25].

Table 1. Capsaicin Contents and Scoville Heat Indexes

First six peppers are dried; last three are fresh.
CAP and DHC are ppm.
Scoville Heat Index (SHI) calculated as per ref. 18.

Variety	CAP	DHC	SHI
Chipotle	520	470	14,900
Ancho	50	30	1,200
Mulato	15	14	400
Pasilla	34	34	1,000
Pulla	400	280	10,000
Costeno	93	61	2,300
Chinese	120	69	2,800
Jalapeño	400	200	9,000
Piquin	820	490	19,700

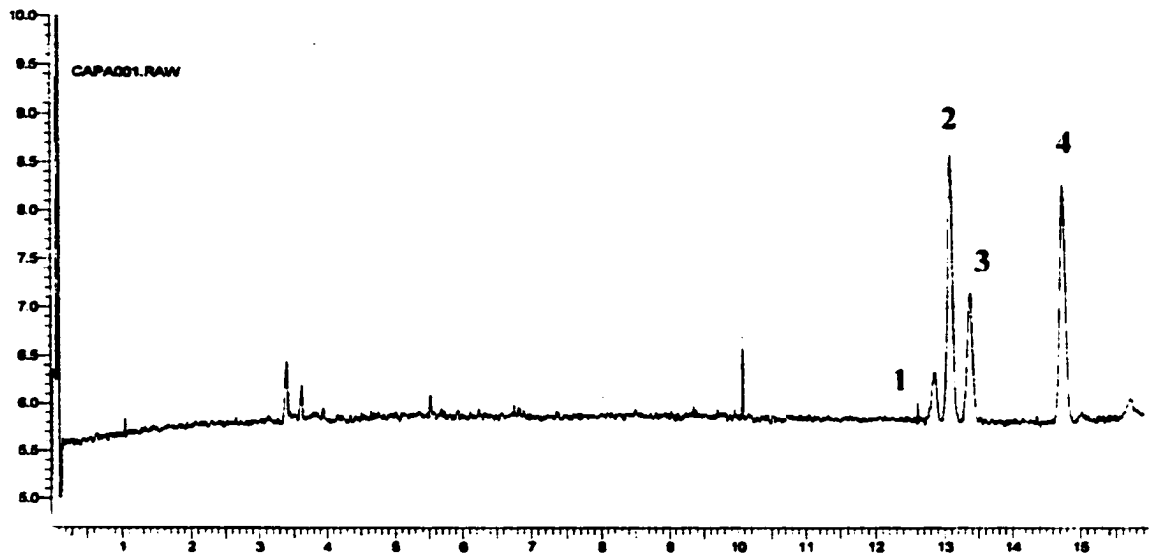

Figure 2. Electropherogram of extract of Chipotle pepper sample. Peak identification: 1, norcapsaicin; 2, capsaicin; 3, N-vanillyl-n-nonamide (internal standard); 4, dihydrocapsaicin.

3.4. HPLC

For comparison, some of the same extracts were analyzed by HPLC using an AOAC method [17]. The mobile phase was 60/40 (v/v) 1% aqueous acetic acid/ACN at 1 mL/min. Sample extract was dissolved in 10 mM SDS and mobile phase. The one-point quantitative standard contained 50 ppm each of CAP and DHC. It was found necessary to clean the HPLC column by flushing with 15mL of pure ACN after every 3 sample injections to remove extracted materials that stuck to the column and changed its efficiency and the retention times of the capsaicinoids. A chromatogram for the Chipotle pepper extract is shown in Figure 3. The quantitative comparison is given in Table 2.

Table 2. Comparison of HPLC and MECC Assays

(CAP and DHC are ppm)

	CAP		DHC	
Variety	MECC	HPLC	MECC	HPLC
Chipotle	520	540	470	490
Pulla	400	410	280	280
Jalapeño	400	390	200	180
Piquin	820	740	490	480

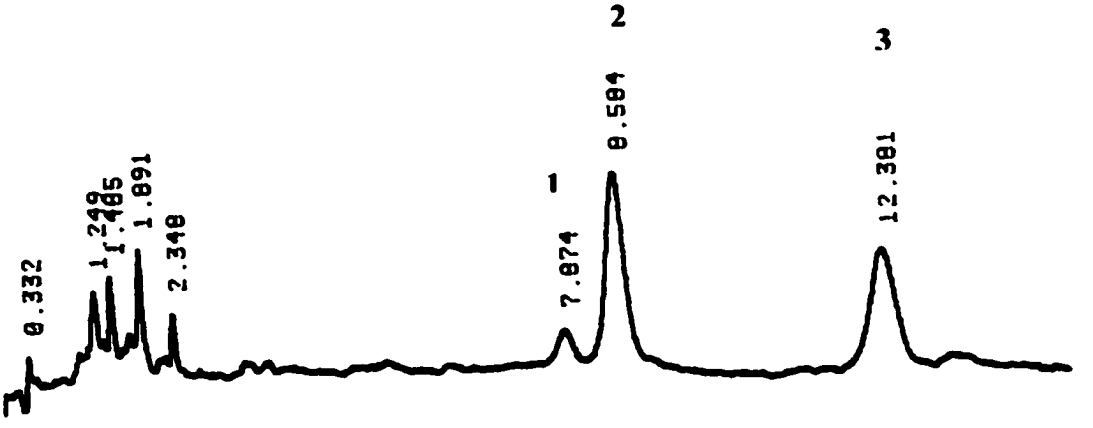

Figure 3. HPLC chromatogram of extract of Chipotle pepper sample.

Peak identification: 1, norcapsaicin; 2, capsaicin; 3, dihydrocapsaicin.

Part II

Study of DNA-Ruthenium (II) Complex Binding using Capillary Zone Electrophoresis

INTRODUCTION

1.1. Metallointercalators

Metallointercalators refer to the transition metal complexes containing planar aromatic heterocyclic ligands which can insert and stack between the base pairs of double helical DNA. The rich chemistry of metallointercalators involves their photophysical, photochemical and redox properties. The considerable interest in metallointercalators arises from their ability to recognize and react with double helical DNA.

The most important unique feature of metallointercalators is their binding to a DNA duplex by intercalation, which means one of the planar chromophor stacks between adjacent DNA base pairs. It is believed that the specific, noncovalent interaction of small organic molecules with duplex DNA is the molecular basis of many antitumor, antiviral and antibiotic drugs. The intercalative drugs can be strongly mutagenic. The intercalation of drug molecules can interfere with and inhibit gene expression, and ultimately affect cell proliferation and differentiation. Therefore, these drugs serve as potent chemotherapeutic agents [1-4].

The redox activity of the complex metal center is another aspect of metallointercalators. A variety of complexes are now available which can

cleave DNA via oxidative or free radical pathways. Many of these reagents have already provided useful footprinting reagents in vitro. In another interesting study, reactive species that are not well stacked in DNA are tethered to and delivered by the intercalator to specific DNA sites through intercalation. In this case, the intercalation property of metallointercalators is used advantageously to provide a path to reactivity [5].

The intense metal-to-ligand charge transfer (MLCT) band in the visible spectrum and luminescence characteristics of metallointercalators provide a sensitive and nonradioactive handle to monitor the conformation and flexibility of helix. The most promising complexes investigated are the complexes containing the dppz (dppz=dipyridophenazine) ligand [6,7,8,9]. Quenched in aqueous solution, the complex luminesces brightly when intercalated into DNA. This luminescent characteristic, coupled with high binding affinity for DNA ($K_b \cong 10^6$) permits its application as a nonradioactive probe of DNA at analytical concentrations.

Another attractive feature of metallointercalators is their optical activity. The octahedral metal complexes exist as enantiomers and exhibit stereoselectivity in presence of DNA. The differential binding with DNA is primarily due to the steric interaction between the non-intercalating ligands and the DNA backbones [10]. The preference in binding has already been

proven by various physical and spectroscopic techniques, such as NMR, circular dichroism, viscosity measurements, X-ray crystallography, UV/Vis absorption, fluorescence, and electrochemical methods [2,11,12]. The study of the stereoselectivity is an important aspect of drug development.

1.2. Structure of B-DNA and non-covalent binding modes

Since the applications of metallointercalators are closely related to their accessing and associating with biomolecules, study of binding mechanisms, binding stoichiometry and binding affinity are crucial. In the binding study, native DNA or synthetic oligonucleotides are frequently used as model biological substances.

Figure 1. Structure of nucleotide.

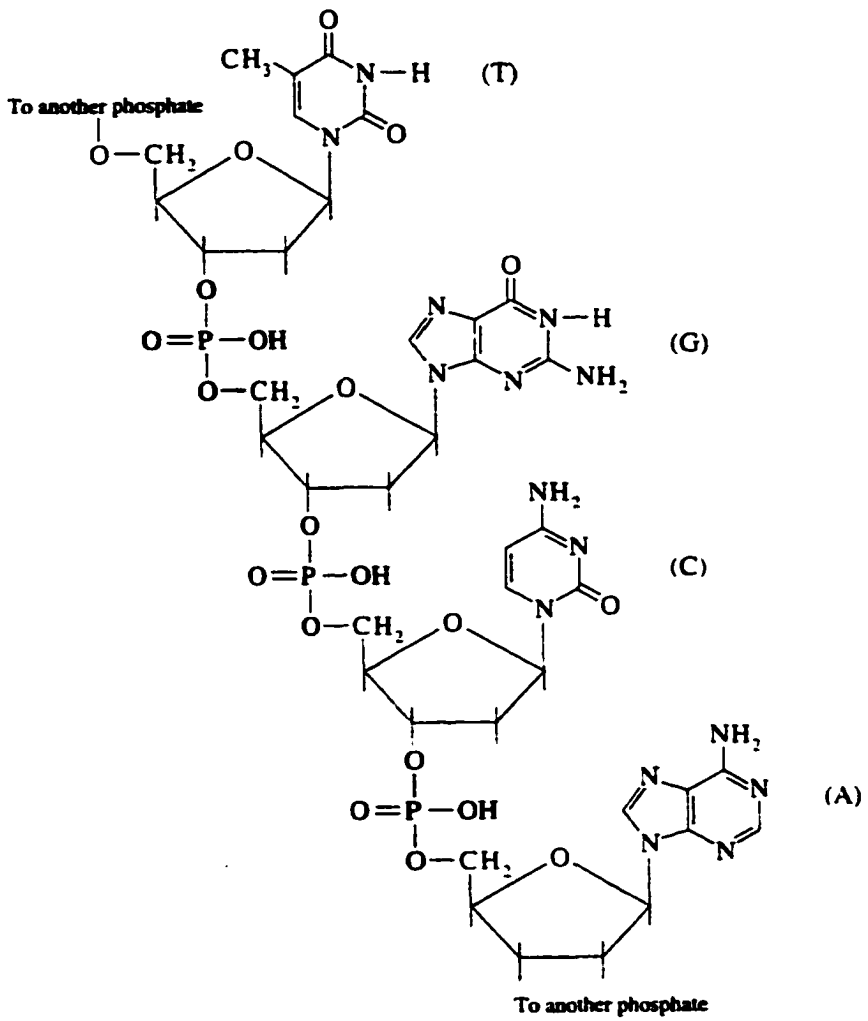

(Reprinted from reference [13] p.551)

Figure 2. Structure of DNA duplex.

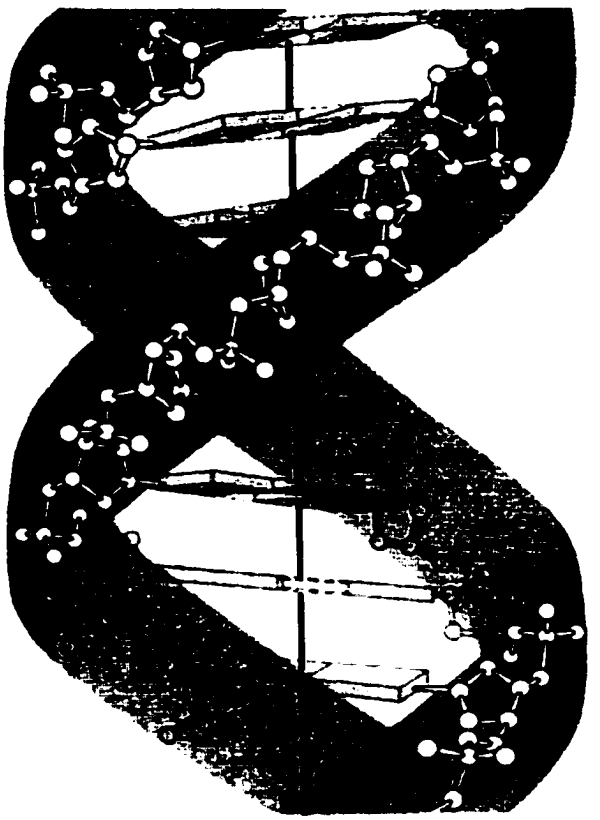

(Reprinted from reference [15] p.181)

Deoxyribonucleic acid (DNA), a major component of chromosomes in living cells, was discovered in 1869 by Swiss physiologist Friedrich Miescher who extracted it from the nuclei of cells. The DNA molecules contain genetic code of life which determines the characteristics of individuals and is passed on from one generation to another [13].

DNA is a polymeric substance made up of thousands of units called nucleotides. The fundamental components of the nucleotides in DNA are phosphoric acid, deoxyribose (a pentose sugar), and the four nitrogen-containing bases, adenine, thymine, guanine, and cytosine (abbreviated as A, T, G, and C). Phosphoric acid is obtained from minerals in the diet; deoxyribose is synthesized in the body from glucose; and the four nitrogen bases are made in the body from amino acids. In 1953, the American biologist James D. Watson and the British physicist Francis H. C. Crick announced their double-stranded helix structure for DNA. Information on the dimensions of polynuleotide double helices were mainly derived from X-ray diffraction studies [13]. Depending on the relative humidity of the DNA fibers, there are a total of three DNA forms: A, B and Z [14].

In the classic B-DNA structure, the helical repeat is a single nucleotide unit, with necessarily all of the nucleotides in the structure having the conformation of this unit. The backbone conformation has C2' *endo* sugar puckers and high *anti* glycosidic angles. The right-handed double helix has 10 base pairs (bp) per complete turn, with the two polynucleotides chains anti-parallel to each other and linked by A-T and G-C base pairs. The paired bases are almost exactly perpendicular to the helix axis and they are stacked over the axis itself. Consequently the base pair

separation is the same as the helical rise, i.e. 3.4 Å. Due to the presence of the phosphate moieties along the backbone of the DNA double helix, the outer region of the DNA is negative and hydrophilic in nature; and the inner region of the macromolecule is mainly hydrophobic due to the presence of the aromatic heterocyclic base pairs in this location. An important consequence of the base pairing arrangement is that the two deoxyribose sugars linked to an individual base pair are on the same side of it. So, when successive base pairs are stacked on each other in the helix, the gap between these sugars forms continuous indentations in the surface that wind along, parallel to the sugar-phosphodiester chains. These indentations are termed grooves. The asymmetry in the base pairs results in two parallel types of groove, whose dimensions are related to the distances of base pairs from the axis of the helix and their orientation with respect to the axis. The wider major (11.6Å in width) is almost identical in depth to the much narrower minor groove (6.0Å in width). In general, the major groove is richer in G-C base pairs than the minor one. This, together with the steric differences between the two, has important consequences for interaction with other molecules [14].

Generally, the contacts of metallointercalators with polynucleotides are noncovalent, and may be categorized as:

Intercalative binding

The planar ligand component inserts between the stacked base pairs. The chromophore is stabilized by van der Waals dispersion interaction between its planar group and the base pairs surrounding it. This results in an extension of the double helix twist (unwinding) for the base pairs at and adjacent to each binding site. The base pairs on either side of an intercalated molecule thus become 6.8Å apart [14].

Surface/Groove binding

By contrast with intercalation, groove binding does not significantly perturb DNA structure. The binding occurs exclusively in the minor groove of B-DNA duplexes. Most groove binding molecules are situated in the narrow minor groove AT regions. The molecules are stabilized in position by close van der Waals interactions with the walls and floor of the groove itself, as well as having hydrogen bonds to the N3 atoms of adenines or O2 of thymines. This is direct sequence readout. Indirect sequence readout is via both groove width and complementation of the negative electrostatic potential in the AT minor groove with positive charge on these drugs. Groove interaction involves the concave curvature of the inner surface of

the drug molecule that of the convex surface of the floor of the DNA minor groove itself [14].

Electrostatic binding

A significant contribution to drug binding is due to the coulombic attraction between the positively charged metal complex ion and the negatively charged DNA phosphate backbone. This interaction is not expected to exhibit sensitivity to the chirality of the drug molecule.

It is generally accepted that intercalation is a strong binding process; electrostatic interaction is a weak binding process and does not induce binding discrimination [71].

1.3. Project introduction

Metallointercalators have been particularly useful because the ligands or metal may be varied in an easily controlled manner to facilitate the individual application. There is a large dynamics of synthesis, modification and characterization of complexes with the ultimate goal of developing new diagnostic and therapeutic agents. Among them the Ru(II) polypyridine system is the most widely investigated family in this rapid developing field. Over the last decade, extensive research has been conducted on the ruthenium family [5-12,16-70].

In this study, the analyte of interest is a group of Ruthenium complexes synthesized by a research group at Queens College [71]. The basic structure is a Ru(II) core with three α-diimine ligands in octahedral coordination. The mirror images of a pair of enantiomeric isomers named delta and lambda are shown in Figure 3. The 3-D structure resembles an electronic fan in which two of the blades are bipyridines and the other one is one of the newly synthesized ligands which are depicted in Figure 4. Figure 5 shows the coordinating sites on the ligands. Since there is only one ligand different, and for the sake of simplicity, in the rest of this section, the ruthenium complexes will be called by their ligand names, e.g., $[Ru(bpy)_2ppz]^{2+}$ is simply called ppz.

The characterization and investigation of interaction with DNA were previously explored through spectroscopic methods including absorption, emission, circular dichroism (CD), fluorescence titration, and fluorescence quenching, and by equilibrium dialysis. Various perturbations of the optical properties upon introduction of DNA provide valuable information on the overall binding. Evidence for intercalation to DNA was mainly the presence of hypochromism in absorption and enhancement in fluorescence emission. The differential optical responses of different isomers proved the enantioselectivity towards DNA. Meanwhile, the binding mode was

characterized as partial intercalation since the binding was found to be weak and salt dependent.

In this dissertation, capillary electrophoresis was utilized as an alternative approach to study the Ruthenium complex binding to DNA. Chiral complexes were resolved due to their differential interactions with DNA-buffer medium. Buffer composition was optimized in terms of DNA concentration and salt concentration. The actual binding constants were obtained by a frontal analysis technique. Minor groove competitive study was performed for the groove binding assessment. The results and analysis of the CE study will be detailed in the following sections.

Figure 3. Mirror images of $\Delta/\Lambda[Ru(bpy)_2L]^{2+}$

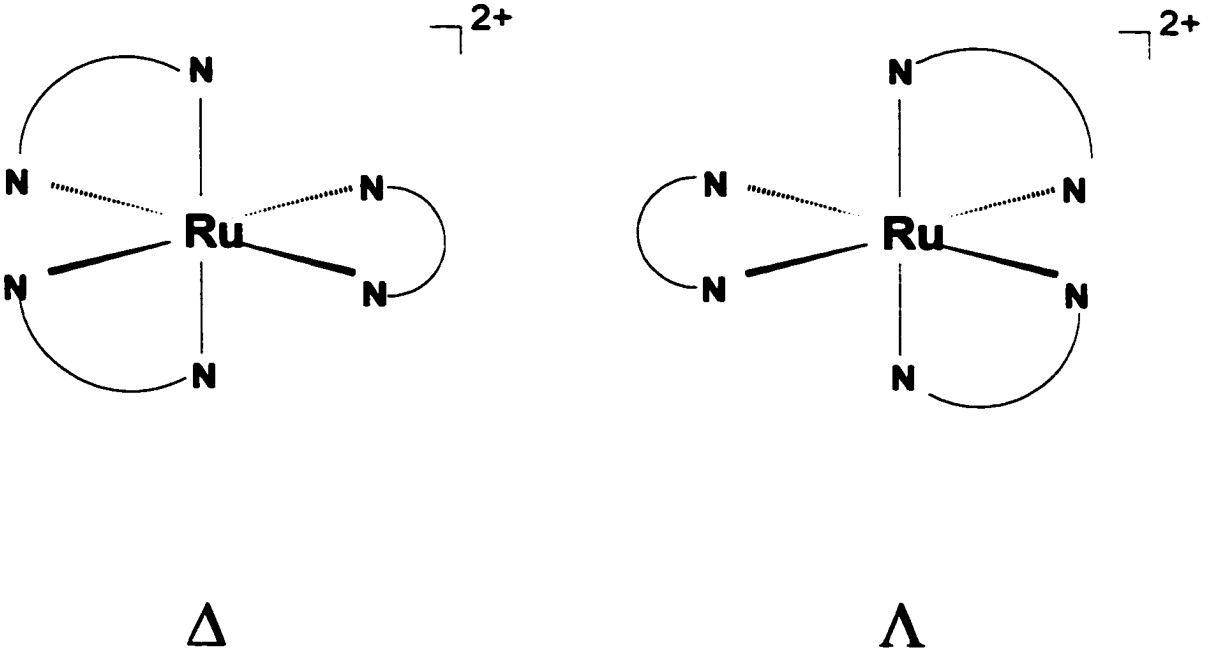

Δ Λ

Figure 4. Structures of α-diimine ligands

bpy (2,2'-bipyridine)

ppz (phenanthrolino pyrazine)

ippz (isophenanthrolino pyrazine)

bzp (benzophenanthroline)

bppz (benzophenanthrolino pyrazine)

mbppz (methyl benzophenanthrolino pyrazine)

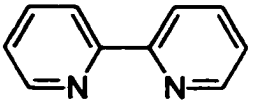

bpy

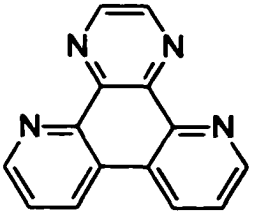

ppz

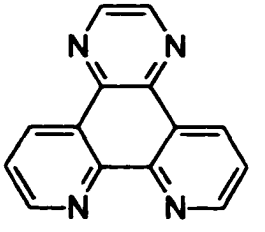

ippz

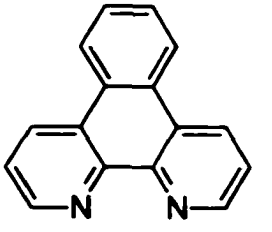

bzp

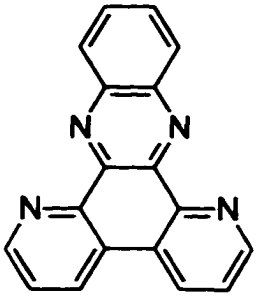

bppz

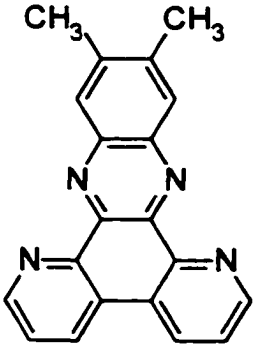

mbppz

Figure 5. Coordination of $[Ru(bpy)_2L]^{2+}$

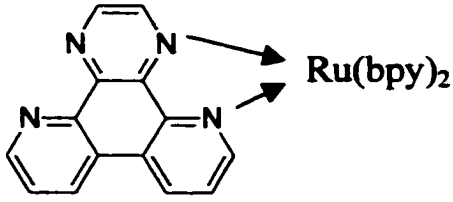

$Ru(bpy)_2ppz^{2+}$

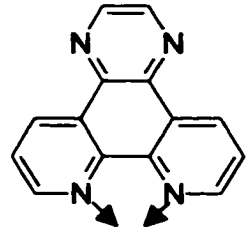

$Ru(bpy)_2\,ippz^{2+}$

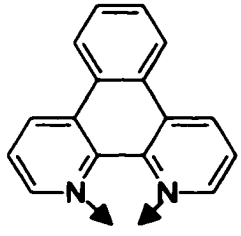

$Ru(bpy)_2bzp^{2+}$

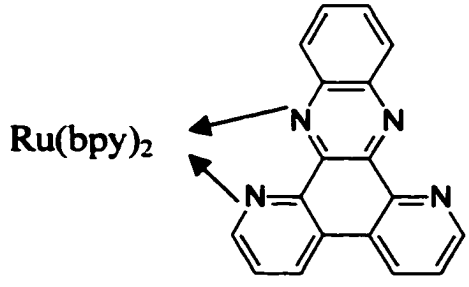

$Ru(bpy)_2\,bppz^{2+}$

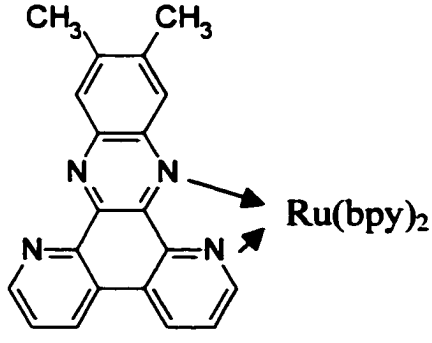

$Ru(bpy)_2\,mbppz^{2+}$

CE METHODOLOGY

As a highly efficient, versatile analytical separation technique, capillary electrophoresis (CE) has been shown to be exceptionally effective for the separation of enantiomeric substances. Extensive applications of CE to chiral mixtures have been directed toward compounds of pharmaceutical origin due to potential differences in pharmacological activity as a function of the isomeric structure [10]. The utilization of CE for separation of optically active metal-ligand complexes, however, is still in its infancy. In 1989, Fanali et al. first used capillary zone electrophoresis (CZE) with salts of D-tartaric acid added to the background electrolyte for the separation of optical isomers of Co(III) complexes [72]. Five years later, Vogt and Werner demonstrated the separation of a racemic mixture of lobaplatin diastereomers using micellar electrokinetic chromatography (MECC) [73], where the diastereomeric platinum complexes were resolved based on their differing partition coefficients inside SDS micelles. More recently, Bushey and co-workers used MECC with bile salts as the chiral detergent to separate enantiomeric Fe(II) ligand complexes [74,75]. The enantiomeric purity of $[M(\alpha\text{-diimine})_3]^{n+}$ transition metal complexes, where the central metals are Ru^{2+}, Ni^{2+}, Fe^{2+}, Cr^{3+}, and Co^{3+}, were assessed in Wheeler's lab [76-78]. A wide range of chiral resolving agents has been evaluated and

threo-D_s[+]-isocitrate, potassium antimonyl-d-tartrate and dibenzoyl-L-tartrate were identified as most efficient. Wheeler and co-workers also pioneered the area of chiral recognition and preferential binding of metal complexes to biological molecules by CE [80,83]. Near-baseline separation of the Λ and Δ isomers of $[Ru(phen)_3]^{2+}$ and $[Ru(bpy)_3]^{2+}$ were noted when calf thymus DNA was employed as the chiral medium in ammonium acetate buffer in 1997. DNA-facilitated enantioseparation of racemic $[Cr(phen)_3]^{3+}$ was later performed. The CE studies have provided valuable insight into the nature and stereoselectivity of metal complex interaction with polynucleotides.

2.1. CZE enantiomeric separation of racemic ruthenium complexes

As the ruthenium complex carries permanent charge, capillary zone electrophoresis (CZE) is chosen as the separation mode. In order to investigate the DNA-Ru complex interaction, enantiomers of racemic ruthenium complex are resolved and binding information is extracted from their CE behavior. To achieve enantiomeric separation, DNA is used as chiral resolving agent in the separation medium into which ruthenium complexes are introduced. During electrophoresis, the two enantiomers of

ruthenium complex interact with DNA differentially, and therefore migrate at different speeds and arrive at the detector at different times.

The background electrolyte composition for enantioseparation is: 50mMTris-HCl buffer, DNA, and salt such as NaCl. Optimization of the enantiomeric separation is mainly to fine-tune the DNA and salt concentrations in the separation medium.

Figure 6. Illustration of mobility vectors

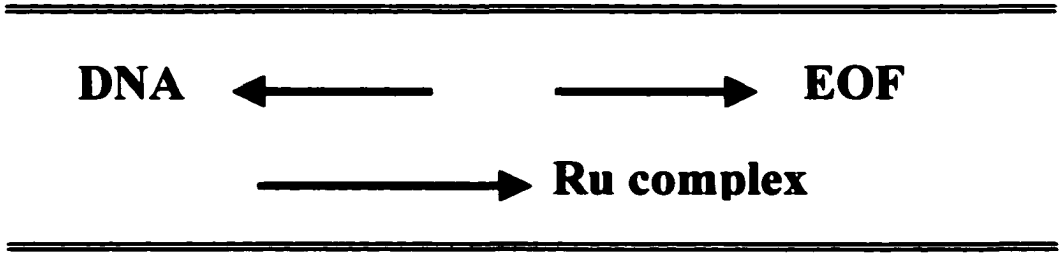

2.2. Frontal Analysis CZE method

The methods applied before in measuring the actual binding constants are mainly equilibrium dialysis and fluorescence titration [71]. In the dialysis method, the racemic complex is dialyzed against DNA and the free ruthenium complex concentration of the solution outside the dialysis bag (dialysate) is measured by UV. The binding constant and the average site size are determined by fitting the data collected from dialysis experiment to the McGhee and von Hippel equation. In the fluorescence titration method, the emission intensity of the ruthenium complex solution is measured as a function of the amount of DNA added and K_b determined as (−1/slope) of Eadie Hofstee plot [71].

Despite its popularity as a separation technique, capillary electrophoresis using chiral selector additives in the BGE has developed into a particularly effective means to determine apparent equilibrium constants for molecular associations in solution. In 1992, Wren and Rowe developed a model [80] for the separation of enantiomeric molecules by CE which shows that the degree of separation depends on the concentration of chiral selector, for which there is an optimum concentration maximizing resolution. The optimum concentration depends inversely on the affinity of the enantiomers of the chiral selector. This model was later used as the

basis for binding studies by CE. Nowadays, the most common method used to estimate binding parameters by CE involves measuring the change in electrophoretic mobility of a solute through a buffer solution containing dissolved complexing agents or ligands. The various graphical and mathematical approaches generally rely on linear plots [81] and nonlinear regression [82-85] based on a 1:1 molecular association model. For studies of association between small molecules and biomolecules, where there are multiple binding sites available along the macromolecule, methods based on 1:1 binding stoichiometry are not applicable. At present, CE methods based on frontal analysis [86-92], the Hummel-Dreyer method [86,89-91] and the vacancy peak method [86,89-91] are available. These CZE methods rely on the separation of the interacting species, on basis of their difference in mobility. Of the three methods, frontal analysis appears to be the most promising because it is simple, robust and requires the smallest amount of sample.

In the frontal analysis method, the solute is first equilibrated with the ligand. A large plug of solution containing the preequilibrated ligand and solute is injected into the CE capillary containing only buffer. After a period of electrophoresis, the free solute separates from the sample plug and the concentration of free solute is calculated directly from its peak size.

The free and bound concentrations of solute are then calculated and used to determine binding constant K_b.

In this study, the binding constant of Ru(II) complexes to calf thymus DNA is defined as

$$K_b = [Ru]_b / [DNA_{b.s}]_f [Ru]_f$$

where $[Ru]_b$ is the bound ruthenium complex concentration, $[Ru]_f$ is the free ruthenium complex concentration, and $[DNA_{b.s}]_f$ is the concentration of free DNA binding sites. $[DNA_{b.s}]_f$ is calculated from the total DNA concentration in base pairs, the average binding site distribution factor n (number of binding site per base pair) and $[Ru]_b$.

$$[DNA_{b.s}]_f = [DNA]_t \cdot n - [Ru]_b$$

The Scatchard Equation was then applied to obtain the binding information [93-97]:

$$r/C_f = K_b n - K_b r$$

where r is the ratio of bound ruthenium complex per DNA base pair,

$$r = [Ru]_b / [DNA]_t$$

Frontal analysis allows the determination of the free ruthenium complex concentration. The bound ruthenium complex concentration and r are then calculated. K_b and n are obtained from the slope and intercept of the r/C vs. r plot.

Figure 7. Schematic elution of frontal analysis

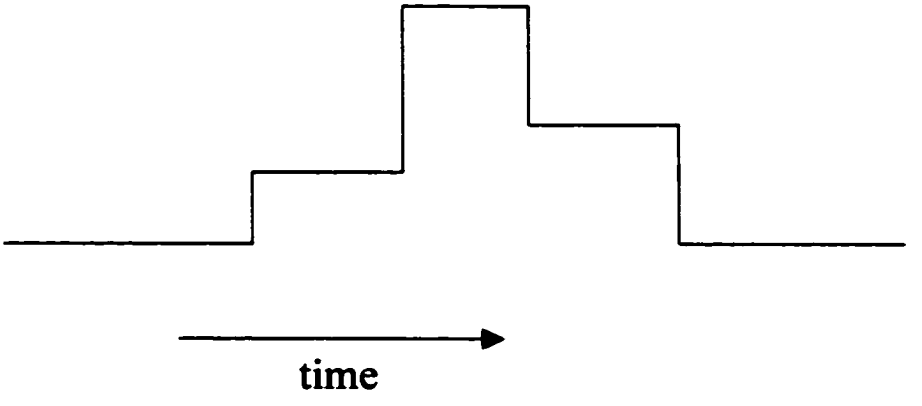

Separation buffer : buffer
Sample : buffer + interacting species

2.3. Partial filling technique

The partial filling technique (PFT) in capillary electrophoresis is an efficient system in which only 50~800 nanoliters of a buffer with additive solution needs to be added in each run. PFT is especially applicable when these additives to the background electrolyte (BGE) are expensive or absorb UV light. The selector dissolved in the BGE is injected into the capillary as a plug, prior to application of the analyte. During the run both ends of the capillary are connected to the BGE. The selector and the analyte may move in opposite direction or in the same direction at different velocities depending on their electrophoretic mobilities so that the selector is not present when the analyte reaches the detector.

This technique was first employed by Valtcheva et al. in 1994 with non-immobilized cellulase as a chiral selector for the enantioseparation of β-blockers [98]. Since its first publication on PFT there are many reports on enantioseparation using different chiral selectors with this technique [99-106]. A PFT-MECC system using surfactants as the micellar phase is another mode of PFT [107]. PFT is also found to be suitable when using CE coupled to mass spectrometry [108-110].

The important features of this technique are the low consumption of selector solution and avoiding detection interference. Meanwhile, separation performance can be optimized by varying the length and/or concentration of the selector plug.

Figure 8. Schematics of complete filling and partial filling techniques

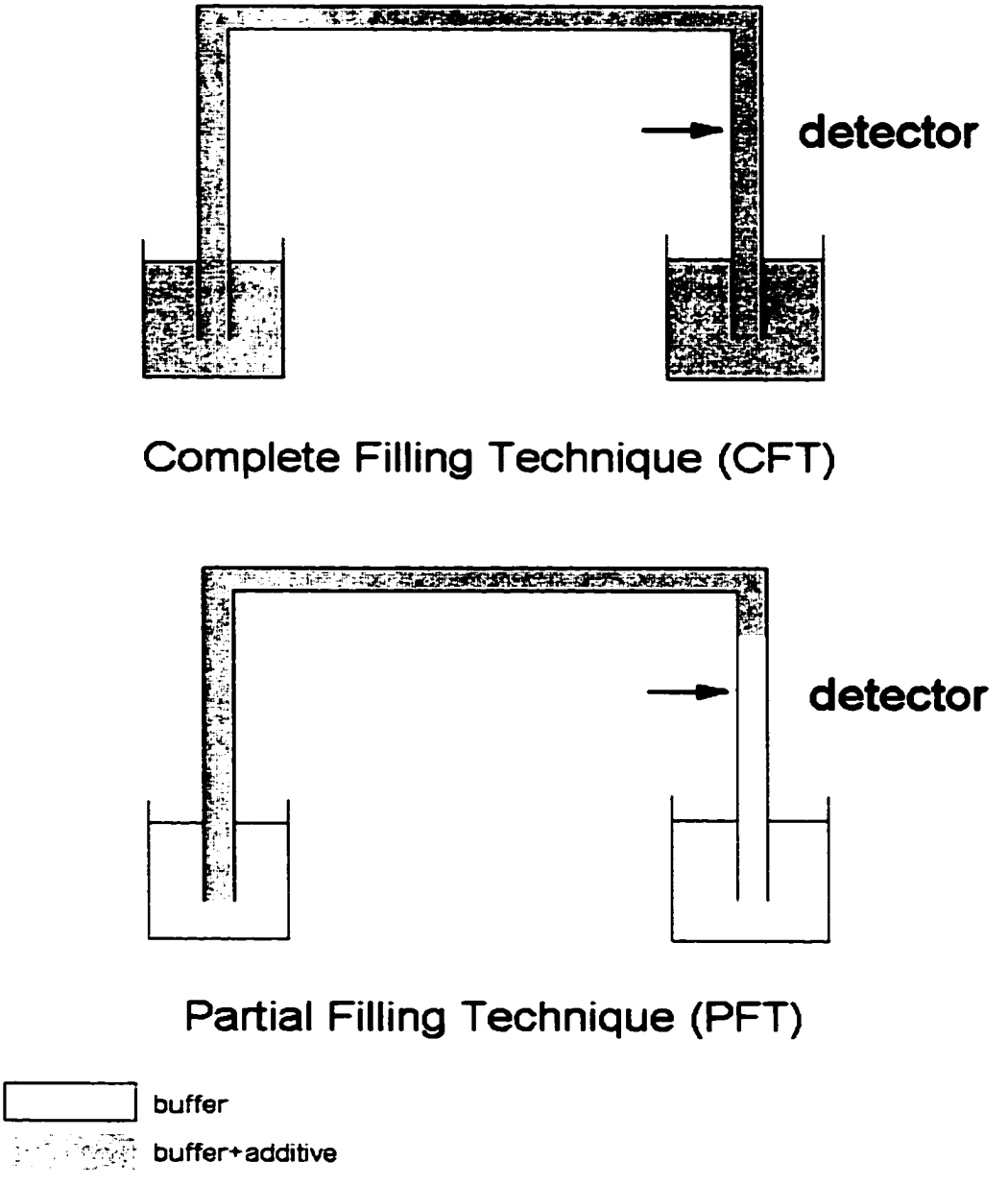

EXPERIMENTAL

3.1. Chemicals and Materials

Five racemic Ruthenium (II) complexes and their enantiomeric isomers in BF_4^- were synthesized by Prof. Baker's research group at Queens College, CUNY. Calf thymus B-DNA, distamycin A and Trisma® base (tris[hydroxymethyl]aminoethane) were purchased from Sigma Chemical Co.(St. Louis, MO). Analytical grade hydrochloric acid, NaCl, KCl, $MgCl_2$, and $CaCl_2$ were obtained from Fisher Scientific (Springfield, NJ).

3.2. Apparatus

CE experiments were carried out using an ISCO 3850 Electropherograph with an adjustable-wavelength UV detector. An uncoated fused-silica capillary with total length 50cm, effective length 30cm and 50μm i.d. was used. Sample injection was accomplished by applying a vacuum at the inlet buffer beaker for a controlled period of time. The electropherograms were recorded on a Spectra-Physics SP-4600 integrator.

3.3. Capillary Conditioning and Flushing

A newly cut capillary was first activated by filling with 1MNaCl over night. After that, the capillary was filled with 0.1mMNaCl. Prior to use, it was flushed thoroughly with water and then equilibrated with the corresponding buffer. Between runs, a water-1.0mM NaCl-water-buffer flushing cycle was applied. After use every day, the capillary was flushed with water, 1.0mM NaCl, 0.1mM NaCl and let stand with 0.1mM NaCl in it.

3.4. Solutions

Water

Water used in all the experiments was purified and deionized to 18MΩ resistance using a Milli-Q system (Millipore, Bedford, MA, USA).

DNA stock solution

Approximately 100mg calf thymus DNA fiber was weighed and dissolved in 50mL 50mM Tris-HCl buffer. The solution was stirred over night, and then centrifuged. The upper layer was transferred to another clean container and stored at ~4°C.

50mMTris-HCl buffer solution

3.03 g Trisma base was weighed and dissolved in about 400mL of water. The pH of the solution was adjusted with HCl to 7.40 and the total volume was then brought to 500mL.

Sample concentrations

$[Ru(bpy)_2L]^{2+}$ samples were dissolved in water and stored as concentrated stock solutions. Aqueous dilutions were prepared to achieve the desired concentration for analyses. All DNA and ruthenium complexes concentrations were established via UV/Vis absorption (molar absorptivities are summarized in Table 1.).

3.5. Electrophoretic Conditions

Electrophoresis voltage was chosen to maintain current below 100μA to minimize Joule heating. All experiments were performed at room temperature.

Table 1. Molar Absorptivities, ε

Complex	ε	λ_{max}
$[Ru(bpy)_2(ippz)]^{2+}$	1.6×10^4	450nm
$[Ru(bpy)_2(ppz)]^{2+}$	1.1×10^4	422nm
$[Ru(bpy)_2(bppz)]^{2+}$	1.04×10^4	544nm
$[Ru(bpy)_2(mbppz)]^{2+}$	1.1×10^4	534nm
$[Ru(bpy)_2(bzp)]^{2+}$	1.8×10^4	452nm
DNA	6.6×10^3	260nm

RESULTS AND DISCUSSION

4.1. Separation of five ruthenium complexes

Figure 9. shows the separation of five ruthenium complexes in DNA-free buffer. The five compounds are being separated and eluting out in order of decreasing charge/mass ratio. Among them, $[Ru(bpy)_2ppz]^{2+}$ and $[Ru(bpy)_2ippz]^{2+}$ have the same charge/mass ratio but differ in coordination sites and are well separated.

Figure 9. Electropherogram of five Ru(II) complexes in DNA-free BGE

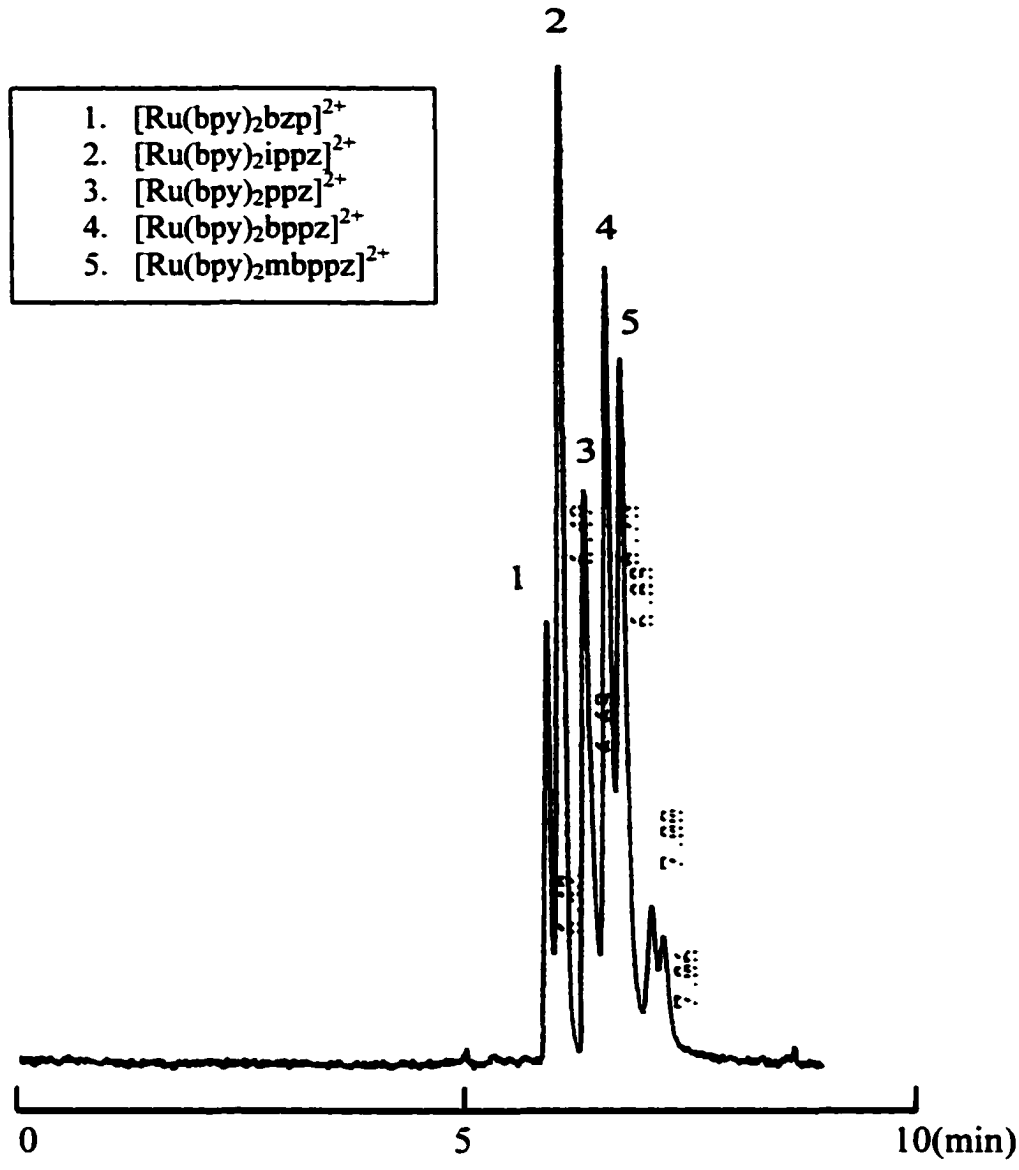

CE separation conditions for Figure 9

Sample:	mixture of racemic Ru(II) complexes (Tabled, ~60μM each)
BGE:	50mM Tris buffer (pH 7.4) with 200mM NaCl
Capillary:	50cm total length/ 30cm effective length, 50μM i.d.
Injection:	5sec, 0.5psi vacuum
Voltage:	+8kV, detector end cathode
Detection:	290nm
Temperature:	room temperature, ~26°C

4.2. Enantiomeric Separation of Racemic Ruthenium Complexes

4.2.1. DNA mobility

At pH 7.4, the DNA molecular surface is negative by charge and DNA migrates against EOF [111]. DNA molecules strongly adsorb to the internal glass wall, forming an immobile anionic DNA network in the capillary.

4.2.2. Effect of DNA concentration

The effect of DNA concentration on the enantioseparation of $[Ru(bpy)_2ppz]^{2+}$ was examined by varying its concentration in BGE as shown in Figure 10. It is clearly seen that as the DNA concentration is increased, both delta and lambda $[Ru(bpy)_2ppz]^{2+}$ isomers exhibit a decrease of net mobility while the mobility difference increases. It is not difficult to understand that more DNA in the buffer medium means more interaction and therefore more separation.

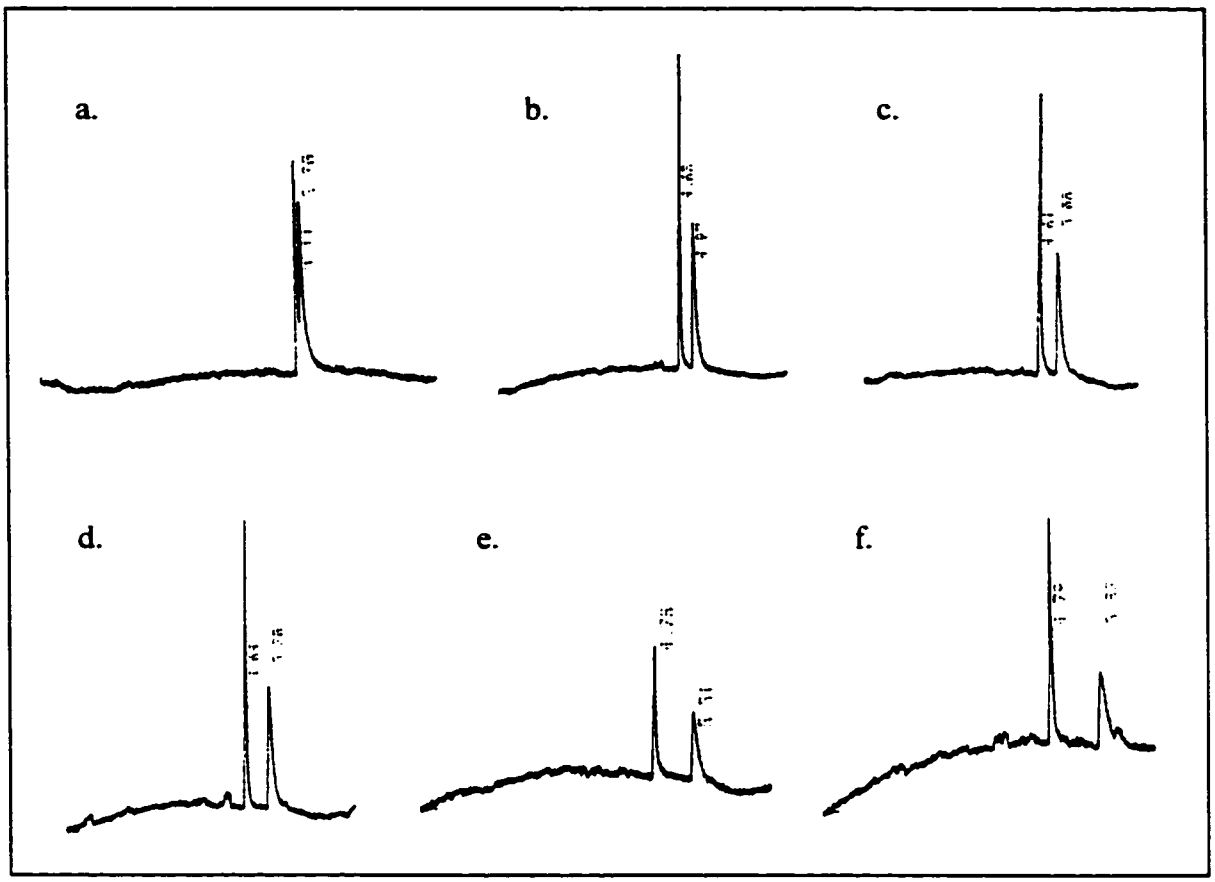

Figure 10. Electropherograms of *rac*-$[Ru(bpy)_2ppz]^{2+}$ in 50mM Tris buffer(pH 7.4) with 100mM NaCl and (a) 0.07mM (b) 0.3mM (c) 0.4 mM (d) 0.5mM (e) 0.6mM (f) 0.8mM DNA. Voltage: 11kV. Other conditions are the same as Figure 9.

Figure 11. DNA concentration effect on enantioseparation

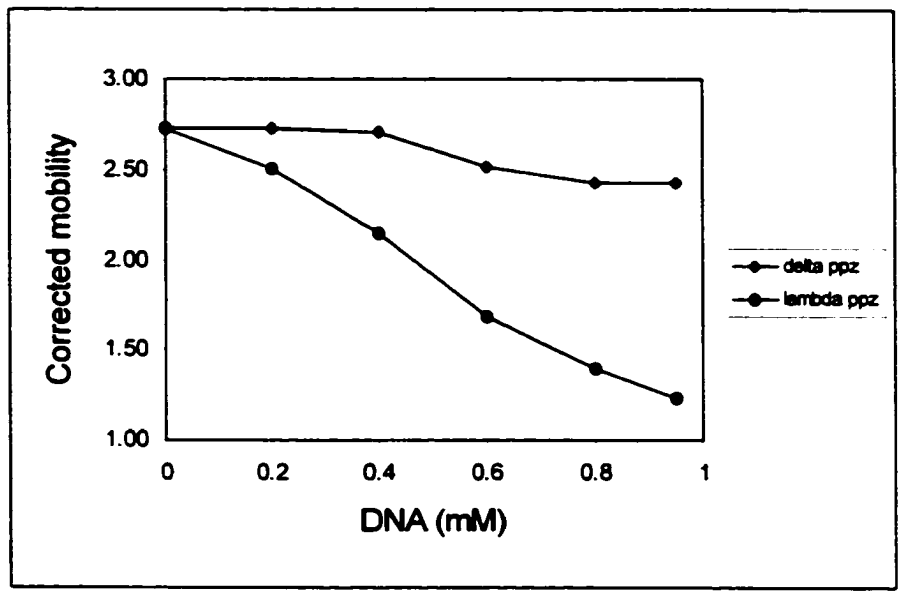

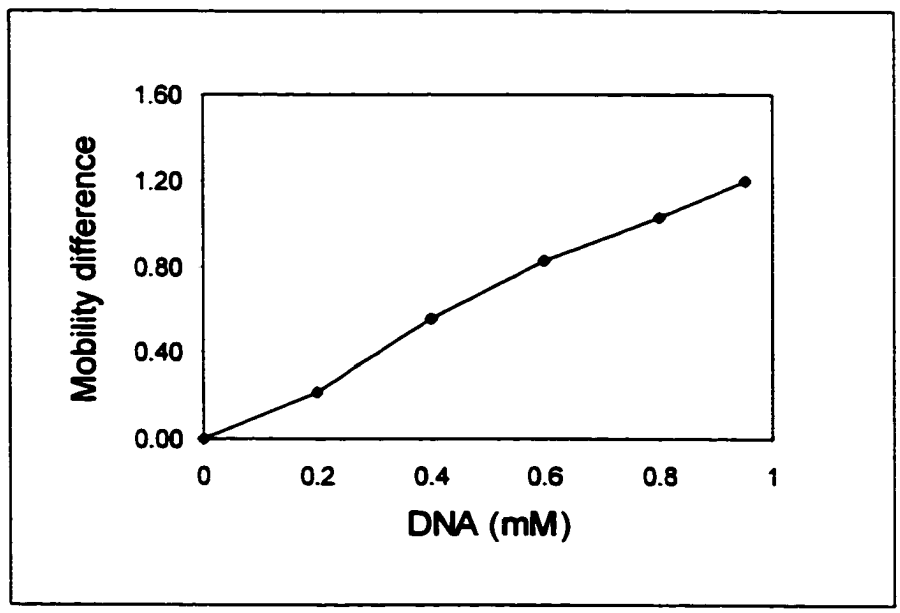

4.2.3. Effect of salt concentration

The dependence of drug-DNA equilibrium constant on salt concentration has been thoroughly examined [47,112-114]. Interpretations are generally based on Manning's polyelectrolyte theory which explains that addition of salt reduces the electrostatic stress by increasing the screening and reduces the concentration gradient stress by reducing the concentration gradient. The salt effect substantially affects the binding constant and provides important insight to the nature of binding.

As a major component in the separation medium, the salt has a significant influence on the separation performance. Figures 12 and 13 show the effect of salt concentration on enantiomeric separation. From the electropherograms (Figure 13), it is clear that at low salt concentrations, the peaks are low and show fronting primarily due to electromigration dispersion. As salt concentration is increased, the peaks become more symmetric and narrower, and the pair of enantiomer peaks migrate closer. The improvement of peak efficiency can be explained by the stacking effect since the addition of salt greatly increases the conductivity of buffer medium relative to the sample conductivity.

On the other hand, the reason for the decrease in resolution is that as more and more counterions are provided to the DNA surface, the

electrostatic attraction between ruthenium complex and DNA is reduced. Although the electrostatic interaction does not directly contribute to the enantiomeric discrimination, it must be present to promote the intercalative interaction. That is why, in some cases, a complete loss of resolution is observed at high salt concentration. This phenomenon indicates that the binding is largely electrostatic in nature.

Figure 12. Plate number and Resolution vs. salt concentration

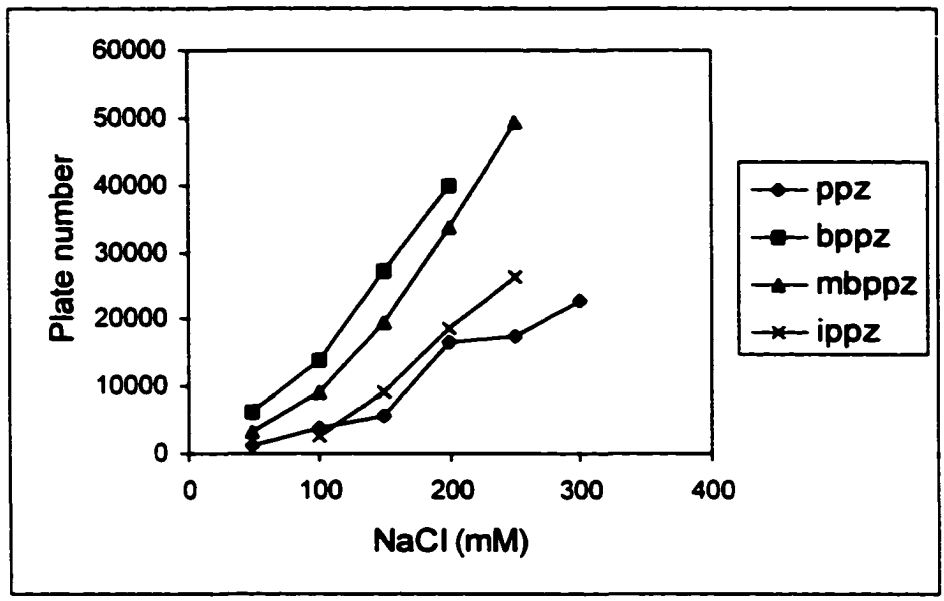

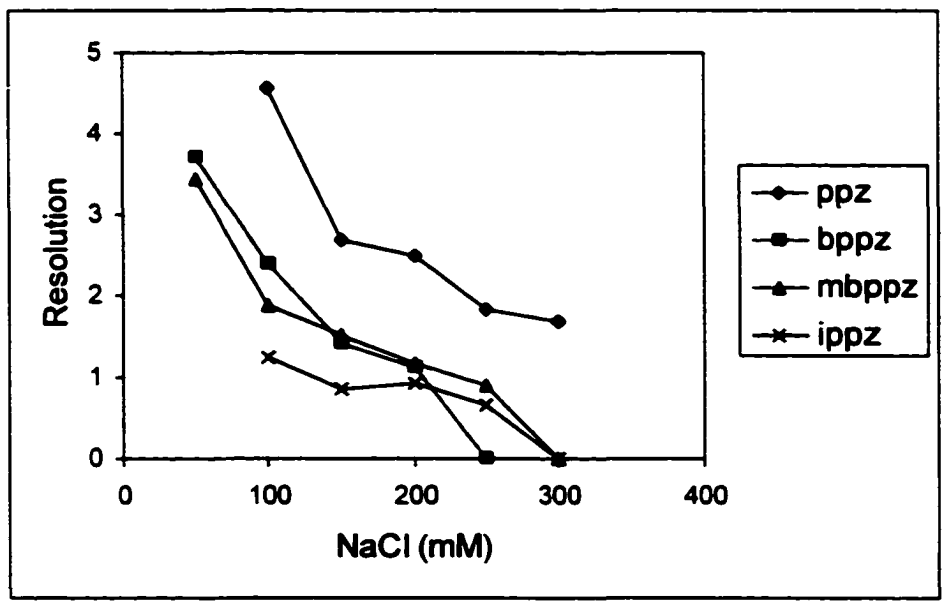

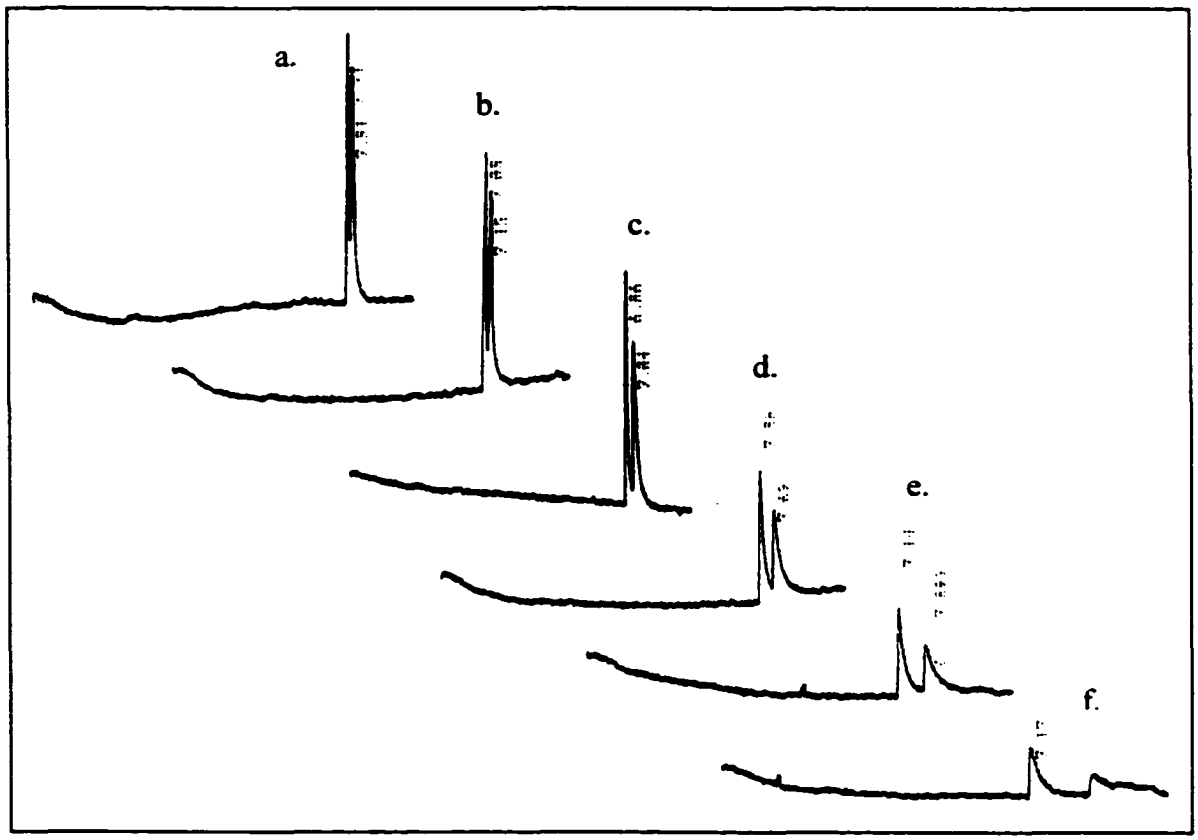

Figure 13-1. Separation of $[Ru(bpy)_2ppz]^{2+}$ in 50mM Tris buffer (pH 7.4) containing 0.1mMDNA and (a) 300mM (b) 250mM (c) 200mM (d) 150mM (e) 100mM (f) 50mM NaCl.

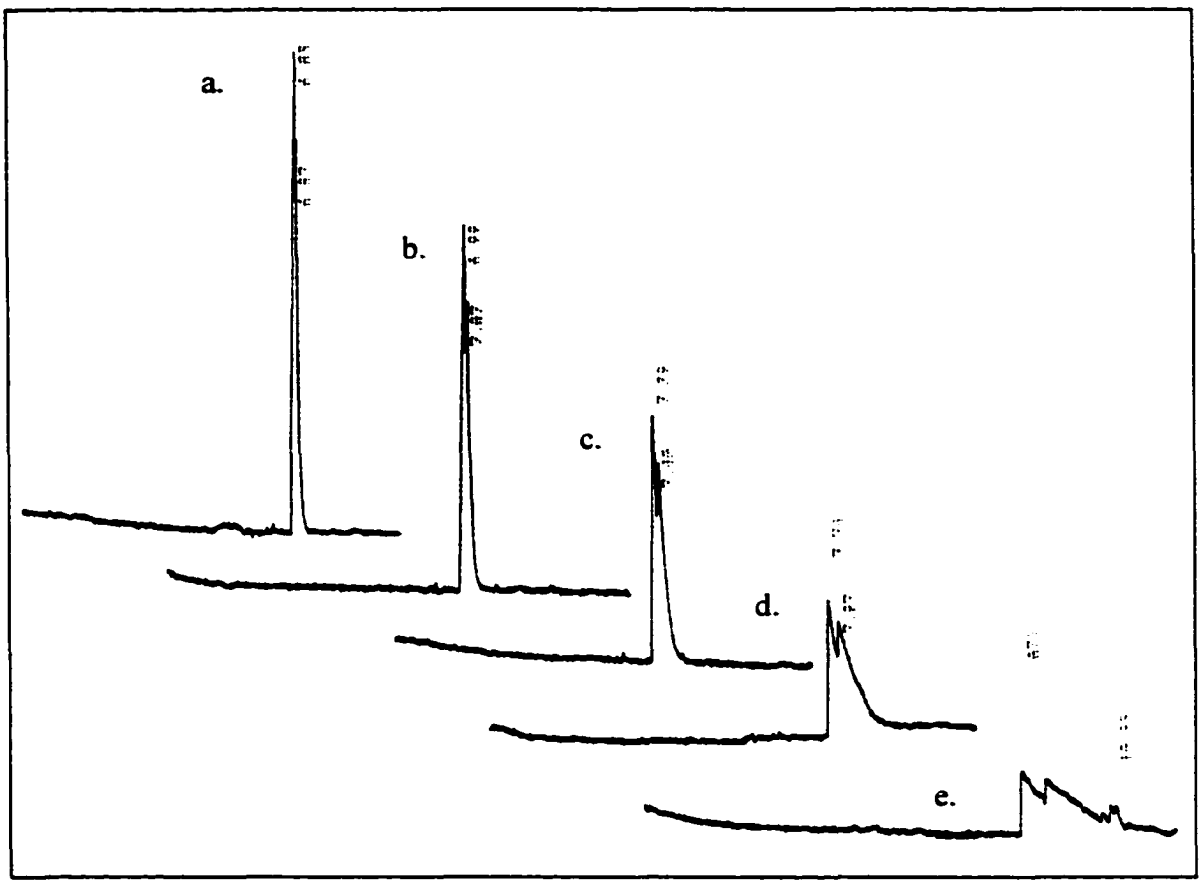

Figure 13-2. Separation of $[Ru(bpy)_2ippz]^{2+}$ in 50mM Tris buffer (pH 7.4) containing 0.1mMDNA and (a) 250mM (b) 200mM (c) 150mM (d) 100mM (e) 50mM NaCl.

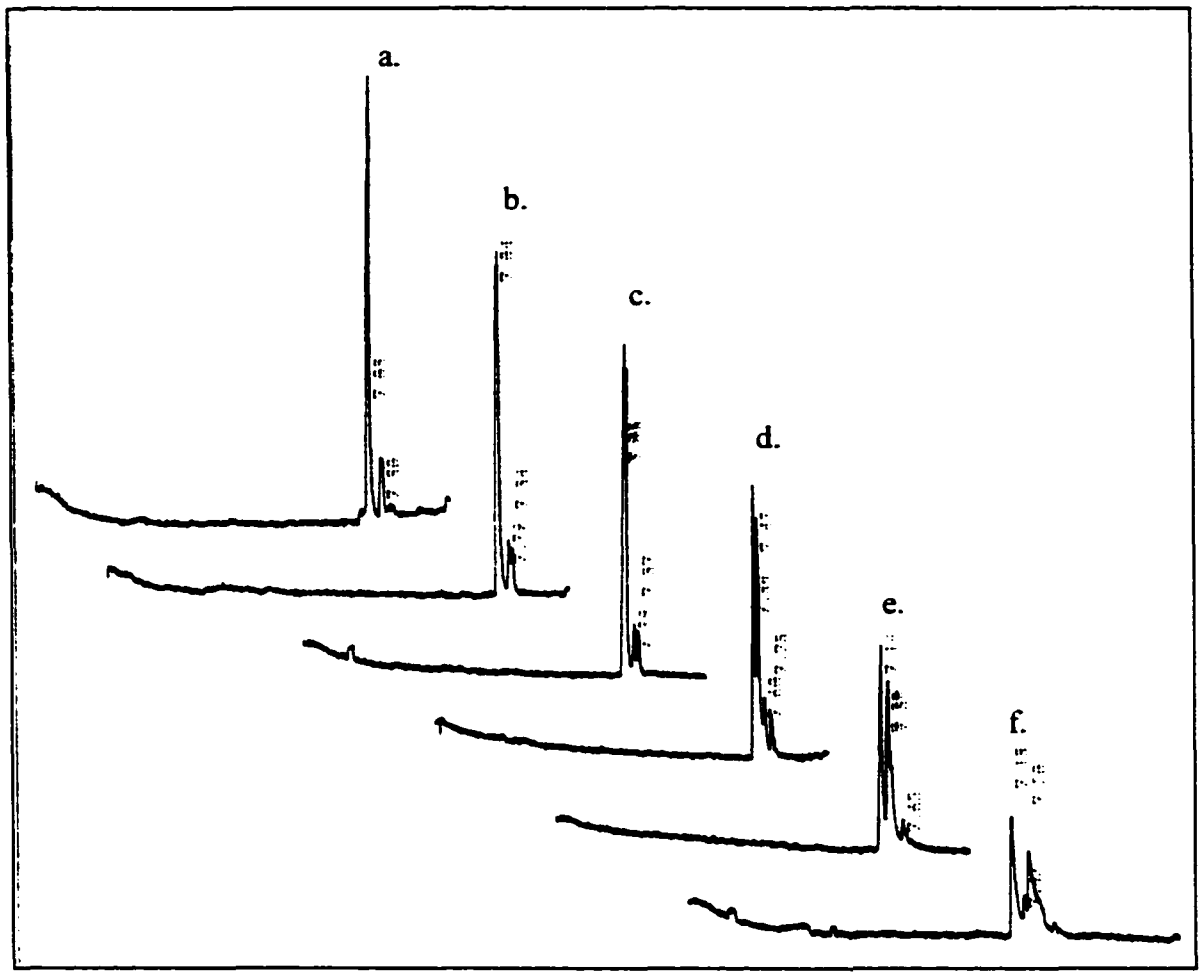

Figure 13-3. Separation of $[Ru(bpy)_2bppz]^{2+}$ in 50mM Tris buffer (pH 7.4) containing 0.1mMDNA and (a) 300mM (b) 250mM (c) 200mM (d) 150mM (e) 100mM (f) 50mM NaCl.

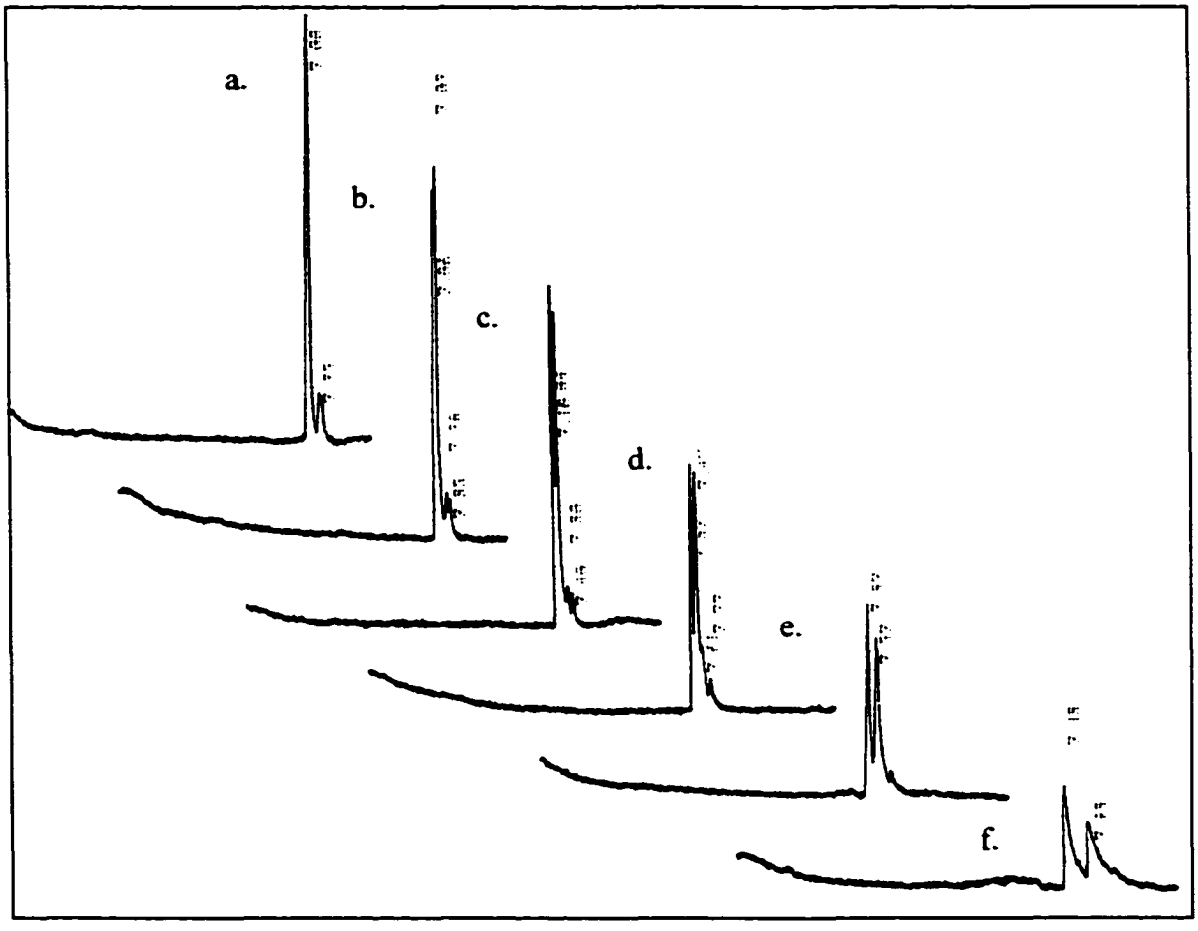

Figure 13-4. Separation of $[Ru(bpy)_2 mbppz]^{2+}$ in 50mM Tris buffer (pH 7.4) containing 0.1mMDNA and (a) 300mM (b) 250mM (c) 200mM (d) 150mM (e) 100mM (f) 50mM NaCl.

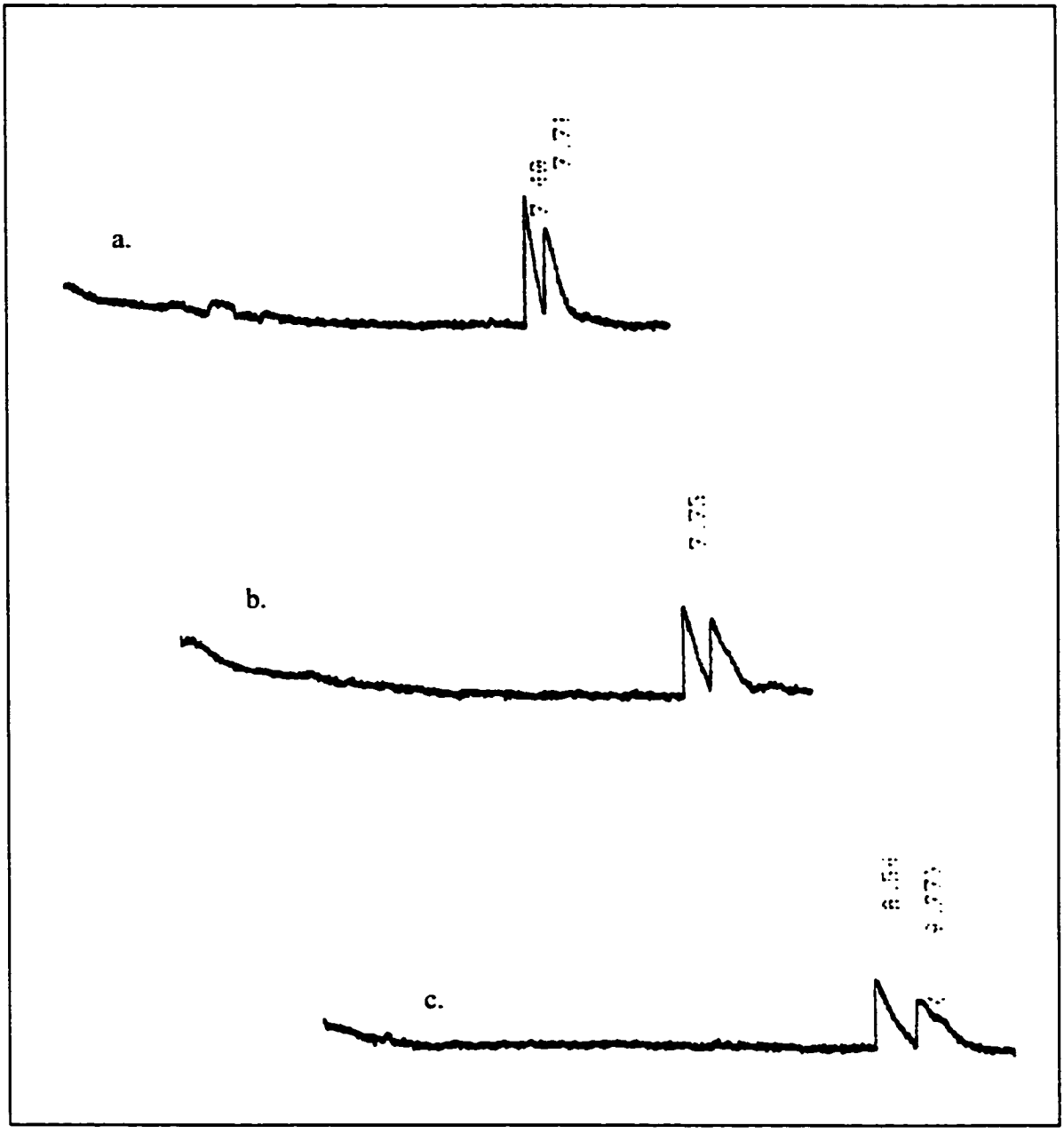

Figure 13-1. Separation of $[Ru(bpy)_2bzp]^{2+}$ in 50mM Tris buffer (pH 7.4) containing 0.1mMDNA and (a) 300mM (b) 250mM (c) 200mM NaCl.

4.2.4. Assessment of different types of salt

The effect of different types of salt was evaluated as well. Table 2 shows the buffer compositions which achieve the same enantioseparation of ppz. The divalent salts exhibit a much greater shielding effect compared to monovalent salts. The advantage of using divalent salts is that the relatively low concentration of salt does not dramatically increase the overall buffer ionic strength. Joule heating is not a problem in this case. Thus, higher voltage can be applied and the migration time is reduced by about 50%.

Table 2. Buffer compositions for $Ru[(bpy)_2ppz]^{2+}$ enantioseparation

DNA	Added Salt	Tris-HCl buffer
0.1mM	200mM NaCl	50mM
0.1mM	200mM KCl	50mM
0.2mM	20mM $MgCl_2$	50mM
0.3mM	20mM $CaCl_2$	50mM

4.3. Stereoselectivity and relative binding constants

Figure 14 illustrates the optimized enantioseparation of each individual ruthenium complex. The enantiomeric elution order is established by spiking experiments. According to the separation mechanism, the longer migration time indicates stronger DNA association. The enantiomeric elution orders determined here confirm the previous spectroscopic studies on binding preferences. For ppz, bppz and mbppz, the elution order is lambda after delta showing a preferential binding by the lambda isomer. In the case of bzp and ippz, a reversed enantiomeric order of migration is observed which indicates that their binding to DNA favors the delta isomer.

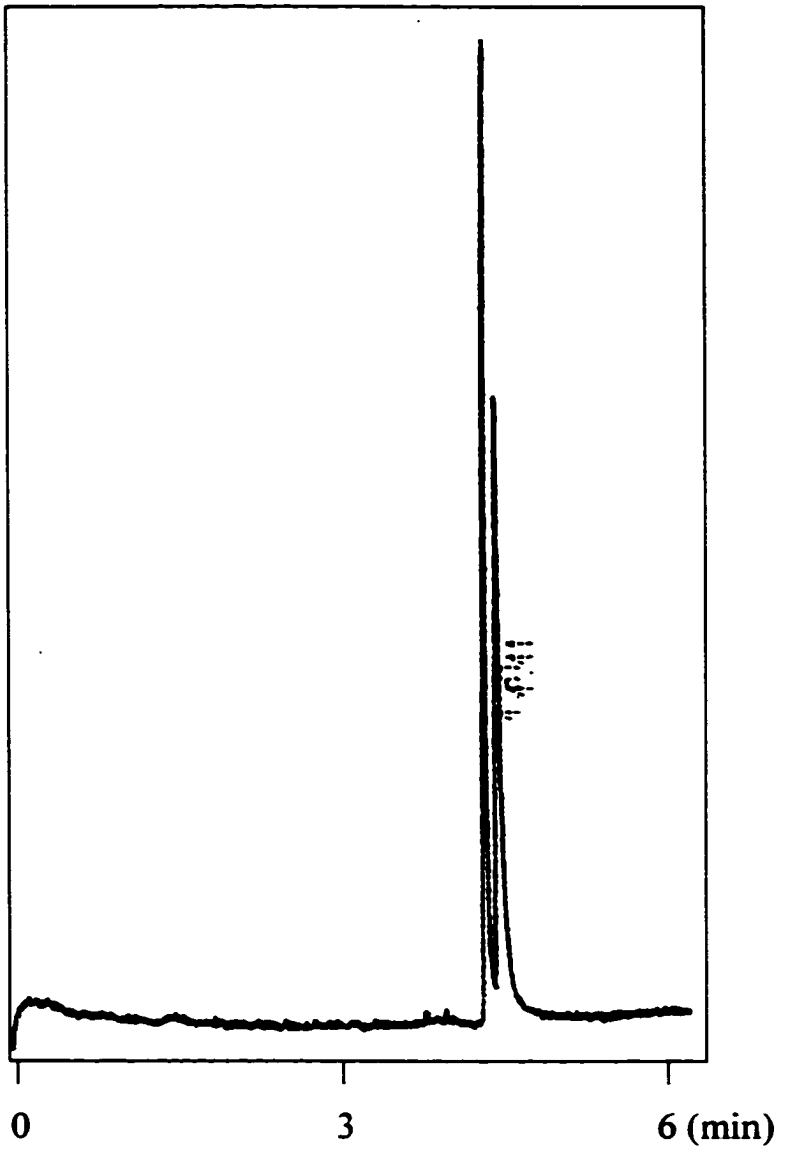

Figure 14-1. Enantioseparation of $[Ru(bpy)_2ppz]^{2+}$ in 50mM Tris buffer (pH 7.4) containing 0.1mM DNA and 200mM NaCl.

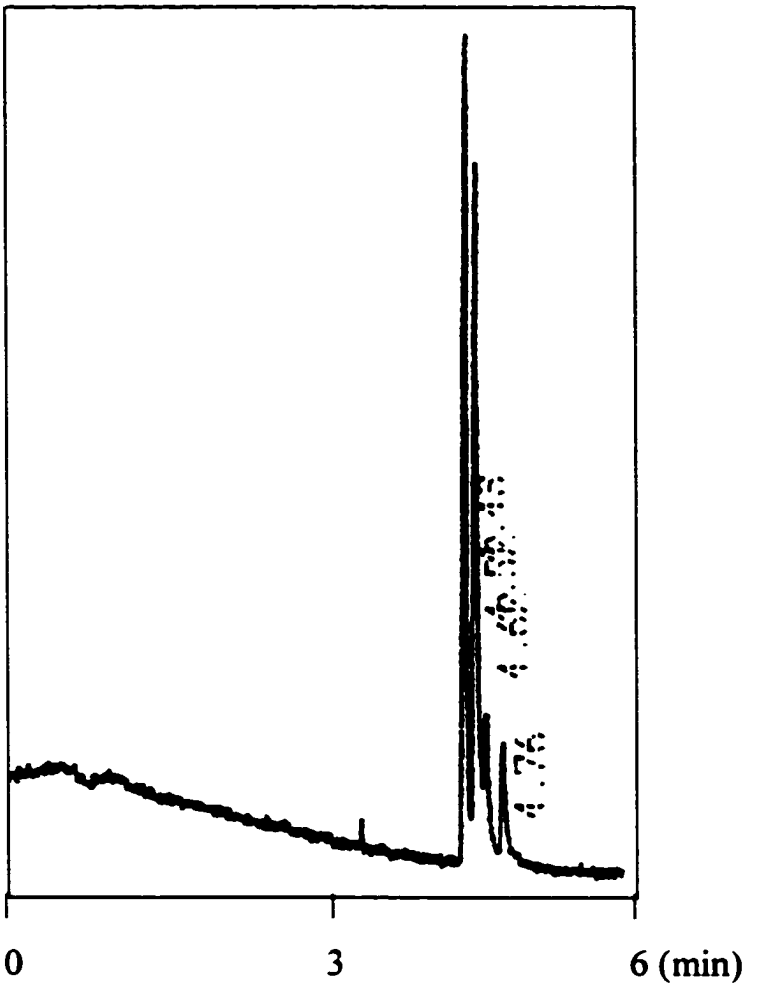

Figure 14-2. Enantioseparation of $[Ru(bpy)_2bppz]^{2+}$ in 50mM Tris buffer (pH 7.4) containing 0.2mM DNA and 200mM NaCl.

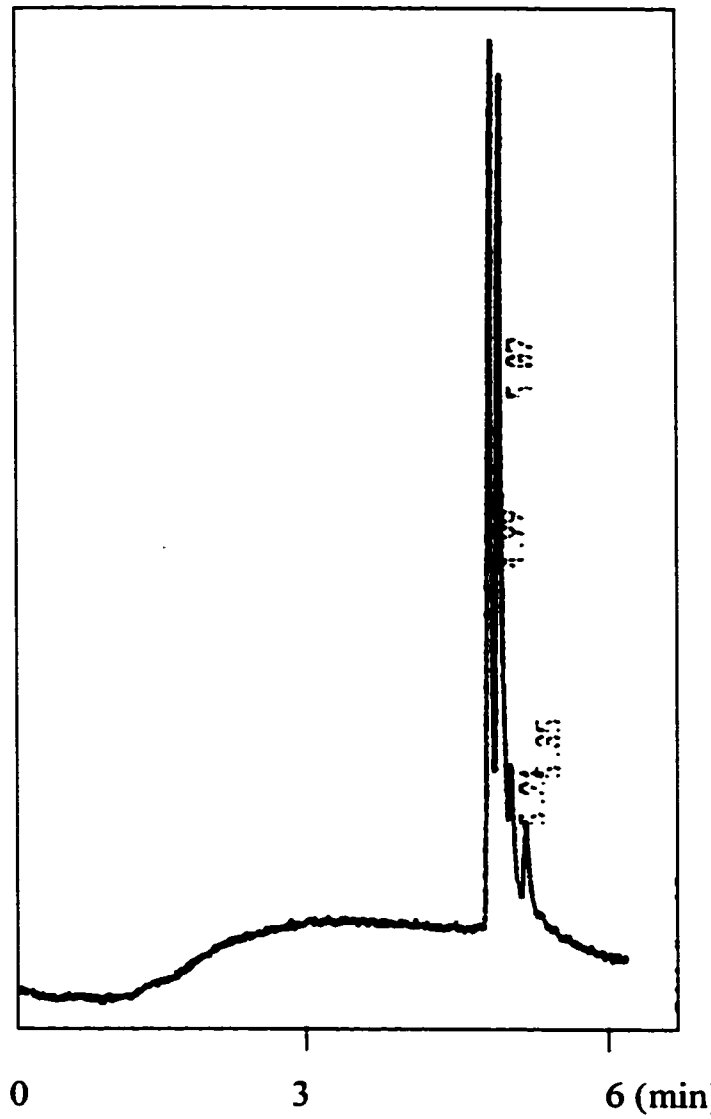

Figure 14-3. Enantioseparation of $[Ru(bpy)_2mbppz]^{2+}$ in 50mM Tris buffer (pH 7.4) containing 0.2mM DNA and 200mM NaCl.

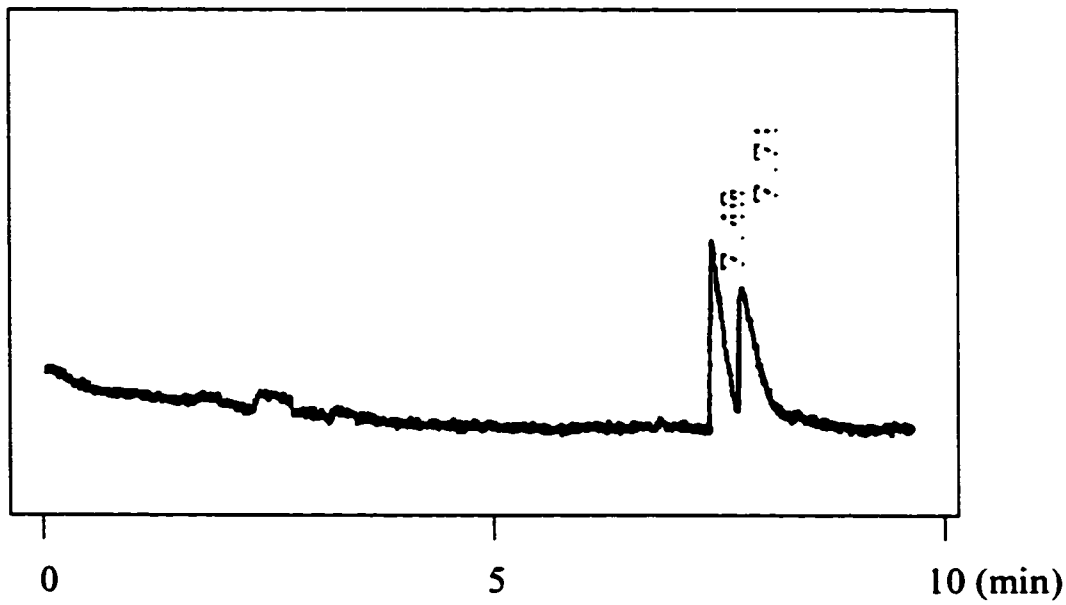

Figure 14-4. Enantioseparation of $[Ru(bpy)_2bzp]^{2+}$ in 50mM Tris buffer (pH 7.4) containing 0.1mM DNA and 300mM NaCl.

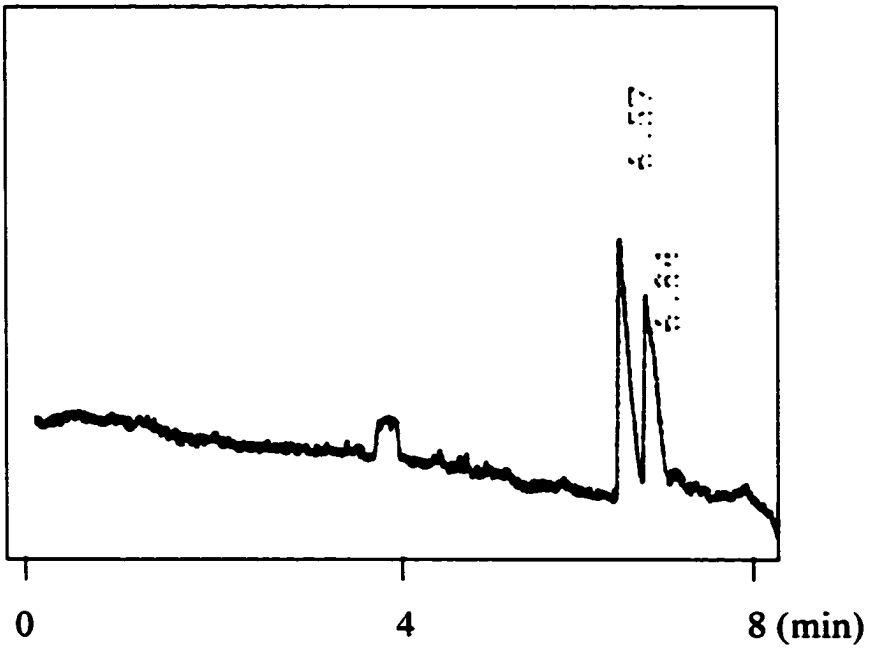

Figure 14-5. Enantioseparation of $[Ru(bpy)_2ippz]^{2+}$ in 50mM Tris buffer (pH 7.4) containing 0.1mM DNA and 300mM NaCl.

To obtain information on the relative binding strengths, an electropherogram was obtained by coinjecting five racemic compounds in the capillary containing 0.5mM DNA and 200mM NaCl (Figure 15). Enantiomeric separation of all of the ruthenium complexes is achieved in the same run. The last eluting pair of peaks (bzp) have the highest binding strength among the five. The ippz pairs is the second highest. The second peak of bppz slightly overlaps the first peak of mbpp, but they are still identifiable. It indicates mbppz has a slightly higher average binding strength than bppz. The delta ppz elutes first; its lambda peak elutes after the bppz and mbppz peaks.

As the migration time reflects relative binding strength, the migration time difference for the pair of enantiomers gives us the information on the degree of stereoselectivity. The greater breadth of ppz enantiomer peaks reflects the big difference in enantioselectivity. In contrast to ppz, ippz has relatively higher average binding strength, but lower degree in stereopreference.

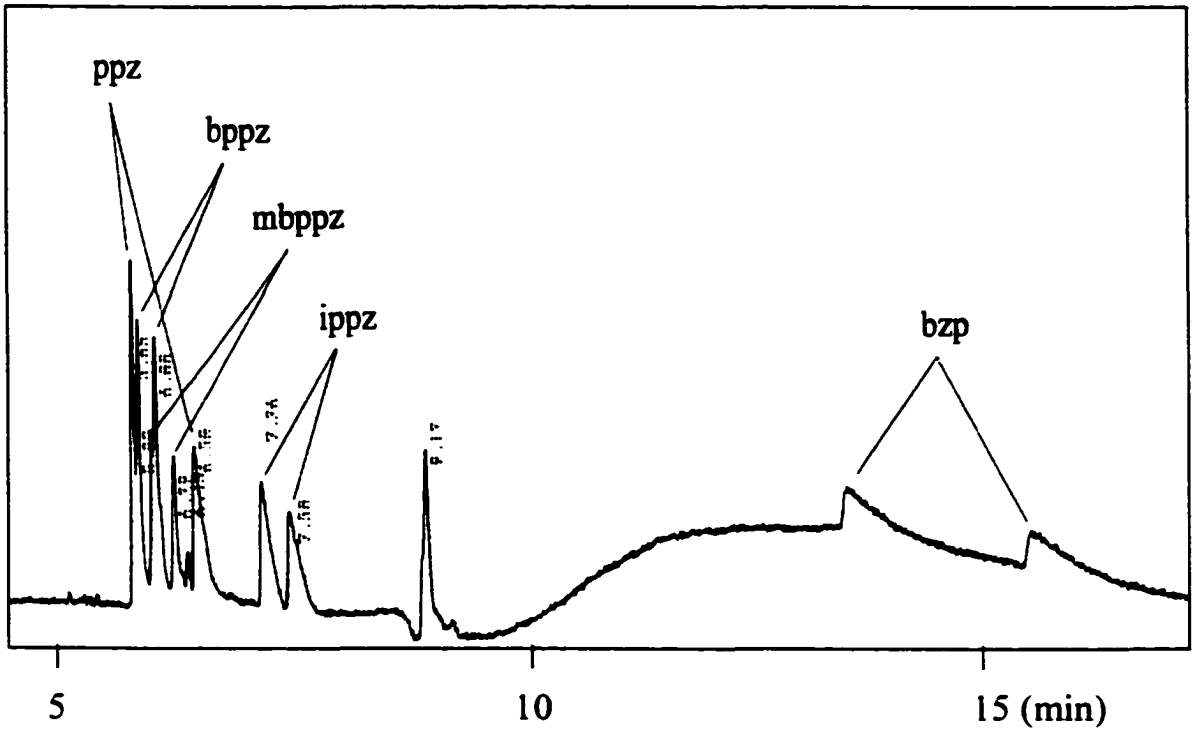

Figure 15. Enantioseparation of five racemic Ru(II) complexes in 50mM Tris buffer (pH 7.4) containing 0.5mM DNA and 200mM NaCl.

4.4. Determination of intrinsic binding constants by frontal analysis

The sample solution for each binding constant measurement was a series of solutions with varying concentrations of Ruthenium complex and fixed concentration of DNA in either 50mM Tris buffer or 50mM Tris buffer with 50mM NaCl. The DNA concentration should be sufficient to cover the low binding strength cases. Sample concentration was carefully chosen to facilitate the plateau height measurement and to achieve good linear regression for the Scatchard Plot and non-linear regression for Isotherm Plot. Assuming that the ruthenium complex-DNA binding is a reversible and kinetically rapid process, each mixture is equilibrated for 30min. A relatively long-time injection (60s) was applied in this study to obtain plateau peaks. After the sample solution was introduced hydrodynamically, the capillary ends were immersed in the running buffer, negative voltage was applied on the detector side and the electrophoresis was carried out. It has been described above that DNA has approximately zero apparent mobility during the electrophoresis. The charge and size of DNA are not significantly altered by the presence of bound ruthenium complex which means that both DNA and bound DNA remain in the initial

sample zone. Only the unbound ruthenium complex migrates apart from the sample zone and a plateau is formed before reaching the detector.

Table 3 summarizes the binding constant measurements. All binding constants are of order 10^4~10^5 which are reasonable for a weak/partial intercalative mode of binding. The CE results are similar to those obtained by fluorescence titration (Table 4). The order of increasing binding strength is bppz, mbppz, ppz, ippz and bzp, the same as their elution order. Due to the limited availability of pure enantiomers, only one full set (racemic and enantiomers) of K_b measurements was produced, for bppz. The higher value of K_b for Λ-bppz is in accord with its enantiomeric elution order assignment. In addition, the lower K_b value measured in case of buffer with salt clearly shows the salt-dependence of binding constant.

Figure 16-1. Scatchard and Isotherm Plots for bzp

Sample concentrations:

Racemic $[Ru(bpy)_2bzp]^{2+}$: 17.6, 19.8, 22.0, 24.2, 26.4, 28.6, and 30.8μM

DNA: 75μM base pair

Buffer: 50mM pH7.4 Tris-HCl

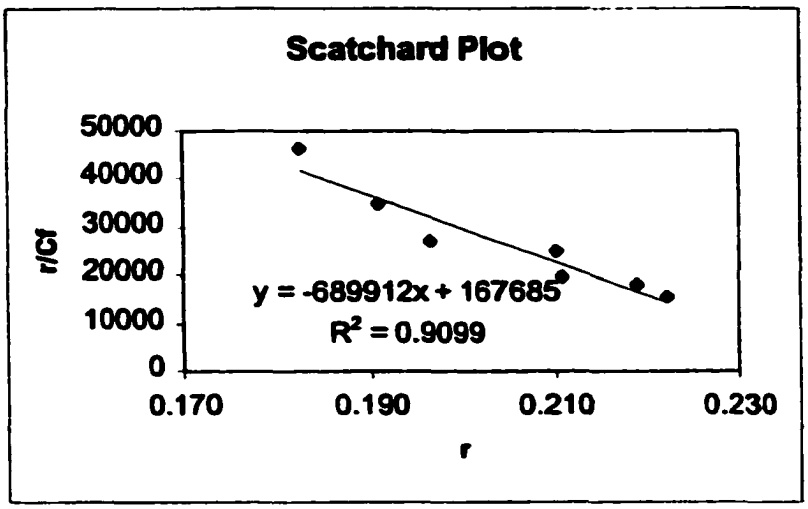

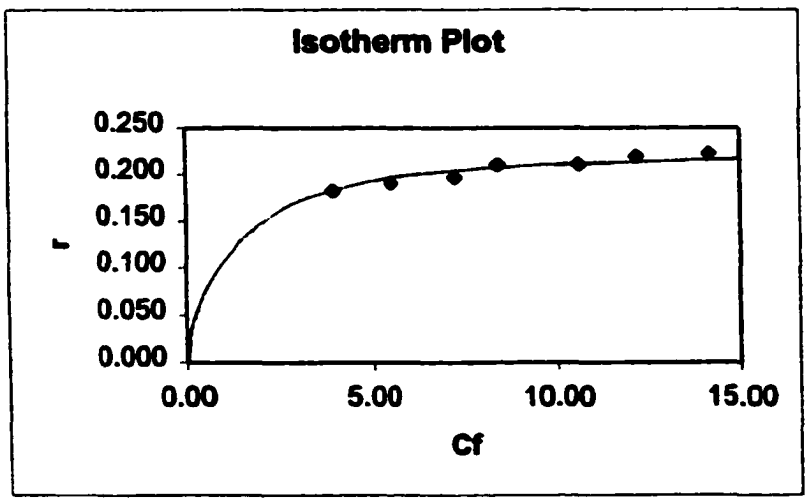

Figure 16-2. Scatchard and Isotherm Plots for bzp

Sample concentrations:

Racemic $[Ru(bpy)_2bzp]^{2+}$:

15.4, 17.6, 19.8, 22.0, 24.2, 26.4, 28.6 and 30.8μM

DNA: 75μM base pair

Buffer: 50mM pH7.4 Tris-HCl + 50mM NaCl

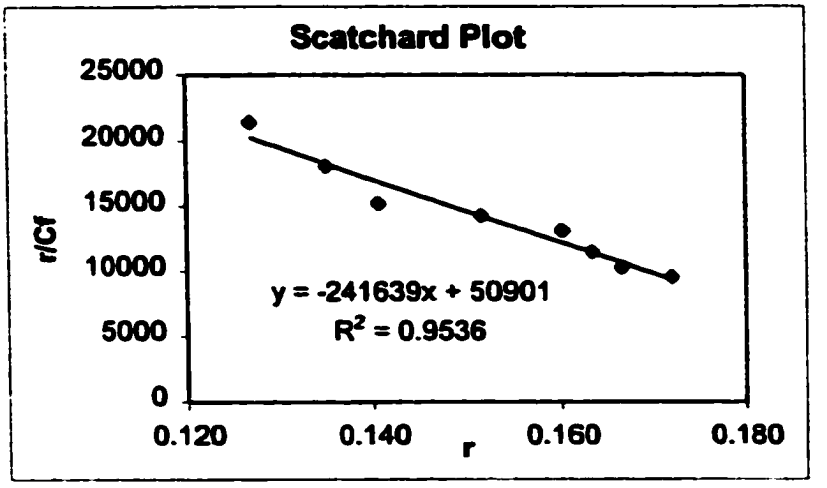

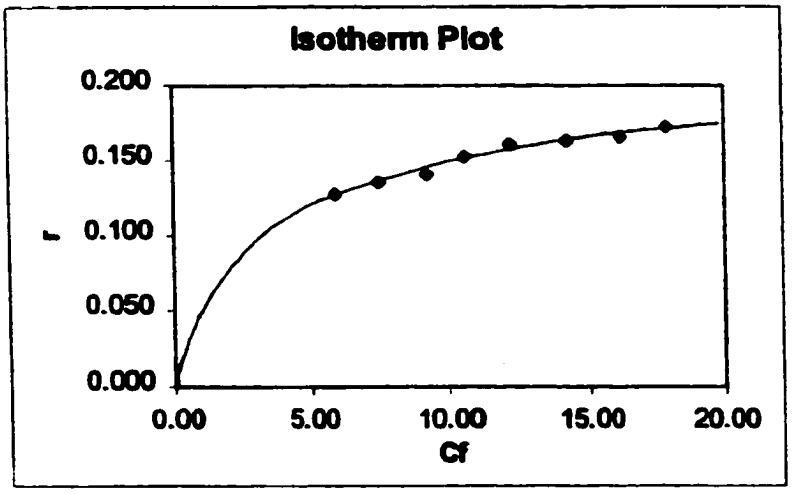

Figure 16-3. Scatchard and Isotherm Plots for ippz

Sample concentrations:

Racemic $[Ru(bpy)_2ippz]^{2+}$:

11.5, 14.38, 17.25, 20.12, 23.0, 25.87, 28.75, 31.62,

34.5 and 37.38μM

DNA: 75μM base pair

Buffer: 50mM pH7.4 Tris-HCl

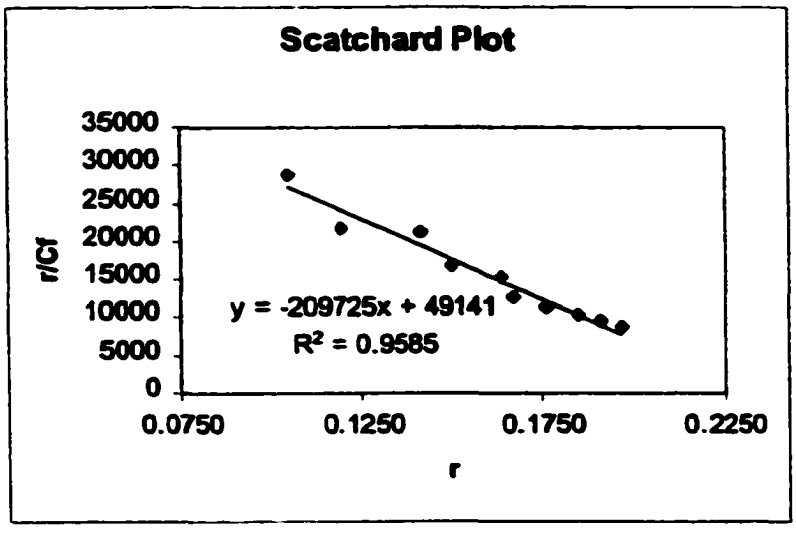

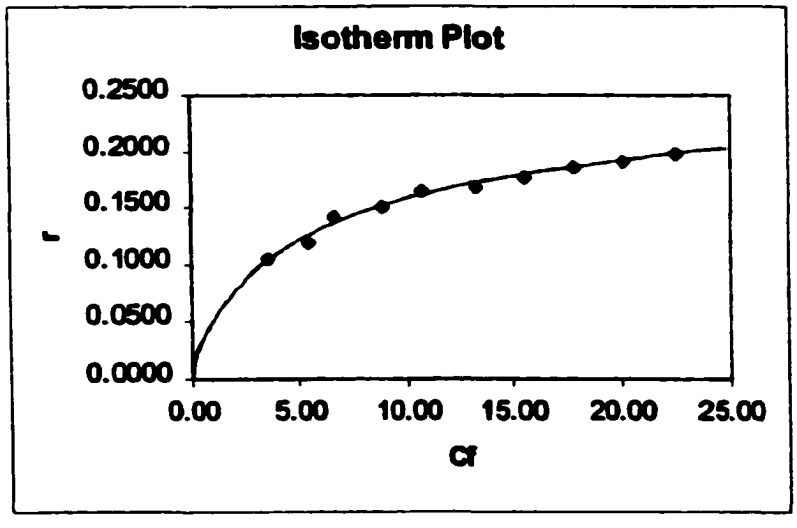

Figure 16-4. Scatchard and Isotherm Plots for ippz

Sample concentrations:

Racemic $[Ru(bpy)_2ippz]^{2+}$:

11.5, 14.38, 17.25, 20.12, 23.0, 25.87, 28.75, 31.62, and 34.5μM

DNA: 75μM base pair

Buffer: 50mM pH7.4 Tris-HCl + 50mM NaCl

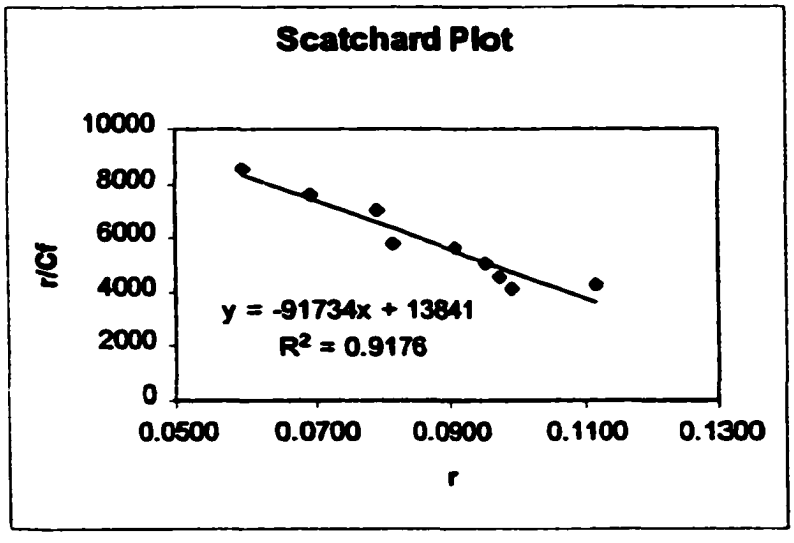

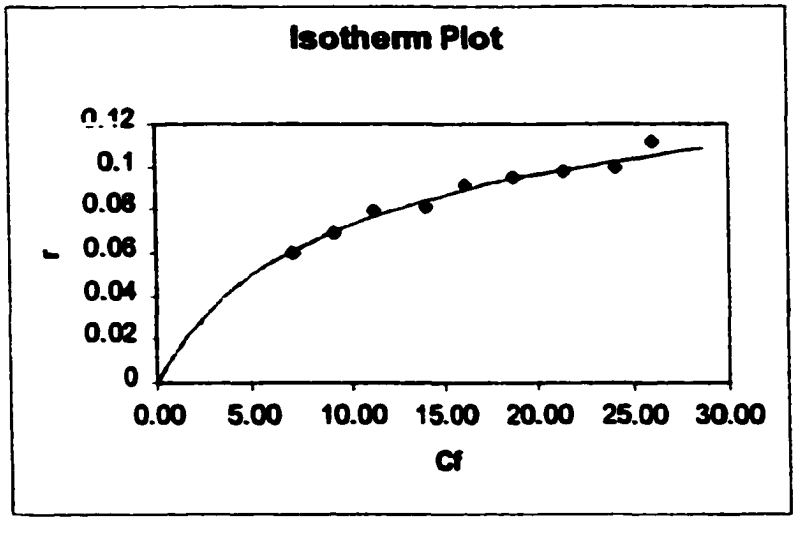

Figure 16-5. Scatchard and Isotherm Plots for ppz

Sample concentrations:

Racemic $[Ru(bpy)_2ppz]^{2+}$:

13.65, 20.48, 27.3, 34.12, 40.95, 47.78, 54.6, 61.42 and 68.25μM

DNA: 75μM base pair

Buffer: 50mM pH7.4 Tris-HCl

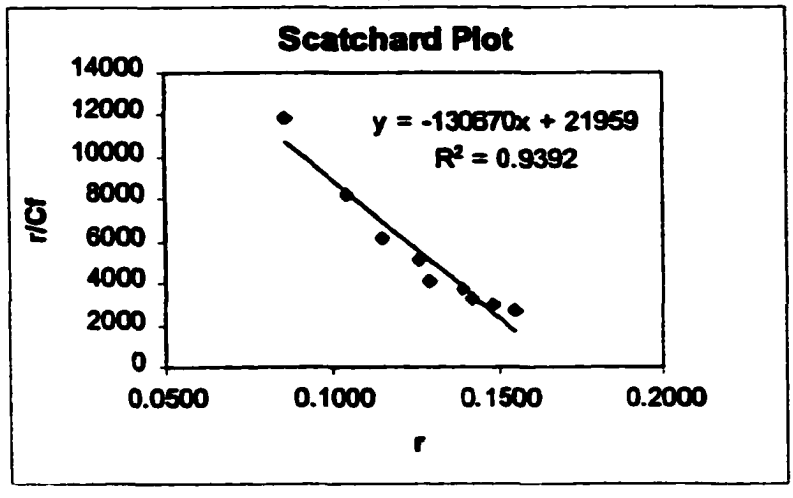

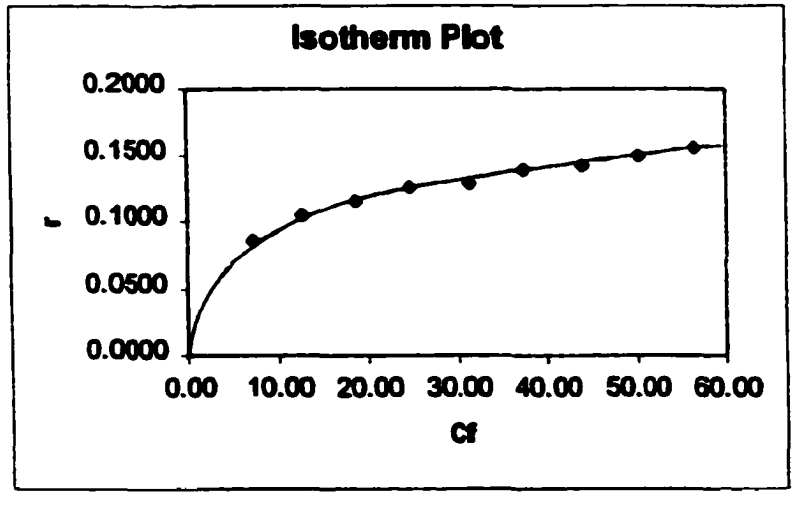

Figure 16-6. Scatchard and Isotherm Plots for ppz

Sample concentrations:

Racemic $[Ru(bpy)_2ppz]^{2+}$:

13.65, 20.48, 27.3, 34.12, 40.95 and 47.78μM

DNA: 75μM base pair

Buffer: 50mM pH7.4 Tris-HCl + 50mM NaCl

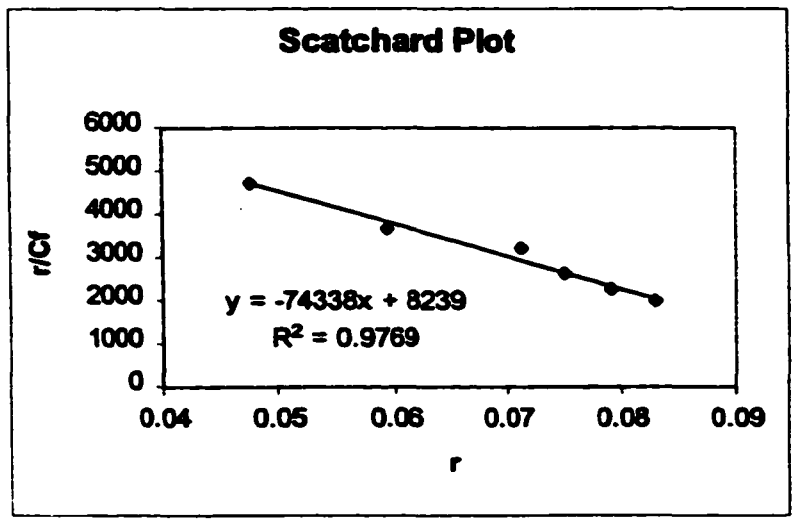

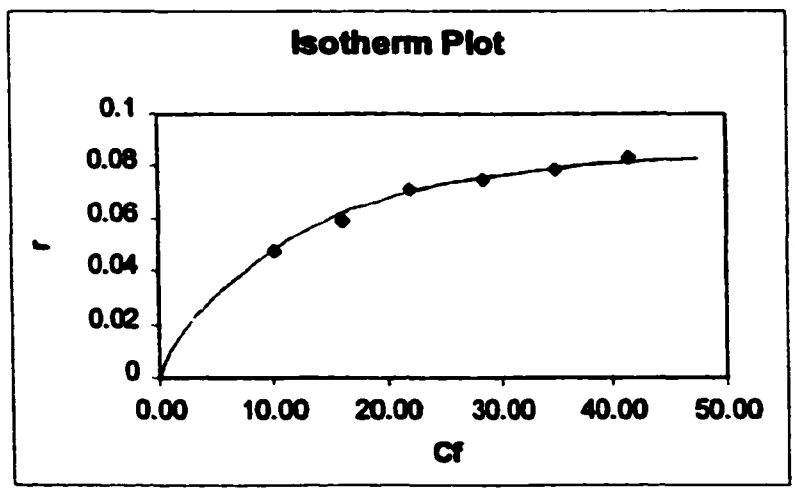

Figure 16-7. Scatchard and Isotherm Plots for mbppz

Sample concentrations:

Racemic $[Ru(bpy)_2 mbppz]^{2+}$:

13.6, 20.4, 27.2, 34.0, 40.8, 47.6, 54.4 and 61.2μM

DNA: 150μM base pair

Buffer: 50mM pH7.4 Tris-HCl

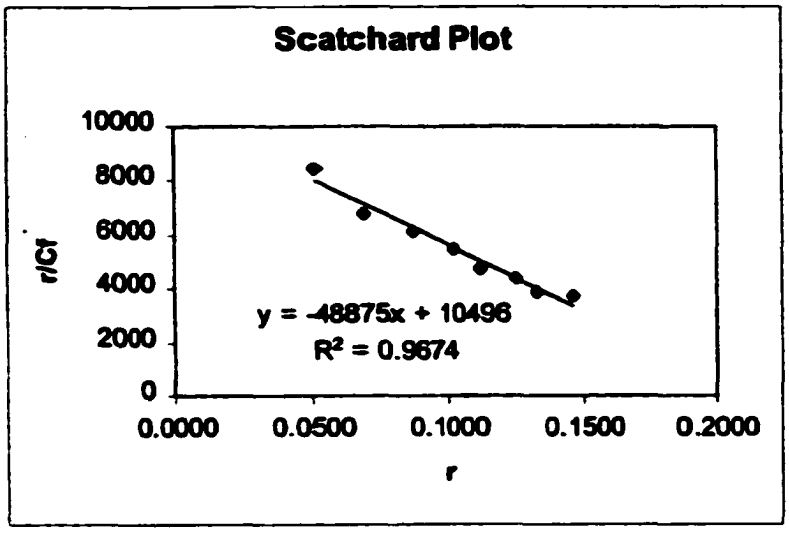

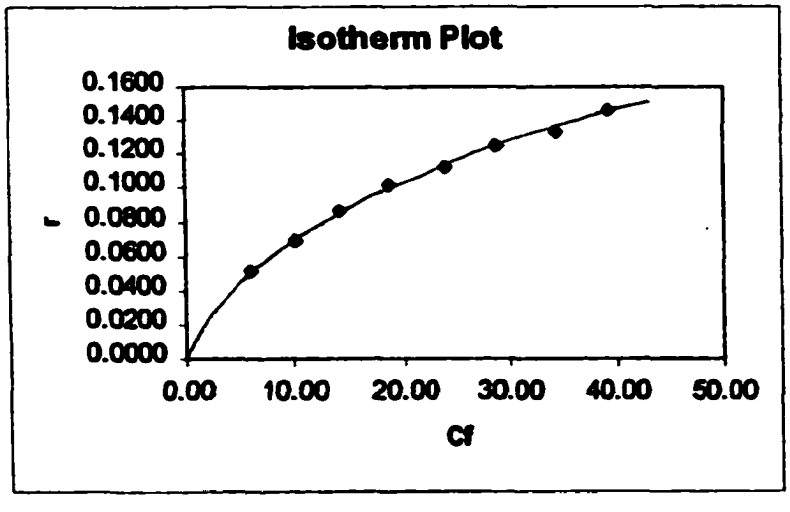

Figure 16-8. Scatchard and Isotherm Plots for mbppz

Sample concentrations:

Racemic $[Ru(bpy)_2 mbppz]^{2+}$:

11.9, 17.85, 23.8, 35.7, 41.65, 47.6 and 53.55μM

DNA: 300μM base pair

Buffer: 50mM pH7.4 Tris-HCl + 50mM NaCl

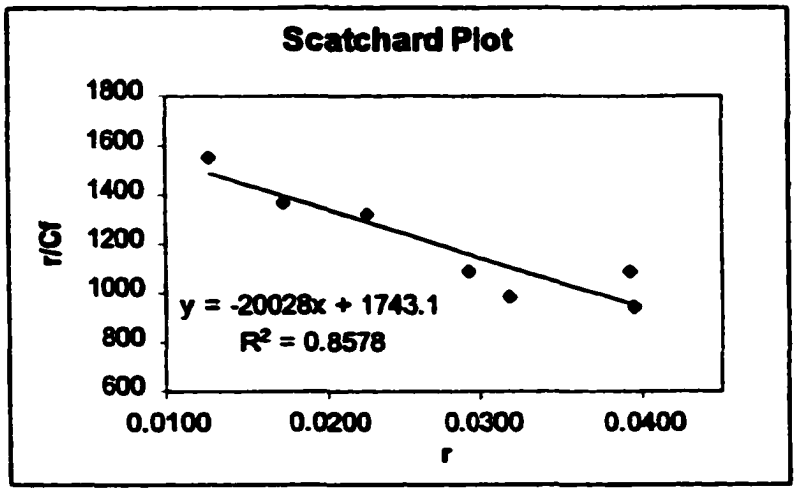

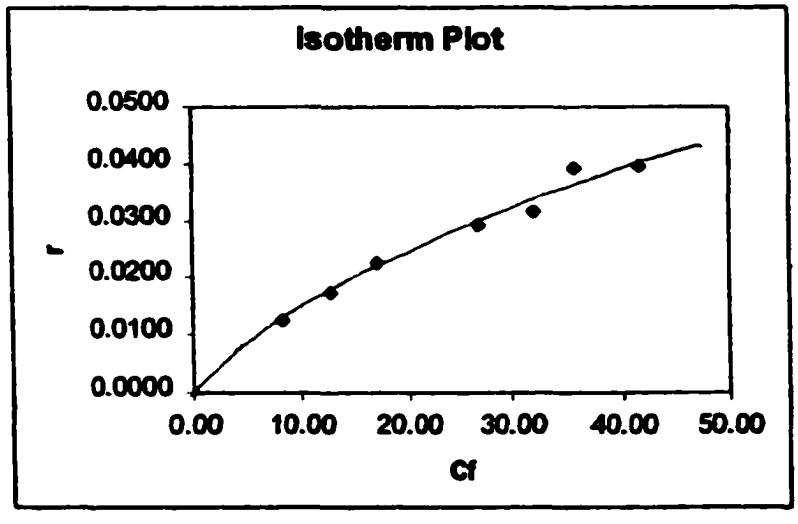

Figure 16-9. Scatchard and Isotherm Plots for bppz

Sample concentrations:

Racemic $[Ru(bpy)_2 bppz]^{2+}$:

13.0, 26.0, 39.0, 52.0, 65.0 and 78.0μM

DNA: 150μM base pair

Buffer: 50mM pH7.4 Tris-HCl

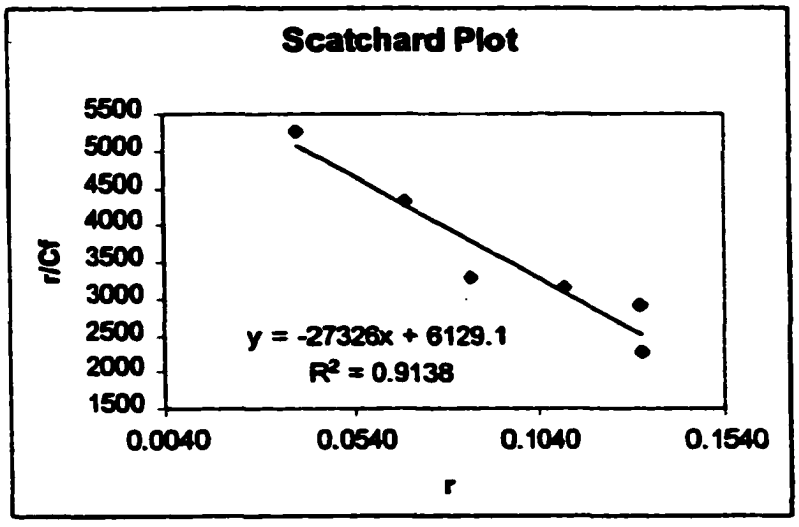

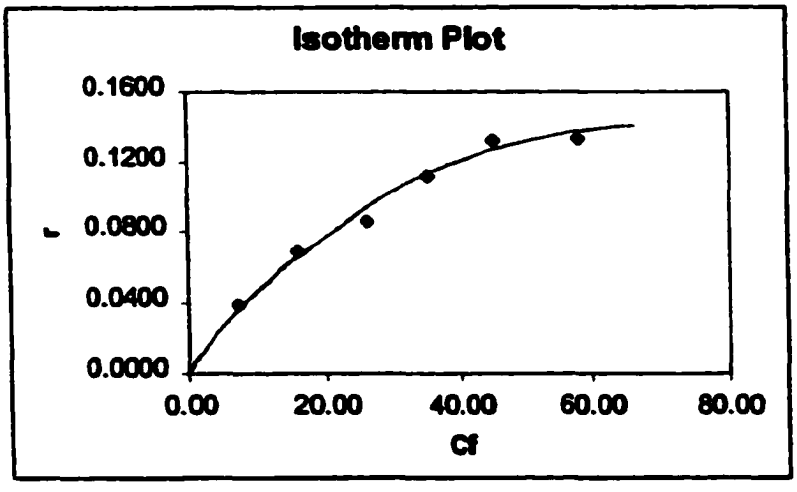

Figure 16-10. Scatchard and Isotherm Plots for bppz

Sample concentrations:

Racemic $[Ru(bpy)_2 bppz]^{2+}$:

13.0, 19.5, 26.0, 39.0, 45.5, 52.0, 58.5 and 65.0μM

DNA: 440μM base pair

Buffer: 50mM pH7.4 Tris-HCl + 50mM NaCl

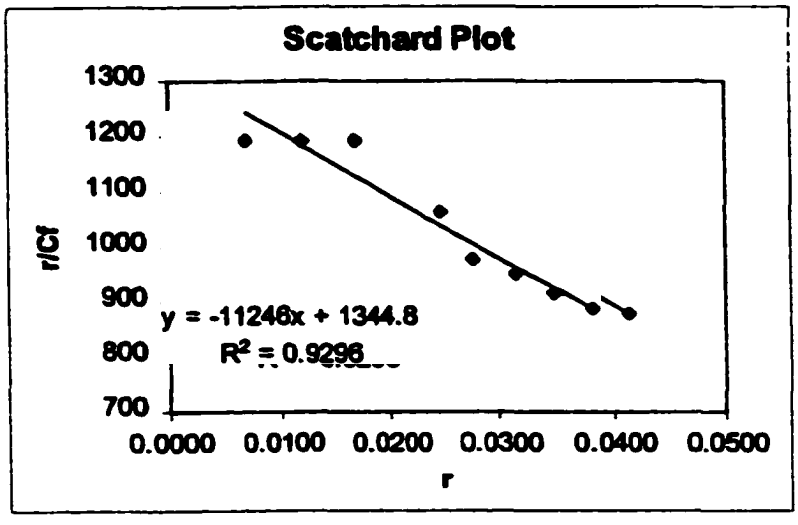

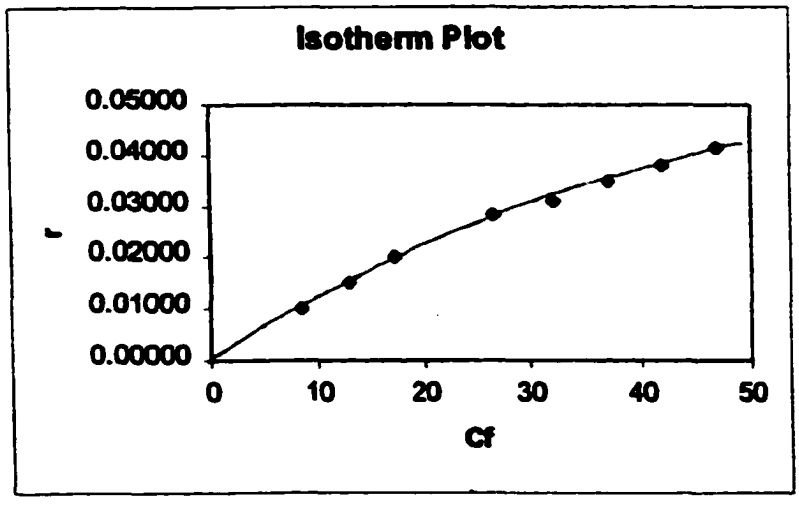

Figure 16-11. Scatchard and Isotherm Plots for Δbppz

Sample concentrations:

Δ- $[Ru(bpy)_2 bppz]^{2+}$:

13.3, 26.6, 39.9, 53.2, 66.5 and 79.8μM

DNA: 150μM base pair

Buffer: 50mM pH7.4 Tris-HCl

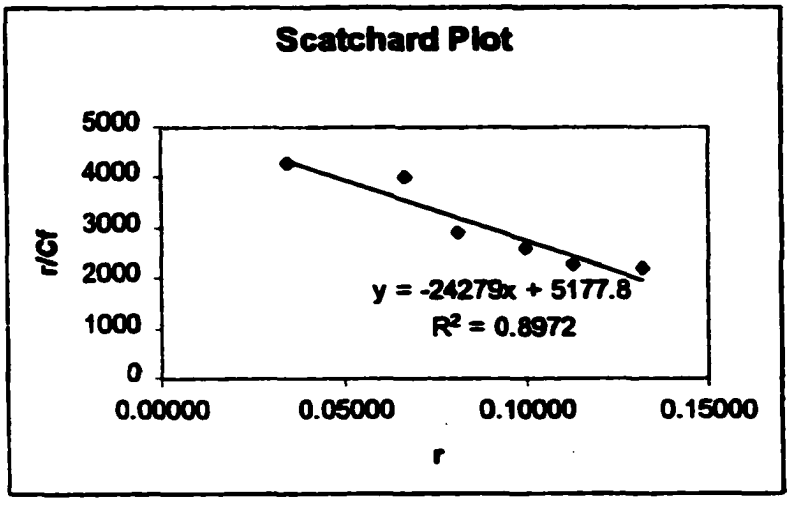

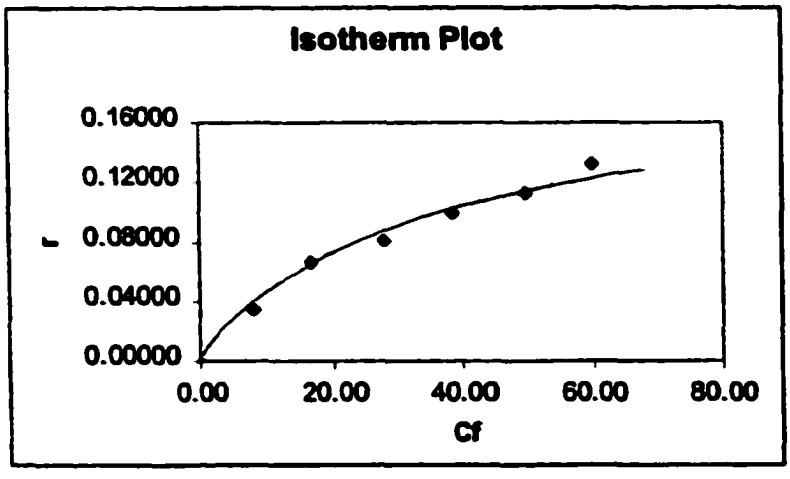

Figure 16-12. Scatchard and Isotherm Plots for Δbppz

Sample concentrations:

Δ- $[Ru(bpy)_2 bppz]^{2+}$:

13.3, 19.95, 39.9, 46.55, 53.2, 59.85 and 66.5μM

DNA: 440μM base pair

Buffer: 50mM pH7.4 Tris-HCl + 50mM NaCl

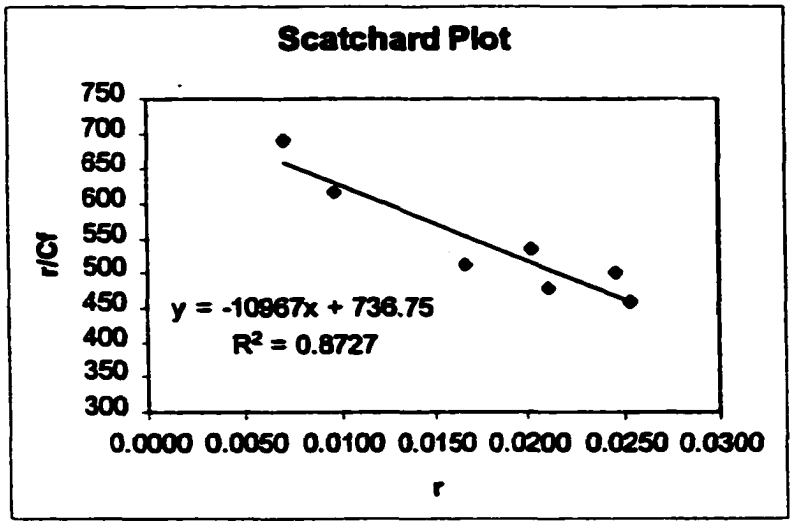

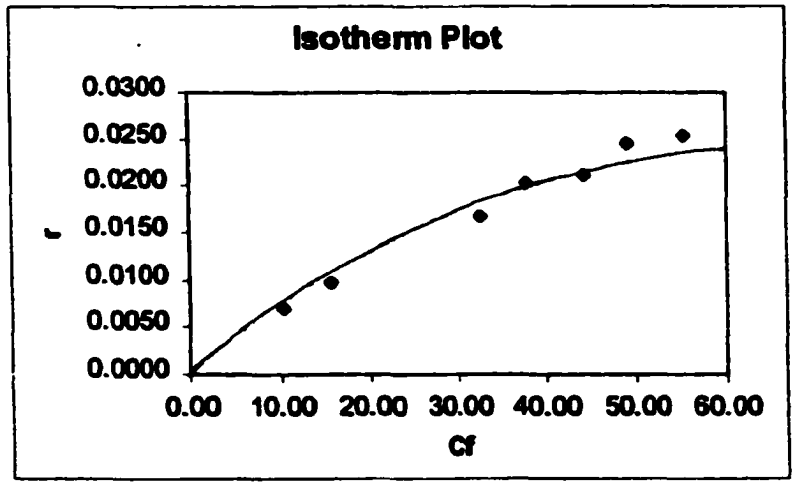

Figure 16-13. Scatchard and Isotherm Plots for Λbppz

Sample concentrations:

Λ- $[Ru(bpy)_2 bppz]^{2+}$:

13.3, 26.6, 39.9, 53.2, 66.5 and 79.8μM

DNA: 150μM base pair

Buffer: 50mM pH7.4 Tris-HCl

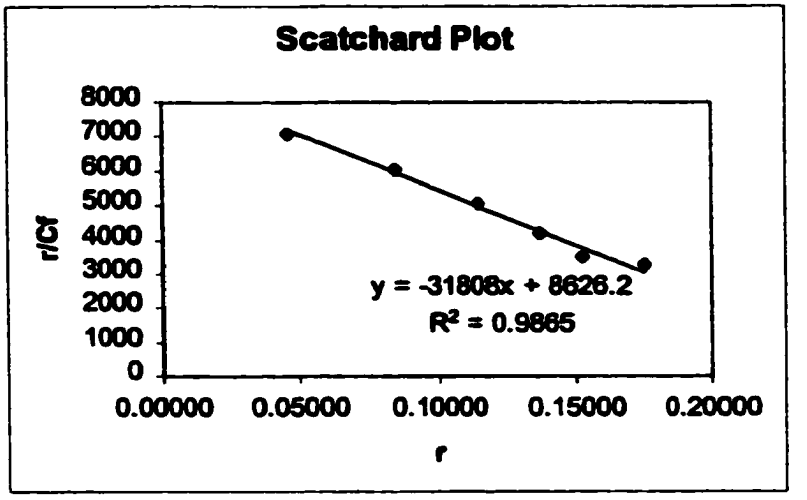

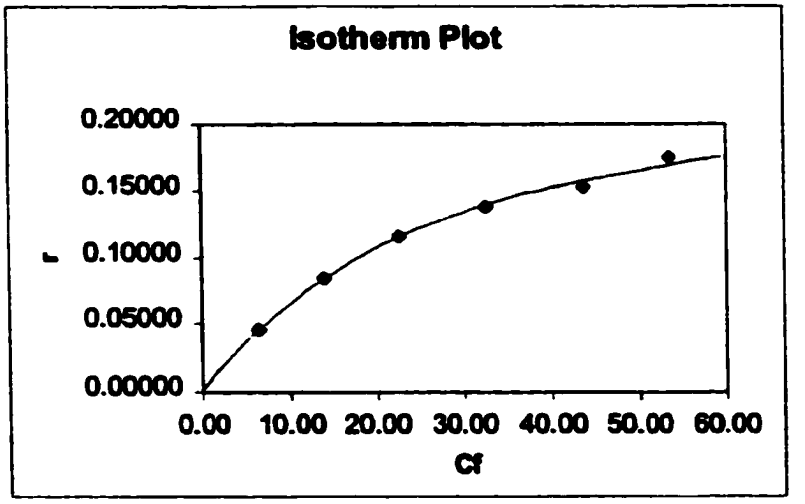

Figure 16-14. Scatchard and Isotherm Plots for Λbppz

Sample concentrations:

Λ- $[Ru(bpy)_2 bppz]^{2+}$:

13.3, 19.95, 26.6, 33.25, 39.9, 46.55, 53.2, 59.85 and 66.5μM

DNA: 440μM base pair

Buffer: 50mM pH7.4 Tris-HCl + 50mM NaCl

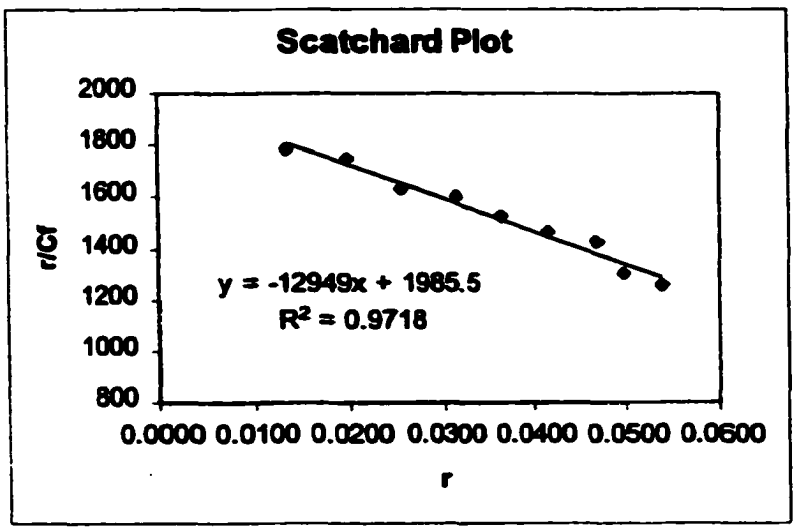

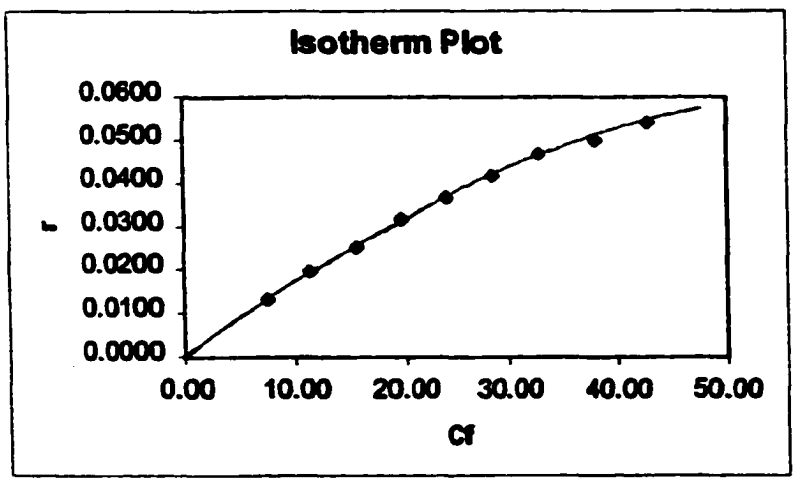

Table 3. K_b and n values measured by Frontal Analysis

	50mMTris - 0NaCl		50mMTris - 50mMNaCl	
	K_b	n	K_b	n
racemic bzp	6.9×10^5	0.20	2.4×10^5	0.21
racemic ippz	2.1×10^5	0.23	9.2×10^4	0.15
racemic ppz	1.3×10^5	0.17	7.4×10^4	0.11
racemic mbppz	4.9×10^4	0.22	2.0×10^4	0.09
racemic bppz	2.7×10^4	0.22	1.1×10^4	0.12
Δ-bppz	2.4×10^4	0.21	1.1×10^4	0.07
Λ-bppz	3.2×10^4	0.27	1.3×10^4	0.15

Table 4. K_b values measured by Fluorescence Titration

(reprinted from reference [71] p.111)

Complex	5mMTris -10mMNaCl	5mMTris-50mMNaCl
Δ-ppz	2.1×10^4	2.8×10^3
Λ-ppz	6.3×10^4	1.1×10^4
Δ-bppz	9.3×10^3	2.4×10^3
Λ-bppz	1.4×10^4	2.4×10^3
Δ-mbppz	2.1×10^4	2.1×10^3
Λ-mbppz	2.5×10^4	3.1×10^3
Δ-bzp	2.2×10^5	1.1×10^5
Λ-bzp	1.3×10^5	7.6×10^4
Δ-ippz	1.6×10^5	3.4×10^4
Λ-ippz	1.0×10^5	2.8×10^4

4.5. Minor groove competitive binding study

An incoming molecule has to have access to the base pairs via a DNA groove. The determination of the DNA binding geometry is an important aspect of the study of the interactions of metallointercalators with nucleic acids. While it has been unambiguously demonstrated that metallointercalators based on the 9, 10-phenanthrenequinone diimine (phi) ligand intercalate from the major groove [42], the DNA binding location of Ru(II) polypyridyls is not yet firmly established. On the basis of NMR evidence, Dupureur and Barton have shown that delta $[Ru(phen)_2dppz]^{2+}$ (dppz = dipyridophenazine) intercalates from the major groove [46,60]. However, on the basis of a similarity of the DNA binding geometry of delta$[Ru(phen)_2dppz]^{2+}$ with actinomycin D, Lincoln et al. have proposed that the metal complex may intercalate from the minor groove [41].

In order to assess the relative importance of minor versus major groove binding in the $[Ru(bpy)_2L]^{2+}$/DNA system, we carried out a CE investigation with both B-DNA and distamycin A in the capillary buffer medium. Distamycin A is a strong AT selective minor groove binder with a large binding constant for B-DNA (Figure 17). It is believed to associate with the DNA molecule by surface binding which means its chain structure fits and winds in the DNA grooves. Its presence in the capillary medium

would be expected to result in the release of both Ru(II) enantiomers if they are both bound in the minor groove.

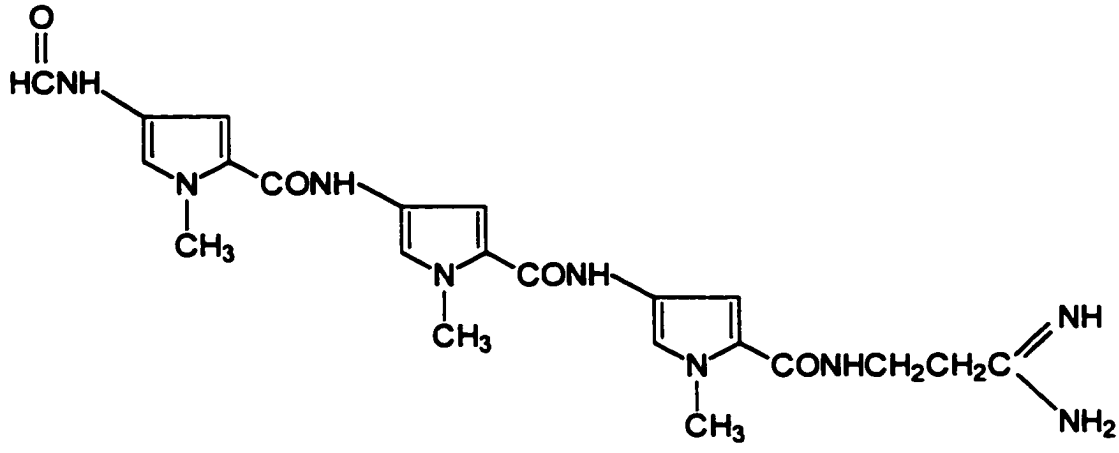

Figure 17. Molecular structure of distamycin A.

The competitive study was conducted on ppz, ippz and bzp, respectively, starting with their optimized enantioseparation conditions (Figures 18-20). In the presence of increasing concentration of distamycin A in the buffer medium, a progressive loss of enantiomeric discrimination

is observed. This observation clearly indicates that the binding for the Ru(II) complexes studied involves association from the minor groove.

According to a reported study [42], distamycin A saturates the poly d(AT) minor groove at an approximate molar ratio of 1 distamycin / 5 bp. Using this ratio, a difference in enantioseparation to addition of distamycin A can be calculated. For ppz (Figure 18), enantiomeric stereoselectivity disappears right after the minor groove is completely blocked by distamycin A suggesting the binding mode characterized by Λ ppz preference occurs primarily in the minor groove. The conclusion seems supportive to the high degree of stereoselectivity of ppz since the steric effect is expected to be greater at the narrower minor groove.

In the case of ippz, bzp, bppz and mbppz (Figures 19-22), enantioseparation is not much affected even when the minor groove is saturated with distamycin A, indicating that the binding mode characterized by Δ preference occurs in both minor and major grooves.

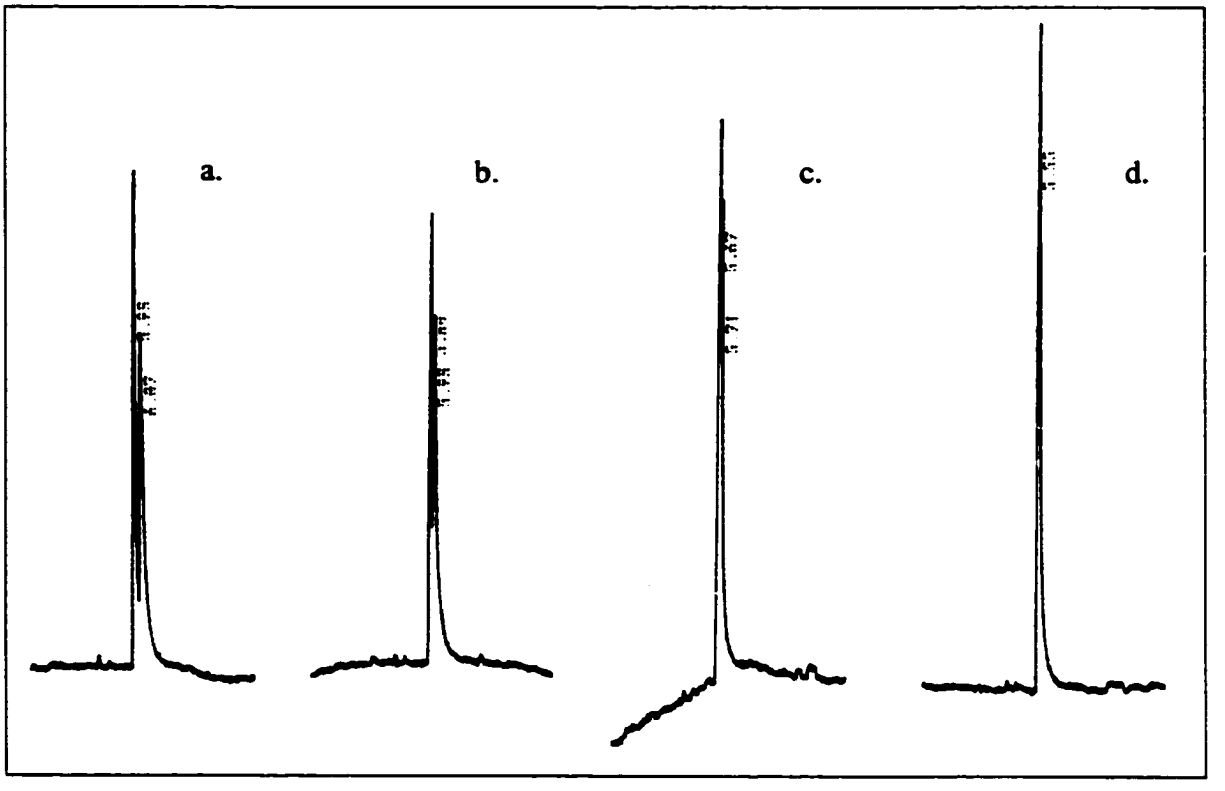

Figure 18. Enantioseparation of $[Ru(bpy)_2ppz]^{2+}$ in 50mM Tris buffer (pH 7.4) with 0.1mM DNA, 200mM NaCl and (a) 0μM (b) 5μM (c) 10μM (d) 15μM addition of distamycin A.

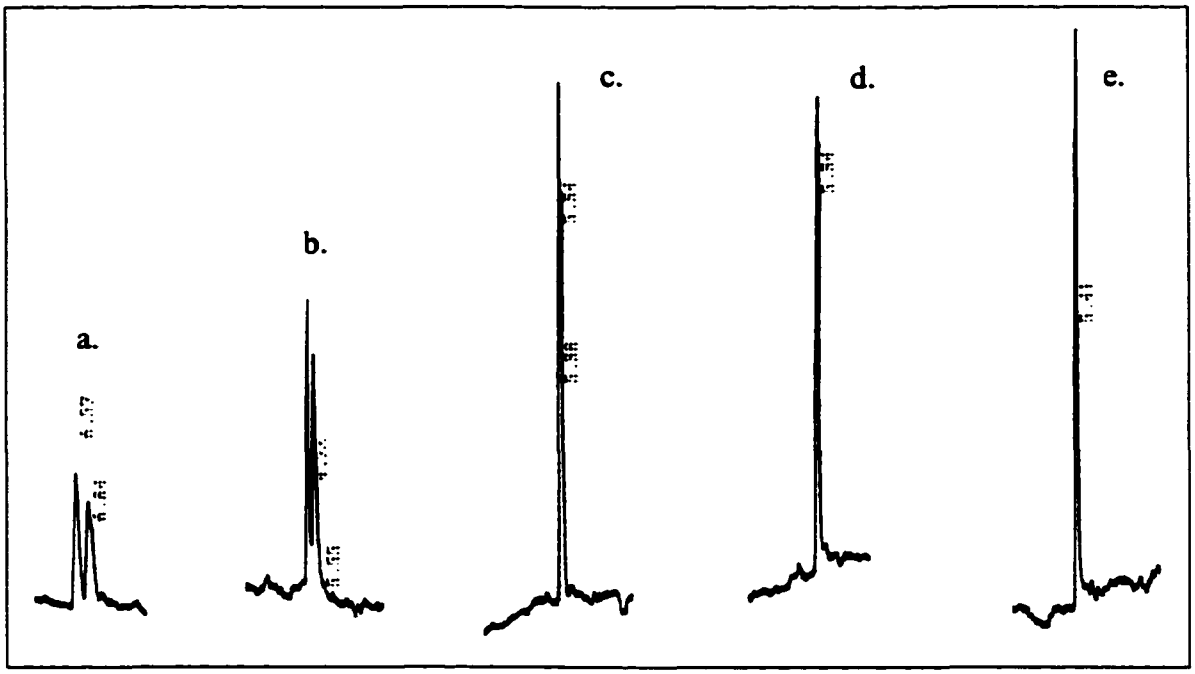

Figure 19. Enantioseparation of $[Ru(bpy)_2ippz]^{2+}$ in 50mM Tris buffer (pH 7.4) with 0.5mM DNA, 200mM NaCl and (a) 0μM (b) 100μM (c) 170μM (d) 200μM (e) 300μM addition of distamycin A.

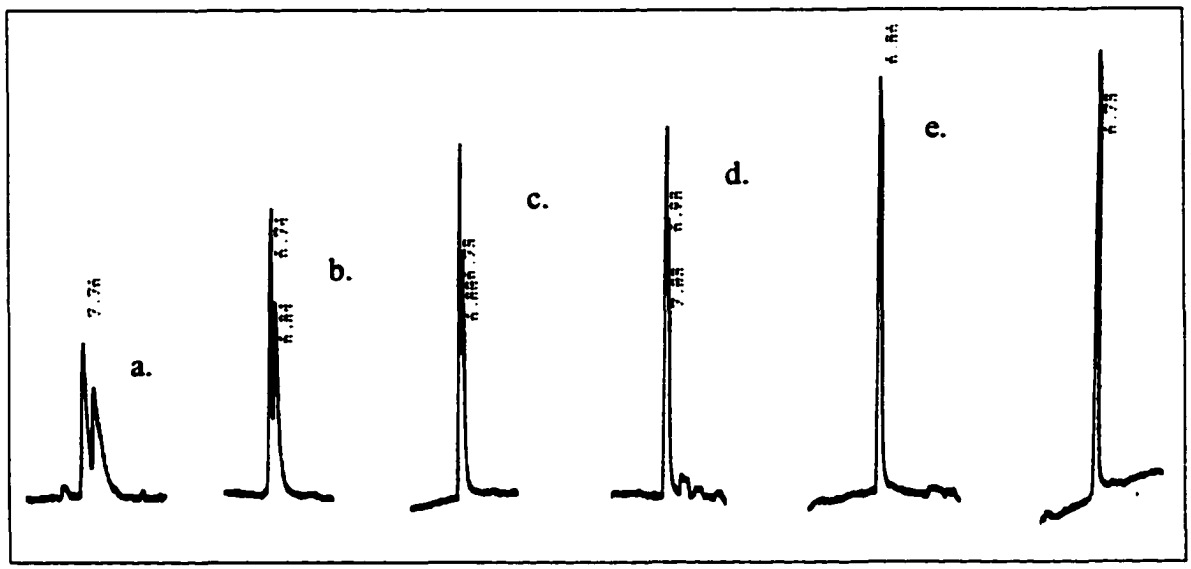

Figure 20. Enantioseparation of $[Ru(bpy)_2bzp]^{2+}$ in 50mM Tris buffer (pH 7.4) with 0.1mM DNA, 300mM NaCl and (a) 0μM (b) 13μM (c) 23μM (d) 31μM (e) 51μM (f) 70μM addition of distamycin A.

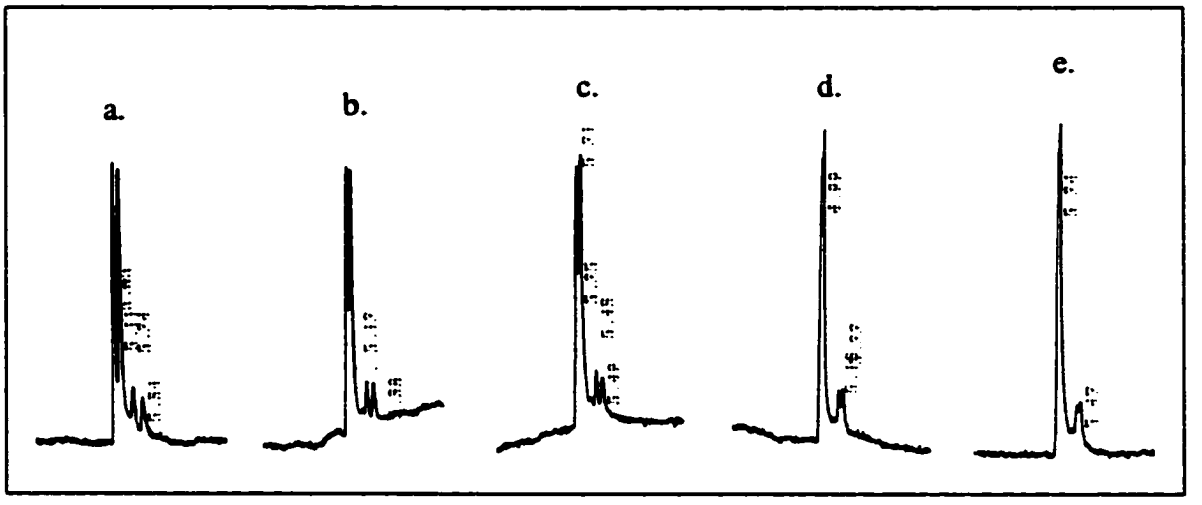

Figure 21. Enantioseparation of $[Ru(bpy)_2bppz]^{2+}$ in 50mM Tris buffer (pH 7.4) with 0.2mM DNA, 200mM NaCl and (a) 0μM (b) 19μM (c) 24μM (d) 36μM (e) 48μM addition of distamycin A.

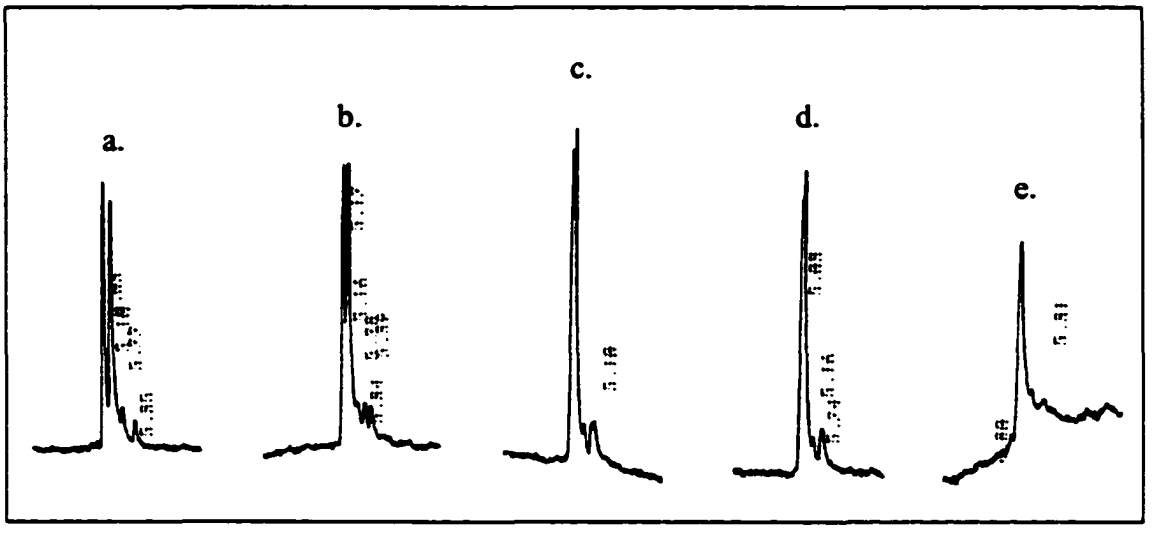

Figure 22. Enantioseparation of $[Ru(bpy)_2mbppz]^{2+}$ in 50mM Tris buffer (pH 7.4) with 0.2mM DNA, 200mM NaCl and (a) 0μM (b) 24μM (c) 36μM (d) 48μM (e) 60μM addition of distamycin A.

4.6. Application of Partial Filling Technique

In the chiral CE experiments performed by Wheeler and co-workers [76,79,115], the detector wavelength for $[M(diimine)_3]^{n+}$ was set at the specific absorption band in visible light region (~400nm) and the sample concentration was on the order of 1.0mM. Because of the high analyte concentration, near-saturation DNA concentrations (2.5~3mM) were required to maximize the enantiomeric resolution. As a result, the overall sensitivity was decreased due to light scattering and absorbance of background DNA and the separation efficiency was low. In a recent CE study [116], a laser-induced fluorescence (LIF) detector was used by Wheeler's group in order to improve analyte detection and analyte resolution. Improved detecability yielded better flexibility in optimizing the chiral resolving agent-to-analyte ratio and experimental conditions.

In our study, all separations were monitored at 290nm. The detection at UV region allows the use of low analyte concentration (60μM) and relatively low DNA concentratons (0.1~0.5mM) to achieve enantiomeric separations. Although the detection wavelength is only 30nm away from DNA specific absorption band (260nm), the interference from DNA background absorption on detection is not significant.

The principles and advantages of the partial filling technique (PFT) were discussed in the earlier section. The partial filling technique was applied here to test its advantages over the complete filling technique (CFT). Figure 23 shows the enantioseparation of ppz accomplished by PFT and CFT.

As the partial filling time is increased, the two enantiomers are gradually resolved. The same separation is accomplished when the filling fraction reaches and exceeds one (Figure 24). Comparing the ppz separation using PFT and CFT at 280nm, the consumption of DNA was reduced by 80% and signal/noise ratio is improved by 15%.

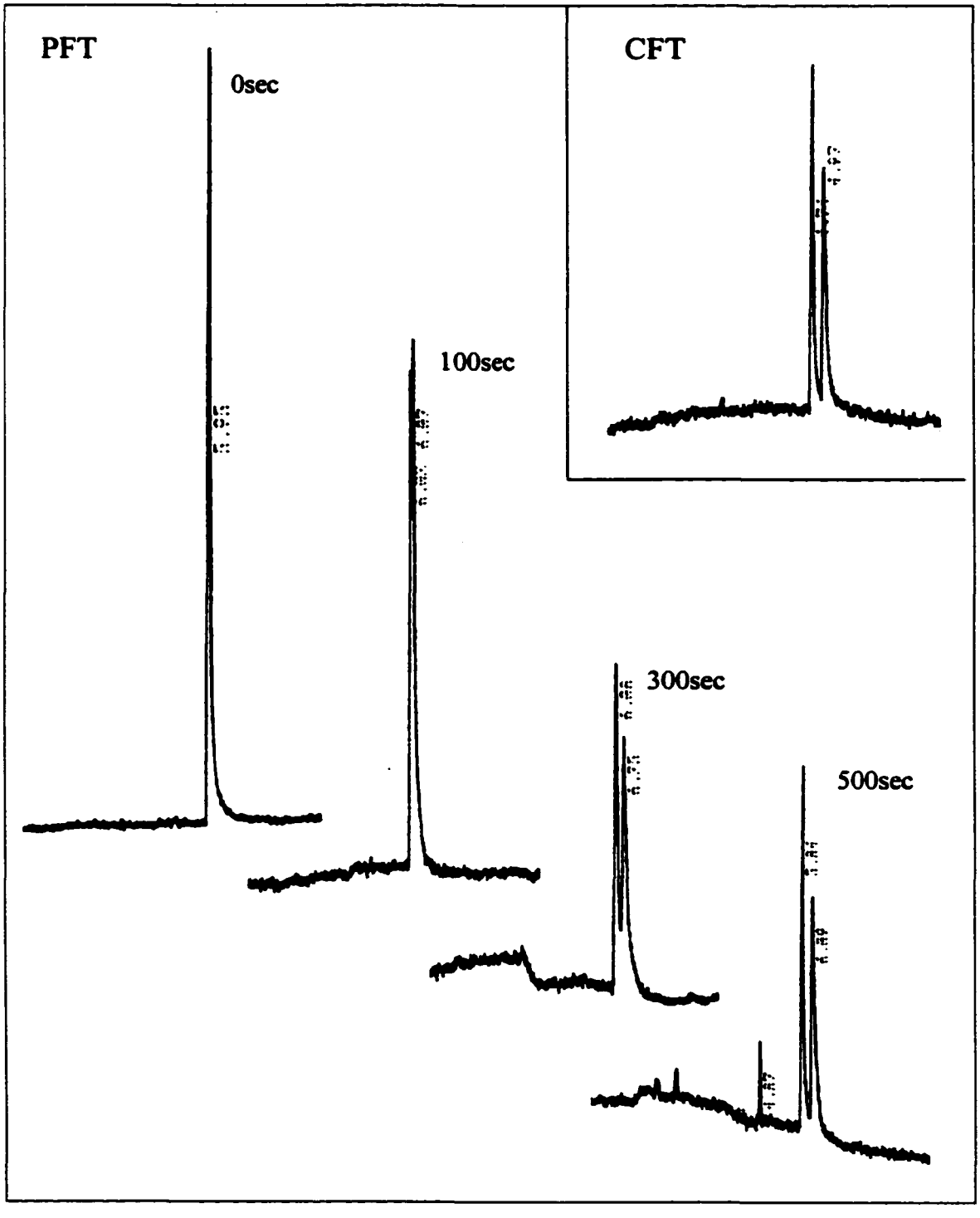

Figure 23. Enantioseparation of $[Ru(bpy)_2ppz]^{2+}$ using complete filling technique (CFT) and partial filling technique (PFT)

Figure 24-. Migration time difference vs. filling fraction, f

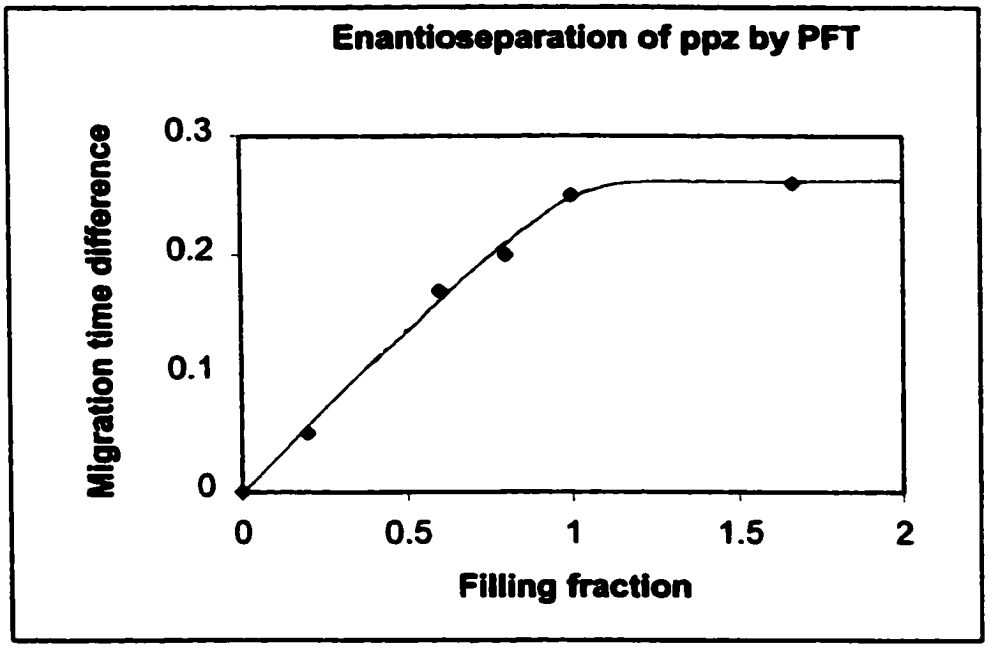

Part III

Evaluation of Conditional Association Constant between Basic Enantiomers and Sulfated-β-cyclodextrin employing the Counter-current Partial Filling CE Technique

INTRODUCTION

1.1. Purpose of project

In Part II, the operating principles and applications of the partial filling capillary electrophoresis technique (PFT) were presented. Since its invention, PFT has been intensively and successfully applied to a variety of separations [1-26]. However, the potential of PFT in evaluation of association constants was rarely explored. Researchers at California State University developed a method for estimating binding constants [27,28] in which the capillary was first partially filled with ligand followed by a sample of receptor and non-interacting standard and electrophoresis then carried out. Analysis of the change in the mobility ratio of the receptor relative to the non-interacting standard as a function of the concentration of the ligand yields a value for the binding constant. Admad and colleagues proposed a linear relationship between the apparent mobility and partial filling fraction based on the assumption that the solute mobility in the separation zone is determined by its degree of complexation [29, 30]. Association constants of drug enantiomers with human α_1-acid glycoprotein and methyl-β-cyclodextrin were obtained.

In previous research on PFT in our research group, a theoretical model proposed a linear relationship between solute migration time and partial filling plug length in counter-current separation mode. The primary aim of this project was to evaluate the association constants between basic enantiomers and negatively charged cyclodextrins (CDs) using this new theoretical model.

1.2. Counter-current partial filling technique

Counter-current partial filling technique was first introduced by Chankvetadze in 1994 [31]. In this special form of PFT, conditions are chosen so that the charged selectors move to the injection end whereas the analytes carry opposite charge and migrate toward the detector end [7, 32-35]. Counter-current PFT is especially applicable to buffer additives with a permanent charge due to the self-mobility effect. Ionic CD derivatives as chiral selectors are presently receiving a great deal of attention. Their attractive properties include good solubility in aqueous media, ability to separate both neutral and charged enantiomers, improved resolution, short analysis time, and low cost of additive [36-45]. In this study, several sulfated cyclodextrins and optically active basic pharmaceuticals were used in the counter-current PFT model system.

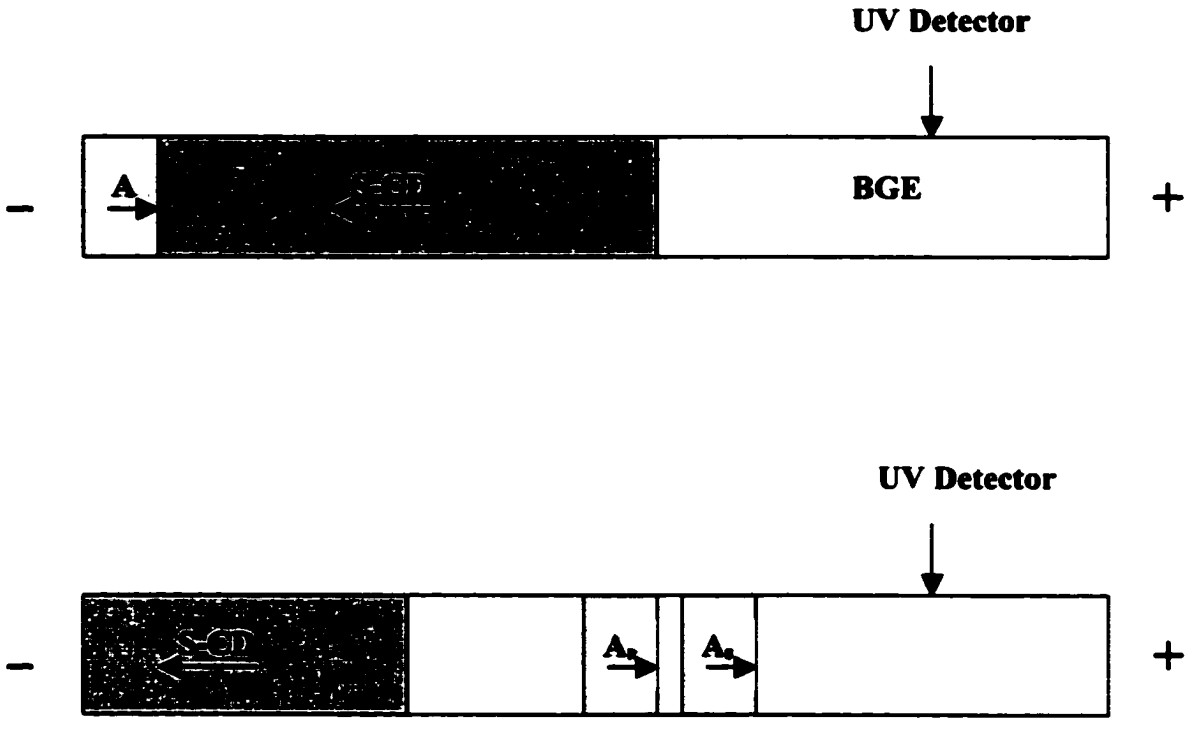

S-CD : sulfated β-cyclodextrin
A_S, A_R : enantiomers
BGE : background electrolyte

Figure 1. Schematic diagram of counter-current partial filling technique

1.3 Theoretical Model

It is assumed one solute (A) interacts with a single chiral selector (C),

$$A + C \leftrightarrow AC \qquad K_a = [AC]/[A][C] \qquad (1)$$

where K_a is the association constant. As illustrated in Figure 1, the differential molecular interaction between the CD and the enantiomers, which results in chiral separation, occurs only within the length of the moving CD band (l_{CD}). EOF is assumed to be the same. The retention time of the analyte can be expressed as the sum of the times spent in the CD band (t_{ACD}) and in the buffer (t_{AB}),

$$t_A = (l_{eff} - l_{CD})/v_{AB} + l_{CD}/v_{ACD} \qquad (2)$$

where l_{eff} is the effective length of the capillary, l_{CD} is the initial length of the capillary filled with CD buffer, v_{AB} is the electrophoretic velocity of the analyte in the CD-free buffer solution, and v_{ACD} is the electrophoretic velocity of the analyte in CD band. v_{ACD} can be expressed as:

$$v_{ACD} = v_{AB}\,\alpha_A - v_{A\text{-}CD}\alpha_{A\text{-}CD}$$

$$= v_{AB}\frac{1}{1+K_a[C]} - v_{A-CD}\frac{K_a[C]}{1+K_a[C]} \qquad (3)$$

where α_A and $\alpha_{A\text{-}CD}$ stand for the mole fraction of uncomplexed analyte and complexed analyte respectively, and $v_{A\text{-}CD}$ stands for the electrophoretic velocity of A-CD complex. Combining equations (2) and (3),

$$t_A = t_{AB} + t_{ACD}$$

$$= (l_{eff} - l_{CD})/v_{AB} + l_{CD}/v_{AC} \qquad (4)$$

$$= l_{eff} \cdot f\left(\frac{1+K_a[C]}{v_{AB} - v_{A-CD}K_a[C]} - \frac{1}{v_{AB}}\right) + \frac{L}{v_{AB}}$$

where f is the fraction of the effective length initially occupied by CD buffer ($l_{CD} = f \cdot l_{eff}$). If mobilities are substituted for velocities using $v = \mu V/L = \mu E$, where L is the total length of the capillary, V is the voltage applied, E is the electric field strength, t_A can also be expressed as:

$$t_A = \frac{l_{eff} \cdot f}{E}\left(\frac{1+K_a[C]}{\mu_{AB} - \mu_{A-CD}K_a[C]} - \frac{1}{\mu_{AB}}\right) + \frac{L}{\mu_{AB}E} \qquad (5)$$

Equation (5) shows that the migration time should vary linearly with the fraction of the capillary filled with CD buffer. If the slope of the t_A vs. f plot is S and the intercept is I, K_a can be calculated:

$$K_a = \frac{\mu_{AB} \cdot S / I}{\mu_{AB} + \mu_{A-CD} + \mu_{A-CD} S / I} \cdot [C] \qquad (6)$$

Ideally, this partial-filled capillary case can be used as a novel way to determine the association constant, K_a, of the solute-additive complex. μ_{AB} can be determined at $[C] = 0$. μ_{AQ} refers to the fully complexed solute mobility.

EXPERIMENTAL

2.1. Chemicals

Three sulphated-β-cyclodextrin sodium salts were used in this study. One, purchased from Aldrich Chem. Co., has an average degree of substitution of 9. Another, purchased from Supelco, has average degree of substitution of 14. A single isomer sulfated-β-cyclodextrin (heptakis-6-sulfato-β-cyclodextrin) was purchased from Regis Technologies, Inc. which has degree of substitution of 7. Norephedrine hydrochloride, isoproterenol hydrochloride and propranolol hydrochloride were obtained from Aldrich Chem. Co.; N,N,N',N'-tetramethyl-ethylenediamine (TEMED) from Spectrum Quality Products, Inc.; and 3-(methacryloyloxy)-propyl-trimethoxysilane from Lancaster Synthesis.

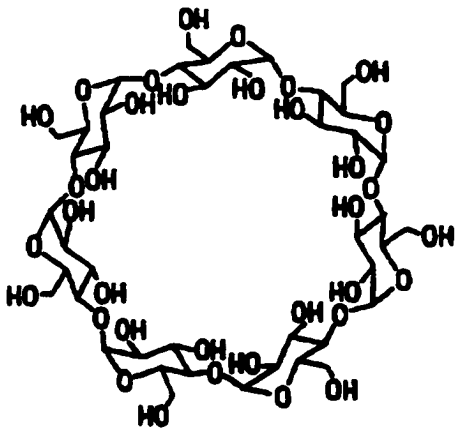

Figure 2. Chemical structure of native β-cyclodextrin

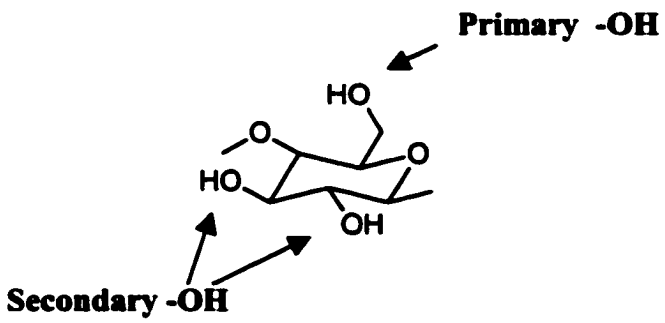

Figure 3. Basic D-glucose unit for β-cyclodextrin

Aldrich S-CD:	randomly sulfated (average degree of substitution 9)
Sepulco S-CD:	randomly sulfated (average degree of substitution 14)
Regis S-CD:	all primary -OH groups are sulfated

Figure 4. Structures of racemic analytes.

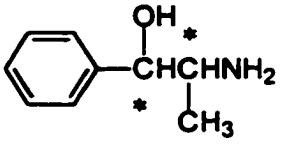

Norephedrine

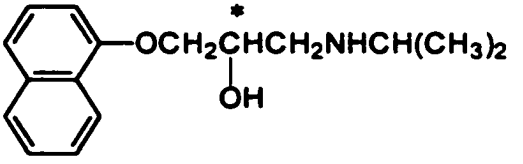

Propranolol

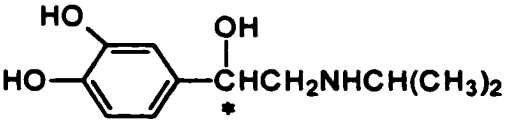

Isoproterenol

2.2. Apparatus

CE experiments were carried out using an ISCO Model 3850 Capillary Electropherograph with Vacum/Electromigration Injection Control Accessary. The electropherograms were recorded on a Spectra-Physics SP-4600 integrator.

2.3. Capillary coating

In the theoretical model, the EOF is assumed to be zero. Capillary coating was performed to cover the active silanol groups on the internal surface. A new fused-silica capillary was internally coated with polyacrylamide according to the method reported by Hjerten [46] as modified. Specifically, the fused-silica capillary was treated with 1M NaOH for 1h and rinsed with water and then dehydrated with methanol for 5min. A solution of 0.5% (v/v) [3-(methacryoxy) propyl]-trimethoxysilane and 0.5% acetic acid in dehydrated methanol was drawn into the capillary and allowed to react with the silica for 1.5h. The capillary was then rinsed with degassed water followed by 4% (w/v) acrylamide aqueous solution containing 0.1% TEMED (v/v) and 0.1% potassium persulphate (w/v). The solution was allowed to polymerize in the capillary for 30min. Finally, the

extra reagent was removed by flushing with water and the capillary was air-dried.

The magnitude of EOF in the coated capillary was found to be approximately 0.06 migration unit ($10^{-4}cm^2/sec.V$). Therefore, coating the capillary wall caused the EOF to be suppressed to a negligible value.

2.4. Capillary conditioning

At the beginning of each day, the coated capillary was rinsed with water and with running buffer before the chiral selector was introduced into the capillary. Between runs, water and running buffer were used to flush the capillary. At the end of the day, the capillary was washed with water and air-dried.

2.5. Solutions

The 250mM buffer stock solution was prepared as follows: 3.45g $NaH_2PO_4 \cdot H_2O$ was accurately weighed and dissolved in about 70mL distilled and deionized water in a 100mL volumetric flask. The pH of this solution was then adjusted to 3.00 with H_3PO_4 using a CORNING 430 pH meter. The total volume was quantitatively brought to 100mL.

For the cyclodextrin stock and working solutions, 25mM phosphate buffer was the solvent. The chiral sample solutions were prepared in water. All working solutions were helium-degassed and filtered through a 0.25μm

Whatman filter before use. All experiments were performed at room temperature, typically 26°C.

2.6. Procedure for partial-filling method

An amount of additive-containing buffer sufficient to fill all or just a fraction of the capillary must be first introduced using vacuum injection. The time required to introduce a certain length was determined as follows. First, the capillary was filled with the plain (CD-free) buffer and a 0.25% (v/v) plug of mesityl oxide was vacuum-injected for 1s. Then the injection end of the capillary was dipped into the sample vial with a solution of a particular CD concentration. The short UV absorbing plug was driven towards the detector by application of vacuum at the detector side with no applied voltage. The peak profile and retention time were recorded by the integrator when the absorber plug passed the detector window. The effective capillary length divided by the retention time gives the hydrodynamic CD solution filling velocity.

For PFT enantioseparations, the capillary was first flushed and equilibrated with buffer. A certain length of CD-containing buffer was introduced for a controlled time and at the known filling velocity. Immediately after, the injection end was placed in the sample vial and the sample introduced hydrodynamically for several seconds at 0.5 psi

vacuum. The capillary was replaced in the inlet and outlet buffer vials, the high voltage applied, and the CE carried on as usual.

RESULTS AND DISCUSSION

3.1. Measurement of complex mobility

In order to determine the association constant, a value for the mobility of the fully complexed species, $\mu_{A\text{-}CD}$, is needed. Several methods have been tried:

(a) Using the conventional CE method, the capillary is continuously filled with buffer containing CD. The apparent mobilities of the enantiomers is plotted versus the concentration of CD. The mobilities of the fully complexed solutes, $\mu_{A\text{-}CD}$, should be equal for both enantiomers, i.e. the plots for the two should converge at some value of *[C]*. For our system, even at the highest usable *[C]* the plots were still diverging.

(b) A mixture of the analytes with a high concentration of cyclodextrin equilibrate as the sample is injected. The complex formed is expected to be separated from the analyte and cyclodextrin through electrophoresis and to be detected and identified due to the inclusion of UV absorbing analyte molecule into the CD cavity.

(c) Cyclodextrin mobility is evaluated by an indirect UV detection method. The CD-analyte complex mobility based on charge-to-size ratio is then estimated:

$$\mu_{A-CD} = \mu_{CD} \cdot \frac{MW_{CD}(n-1)}{n(MW_{CD} + MW_{analyte})} \quad (7)$$

MW represents molecular weight, *n* is the average charge on one cyclodextrin molecule.

(d) PFT is carried out at two different CD concentrations. According to equation (6),

$$K_a = \frac{\mu_{AB} \cdot S_1 / I_1}{\mu_{AB} + \mu_{A-CD} + \mu_{A-CD} S_1 / I_1} \cdot [C_1] \quad (8)$$

$$K_a = \frac{\mu_{AB} \cdot S_2 / I_2}{\mu_{AB} + \mu_{A-CD} + \mu_{A-CD} S_2 / I_2} \cdot [C_2] \quad (9)$$

Combining equations (8) and (9), the complex mobility can be deduced:

$$\mu_{A-CD} = \mu_{AB} \frac{C_1 \frac{S_1}{I_1} - C_2 \frac{S_2}{I_2}}{(\frac{S_1}{I_1} + 1)\frac{S_2}{I_2} \cdot C_1 - (\frac{S_2}{I_2} + 1)\frac{S_1}{I_1} \cdot C_2} \quad (10)$$

However, none of the above methods gave reasonable K_a or $\mu_{A\text{-}CD}$ values. Neither the application of single isomer CD nor viscosity correction of the CD plug helped to solve the problem. While the accuracy of complex mobility measurement was suspected, a nonlinear increase of migration time with CD plug length was observed.

Figure 5 is a plot of migration times of isoproterenol enantiomers versus f using partial filling with 5mM single isomer sulfated-β-cyclodextrin (SICD). It shows clearly that the migration times do not vary linearly with the filling fraction. Experiments with other sulphated CDs and basic enantiomers show the same results that the migration time first increases then decreases with the partial filling fraction.

Figure 5. Migration time of isoproterenol enantiomers as a function of filling fraction

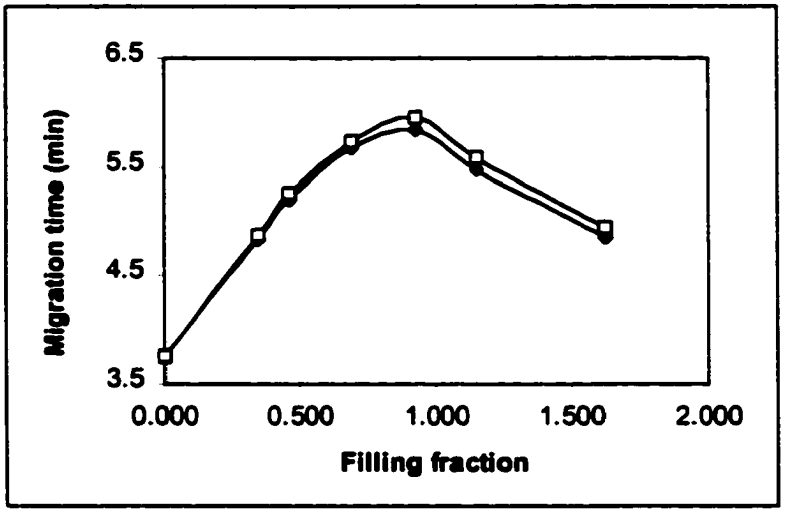

CE conditions: partial filling solution, 5mM SICD in BGE; BGE, 25mM phosphate at pH 3.0; sample, 0.02mg/mL isoproterenol; injection, 0.5psi vacuum injection, 5sec; capillary, polyacrylamide-coated 48 cm x 50μm i.d. (29.5cm effective length)

3.2. Field Strength Effect

As the experimental results disapprove the original theoretical model, an explanation based on a field strength effect is proposed. What might be incorrect about the original theory is the assumption that the electric field strength is uniform over the entire capillary. Due to the conductivity difference and self-migration of sulfated CD, the potential drops and field strengths in the CD plug and CD-free plug are not equal and both of them vary with the electrophoresis time. Considering the intrinsic analyte mobility μ is a constant,

$$v = \mu E$$

so the solute velocity changes as the field strength varies. As the variation of field strength is not negligible, the conversion from equation (4) to equation (5) is fundamentally wrong.

Further interpretation using computer-assisted mathematical calculations is demonstrated below:

The system is considered as a series circuit (As illustrated in Figure 6.) At a point in time (t) during the separation, the potential drop over the CD zone (V_1) and the potential drop over the BGE zone (V_2) are given as:

$$V_1 = R_1 \cdot I_t = S_1 \cdot (l_{eff} \cdot f - v_{CD} \cdot t) \cdot I_t \qquad (11)$$

$$V_2 = R_2 \cdot I_t = S_2 \cdot (L - l_{eff} \cdot f + v_{CD} \cdot t) \cdot I_t \qquad (12)$$

Where I_t, R, and S, are the electric current at time t, the resistance and specific resistance of each region respectively. As above, l_{eff} and v_{CD} are the capillary effective length and CD plug migration speed. The total potential drop (V) applied over the entire capillary is constant.

$$V = V_1 + V_2 = (R_1 + R_2) \cdot I_t \tag{14}$$

Thus,

$$V_1 = V \cdot \frac{R_1}{R_1 + R_2}$$

$$= V \cdot \frac{l_{eff} \cdot f - v_{CD} \cdot t}{(l_{eff} \cdot f - v_{CD} \cdot t) + S_2 / S_1 (L - l_{eff} \cdot f + v_{CD} \cdot t)} \tag{15}$$

and the field strength in CD zone (E_1) is

$$E_1 = V \cdot \frac{1}{(l_{eff} \cdot f - v_{CD} \cdot t) + S_2 / S_1 (L - l_{eff} \cdot f + v_{CD} \cdot t)} \tag{16}$$

The potential drop and field strength equations for the BGE zone can be deduced similarly.

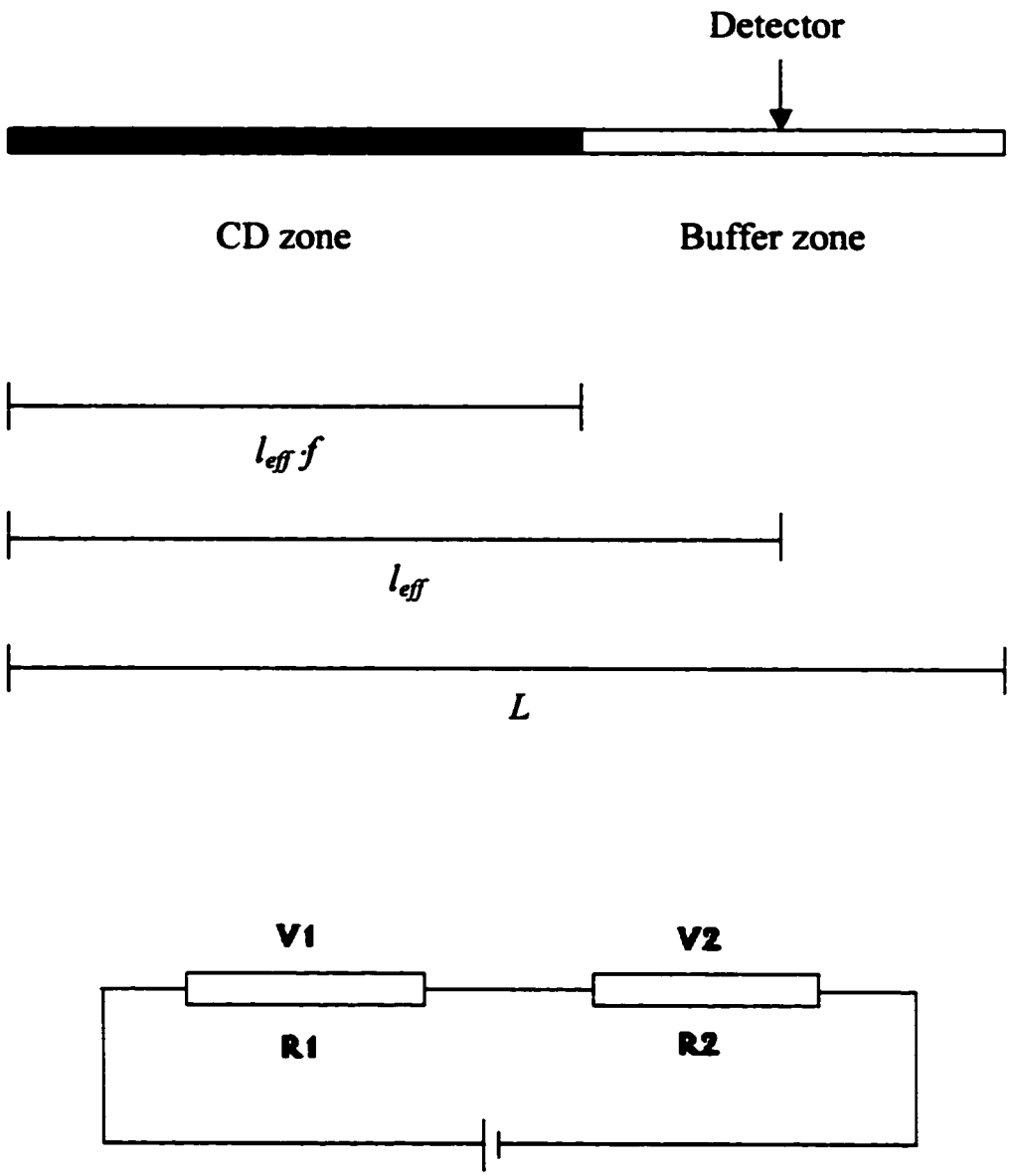

Figure 6. Schematic of series circuit.

Since the BGE zone is less conductive than the CD containing zone, $S_2/S_1>1$. V, $leff$, f and v_{CD} are constants in equation (16). As a function of t, E_1 decreases as t increases.

Figures 7 and 8 illustrate the computer-simulated potential drop and field strength distribution as a function of time using equations (15) and (16). The calculations use experimental data for are: V=26kV, l_{eff}=29.5cm, v_{CD}=11.6cm/min measured by the indirect detection method, and S_2/S_1 is determined by comparing the initial currents when the capillary is completely filled by BGE or the CD solution of interest. Thus S_2/S_1=current ratio=1.325 when 2.0mM CD is used. Three initial filling fractions are used for the calculations: f=0.5, when the effective length is half occupied by CD solution; f=1, when the CD solution is filled to the detector window; and f=1.627, when the capillary is fully filled with CD solution.

The clear trend shown in Figure 7 is that the potential drop over the CD zone decreases with time, and potential drop over the CD-free buffer zone changes the other way round. The reason is that while the polyanionic cyclodextrins migrate out the capillary, the overall resistance as well as the potential drop over the CD plug is reduced. On the other hand, the BGE zone is extended and the potential drop increases.

Figure 7. Computer simulated potential drop distribution as a function of time.

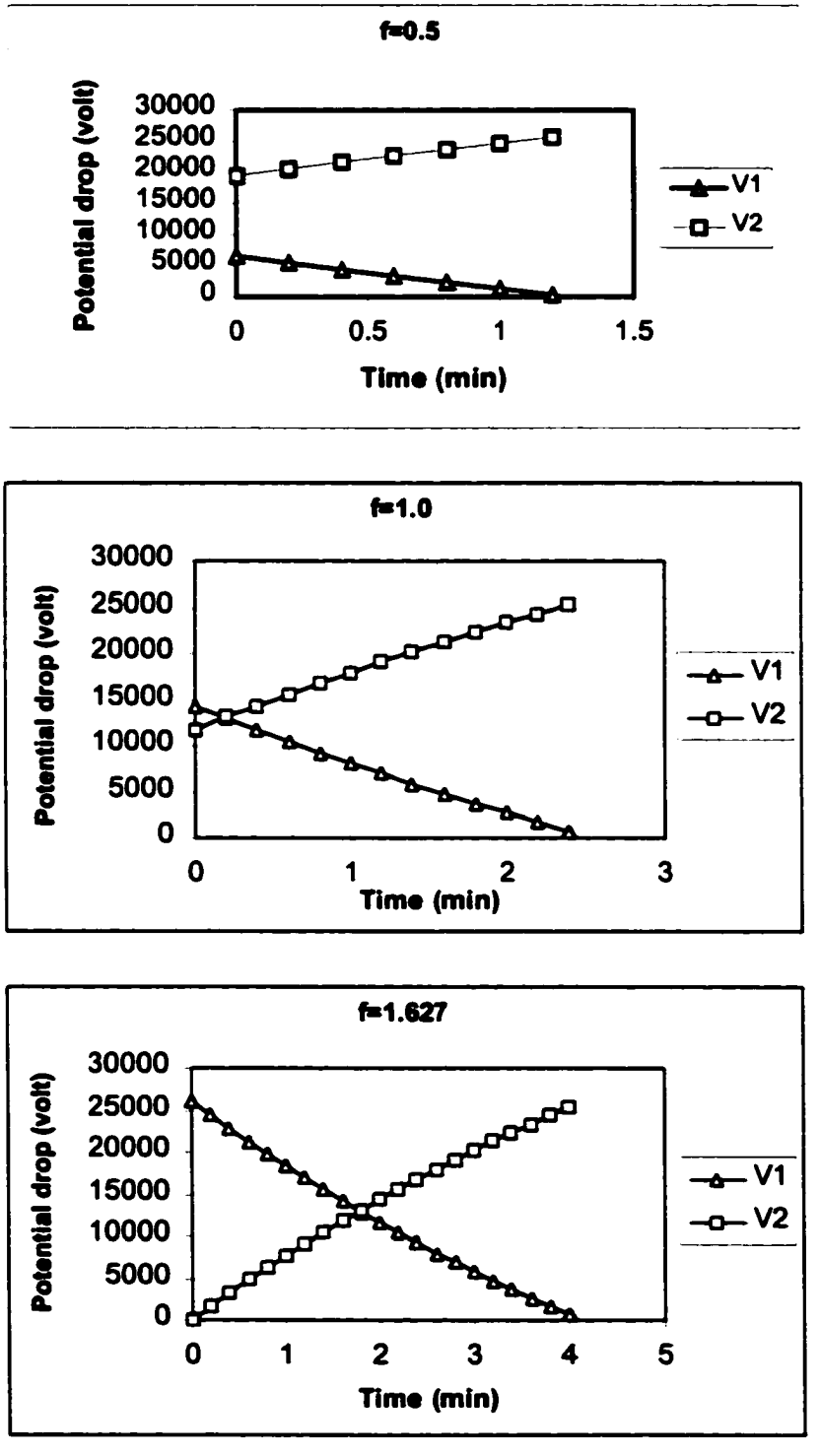

It can be seen in Figures 8.1 and 8.2 that both the field strengths in the CD zone and the field strength in the BGE zone decrease with separation time. Meanwhile, at a same point in time, the field strength is always higher at the higher filling fraction. Figure 8.3 shows that the field strength in the BGE zone is always higher than the field strength in the CD zone. Considering that the intrinsic solute mobility is constant, the solute velocity is proportional to field strength — the higher the field strength, the greater the velocity. Starting with a specific f, the solute migrates slower in the CD zone than its does in the CD-free BGE zone due to its interaction with the CD and the presence of a lower field strength. However, it is not straightforward to compare the overall migration time starting with different initial partial filling fraction. When a longer CD separation zone is applied (bigger f), although the solutes experience more interactions, they also experence higher field strength, giving a greater driving force toward the detector end. Therefore, a longer filling zone does not always result in a longer migration time. The remarkable decrease in migration time at the high filling fraction is observed when high CD concentration was applied (Figure 9) because of higher difference in conductivity.

In conclusion, due to the variation of field strength, migration time is not a linear function of partial filling fraction. The original theoretical

model might be suitable to obtain association constants when the buffer additive is not very conductive.

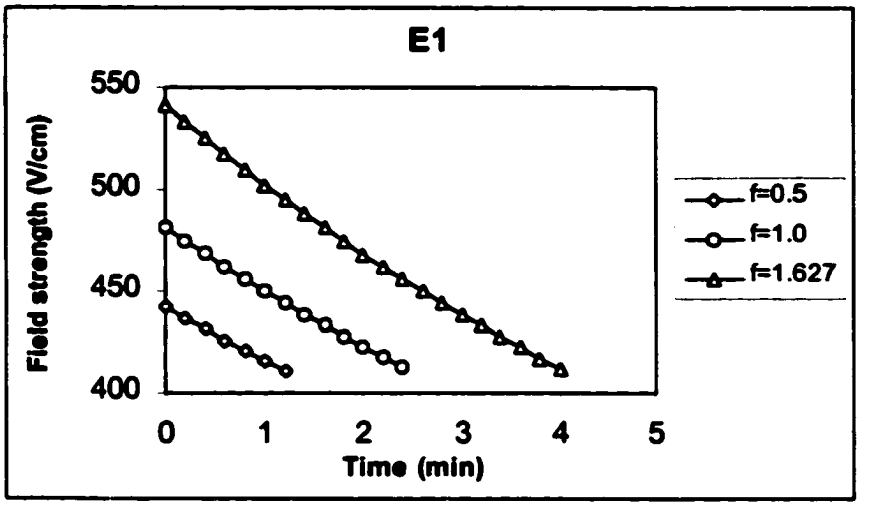

Figure 8.1. Field strength in CD zone as a function of time.

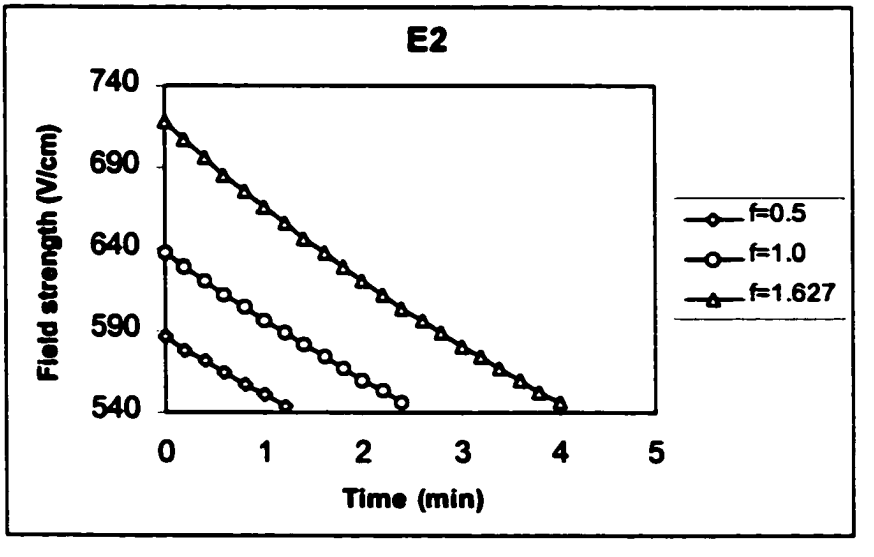

Figure 8.2. Field strength in BGE zone as a function of time.

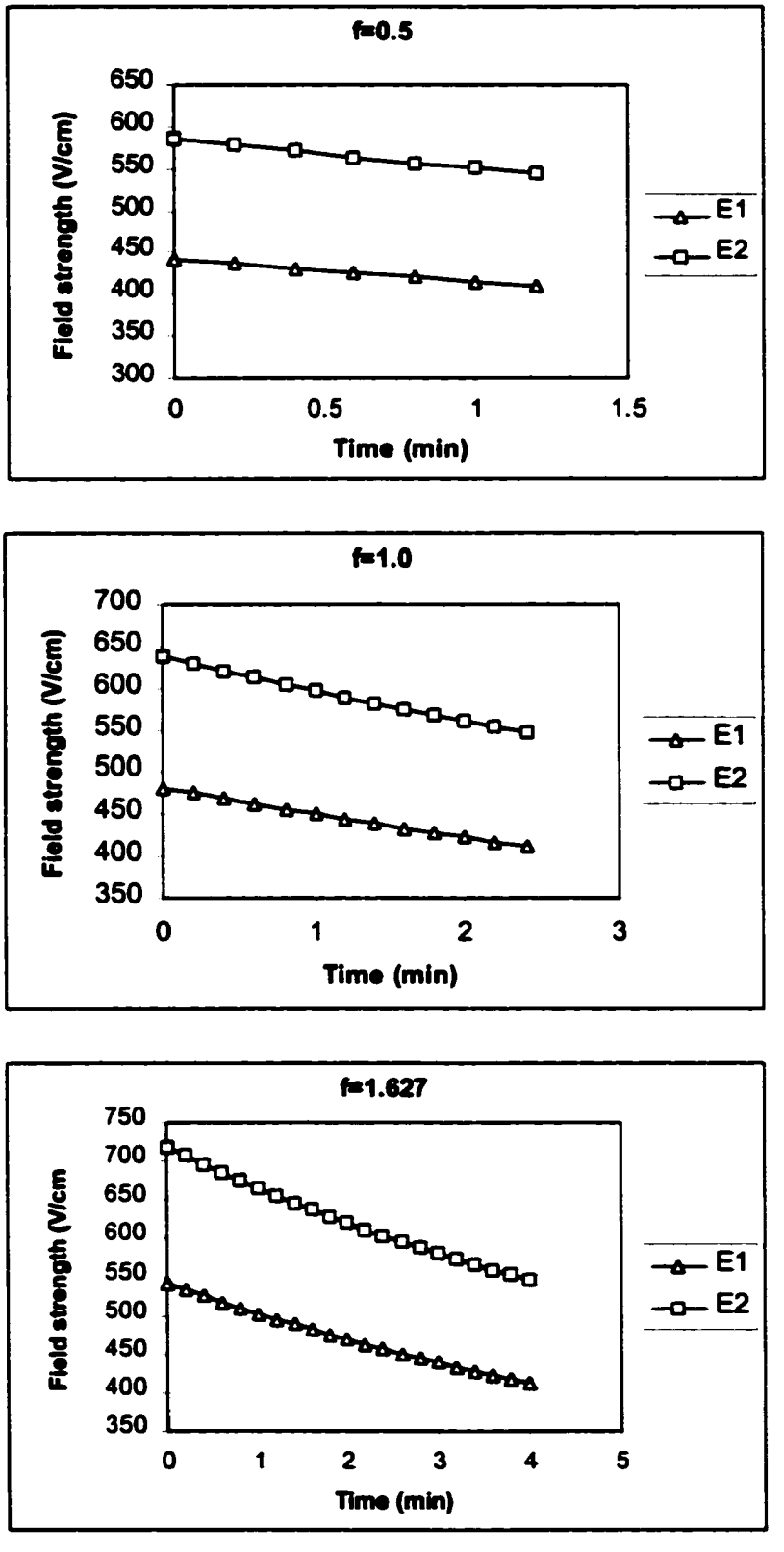

Figure 8.3. Comparison of field strength in CD zone and BGE zone.

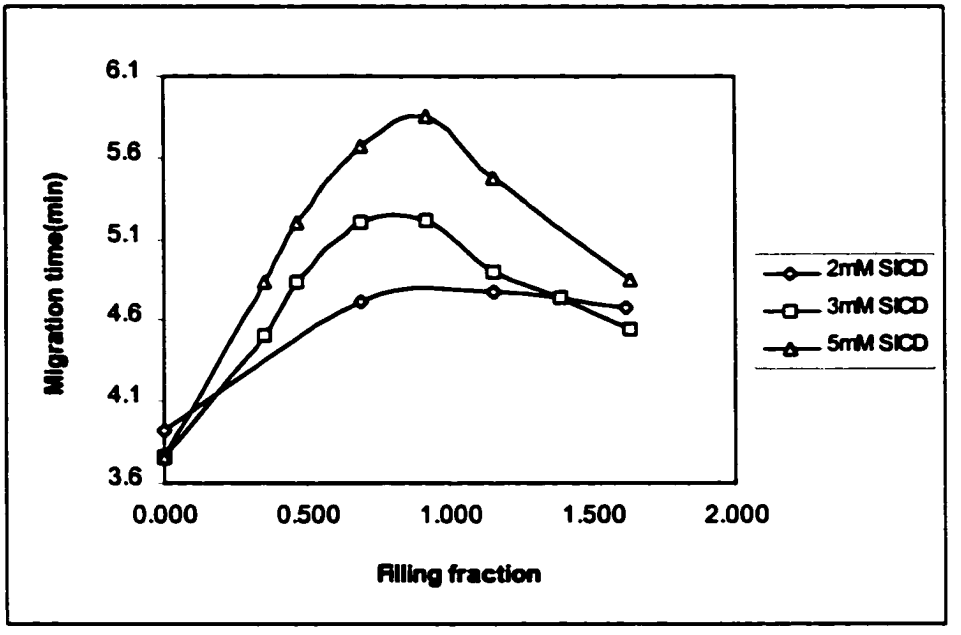

Figure 9. t_A as a function of f at different CD partial filling concentrations.

(CE conditions: same as Figure 5)

REFERENCES

Part I

1. Govindarajan, V. S.; Sathyanarayana, M. N., *Food Science and Nutrition,* 29 (1991) 435
2. Rouhi, A. M., *Chem. & Engr. News.*, 26 (26 January 1998) 31
3. *Official Analytical Methods of the American Spice Trade Association* 2nd Ed., ASTA: Englewood Cliffs, NJ, 1968; Method 21.0
4. Palacio, J. J. R., *J.AOAC.,* 62 (1979) 1168
5. Drcecco, J. J., *J. AOAC.,* 62 (1979) 998
6. Bajaj, K. L., *J. AOAC.,* 63 (1980) 1314
7. Spanyar, P.; Blazovich, M., *Analyst.*, 94 (1969) 1084
8. Todd, P. Jr., Bensinger, M.; Biftu, T., *J. Chromatogr. Sci.*, 13 (1975) 577
9. Hawer, W. S.; Ha, J.; Hwang, J.; Nam, Y., *Food Chem.*, 49 (1994) 99
10. Thomas, B. V.; Schreiber, A. A.; Weisskopf, C. P., *J. Agric. Food Chem.*, 46 (1998) 2655
11. Krajewska, A. M.; Powers, J. J., *J. AOAC.,* 70 (1987) 926

12. Kawada, T.; Watanabe, T.; Katsura, K.; Takami, H.; Iwai, K., *J. Chromatogr.*, 329 (1985) 99

13. Iwai, K.; Suzuki, T.; Fujiwake, H.; Oka, S., *J. Chromatogr.*, 172 (1979) 303

14. Cooper, T. H.; Guzinski, J. A.; Fisher, C., *J. Agric. Food Chem.*, 39 (1991) 2253

15. Johnson, T. S.; Ravishankar, G. A.; Venkataraman, L. V., *J. Agric. Food Chem.*, 40 (1992) 2461

16. Yao, J.; Nair, M. G.; Chandra, A., *J. Agric. Fooc Chem.*, 42 (1994) 1303

17. Lopez-Hernandez, J.; Oruna-Concha, M. J.; Simal-Lozano, J.; Gonzalez-Castro, M. J.; Vazquez-Blanco, M. E., *Deutsche Lebensmittel-Rundschau.*, 92 (1996) 393

18. Parrish, M., *J. AOAC Int.*, 79 (1996) 738

19. Peusch, M.; Muller-Seitz, E.; Petz, M.; Muller, A.; Anklam, E., *Z. Lebensm Unters Forsch.*, A 204 (1997) 351

20. Betts, T. A., *J. Chem Educ.*, 76 (1999) 240

21. Batchelor, J. D.; Jones, B. T., *J. Chem. Ed.*, 77 (2000) 266

22. Huang, J.; Mabury, S. A.; Sagebiel, J. C., *J. Chem. Ed.*, 77 (2000) 1630

23. Khaled, M. Y.; Anderson, M. R.; McNair, H. M., *J. Chromatogr. Sci.*, 31 (1993) 259

24. Laskaridou-Monnerville, A., *J. Chromatogr.*, 838 (1999) 293

25. Suzuki, T.; Iwai, K., in The Alkaloids: Chemistry and Pharmacology, A. Brossi (ed), Vol. 23 (1984), Chaper 4.

Part II

1. Messori, L.; Casini, A.; Vullo, D.; Haroutiunian, S. G.; Dalian, E. B.; Orioli, P., *Inorg. Chim. Acta,* 303 (2000) 283

2. Abufarag, A.; Reedijk, J., *J. Inorg. Biochem.*, 59 (1995) 137

3. Lippard, S. J., *J. Am. Chem . Soc.*, (1978) 211

4. Lippard, S. J.; Bond, P. J., Wu, K. C.; Bauer, W. R., *Science,* 19 (1976) 726

5. Erkkia, K. E.; Odom, D. T.; Barton, J. K., *Chem. Rev.*, 99 (1999) 2777

6. Friedman, A. E.; Chambron, J. C.; Sauvage, J. P.; Turro, N. J.; Barton, J. K., *J. Am. Chem. Soc.*, 112 (1990) 4960

7. Dupureur, C. M.; Barton, J. K., *Inorg. Chem.*, 36 (1997) 33

8. Liu, J. G.; Ye, B. H.; Li, H.; Ji, L. N.; Li, R. H.; Zhou, J. Y, *J. Inorg. Biochem.*, 73 (1999) 117

9. Olson, E. J. C.; Hu, D.; Hormann, A.; Jonkman, A. M.; Arkin, M. R.; Stemp, E. D. A.; Barton, J. K.; Barbara, P. F., *J. Am. Chem. Soc.*, 119 (1997) 11458

10. Barton, J. K.; Dannenberg, J. J.; Raphael, A. L., *J. Am. Chem. Soc.*, 106 (1984) 2172

11. Liu, J. G.; Zhang, Q. L.; Shi, X. F.; Ji, L. N. *Inorg. Chem.*, 40 (2001) 5045

12. Colmenarejo, G.; Holmen, A.; Norden, B., *J. Phys. Chem. B*, 101 (1997) 5196

13. Hein, M.; Arena, S., "The foundations of Chemistry", Brook/Cole, 1998

14. Neidel, S., "DNA Structure and Recognition", Oxford, New York, 1994.

15. Stenesh, J., "Biochemistry", Plenum, New York, 1998.

16. Barton, J. K. *Science*, 233 (1986) 727

17. Murphy, C. J.; Barton, J. K., *Methods Enzymol.*, 226 (1993) 576

18. Jackson, B. A.; Alekseyev, V. Y.; Barton, J. K., *Biochemistry*, 38 (1999) 4655

19. Hall, D. B.; Holmlin, R. E.; Barton, J. K., *Nature,* 382 (1996) 731

20. Dandlier, P. J.; Holmlin, R. E.; Barton, J. K., *Science,* 274 (1997) 1465

21. Sigman, D. S.; Mazumer, A.; Perrin, D. M., *Chem. Rev.,* 93 (1993) 2295

22. Pyle, A.; Barton, J. K., In Progress in Inorganic Chemistry; Lippard, S. J., Ed.; John Wiley & Sons: New York, 38 (1990) 413

23. Erkkia, K. E.; Odom, D. T.; Barton, J. K., *Chem. Rev.,* 99 (1999) 2777

24. Norden, B.; Lincoln, P.; Akermann, B.; Tuite, E., Metal Ions in Biological Systems; Sigel, A., Sigel, H., Eds.; Marcel Dekker: New York, 33 (1996) 177

25. Moucheron, C.; Mesmaerer, A. K.-D.; Kelly, J. M., Structure and Bonding; Clarke, M. J., Ed.; Springer-Verlag: Berlin, 92 (1998) 163

26. Xiong, Y.; Ji, L. N., *Coord. Chem. Rev.,* 185-186 (1999) 711

27. Xiong, Y.; He, X. F.; Zou, X. H.; Wu, J. Z.; Chen, X. M.; Ji, L. N., J. *Chem. Soc., Dalton Trans.,* (1999) 19

28. Zou, X. H.; Ye, B. H.; Li, H.; Liu, J. G.; Xiong, Y.; Ji, L. N., J. *Chem. Soc., Dalton Trans.,* (1999) 1432

29. Zhen, Q. X.; Zhang, Q. L.; Liu, J. G.; Ye, B. H.; Ji, L. N.; Wang, L., *J. Inorg. Biochem.*, 78 (2000) 293

30. Liu, J. G.; Ye, B. H.; Li, H.; Zhen, Q. X.; Ji, L. N.; Fu, Y. H., *J. Inorg. Biochem.*, 76 (1999) 265

31. Liu, J. G.; Ye, B. H.; Chao, H.; Zhen, Q. X.; Ji, L. N, *Chem. Lett.*, (1999) 1085

32. Liu, J. G.; Ye, B. H.; Zhang, Q. L.; Zou, X. H.; Zhen, Q. X.; Tian, X.; Ji, L. N., *J. Biol. Inorg. Chem.*, 5 (2000) 119

33. Rehmann, J. P.; Barton, J. K., *Biochemistry*, 29 (1990) 1701

34. Yamagishi, A., *J. Phys. Chem.*, 88 (1984) 5709

35. Hiort, C.; Norden, B.; Graslund, A., *J. Am. Chem. Soc.*, 114 (1992) 4933

36. Satyanarayana, S.; Dabrowiak, J. C.; Chairs, J. B., *Biochemistry*, 32 (1993) 2573

37. Coggan, D. Z. M.; Haworth, I. S.; Bates, P. J.; Robinson, A.; Rodger, A., *Inorg. Chem.*, 38 (1999) 4486

38. Greguric, I.; Aldrich-Wright, J. R.; Collins, J. R., *J. Am. Chem. Soc.*, 119 (1997) 3621

39. Collins, J. G.; Sleeman, A. D.; Aldrich-Wright, J. R.; Greguric, I.; Hambley, T. W., *Inorg. Chem.*, 37 (1998) 3133

40. Collins, J. G.; Sleeman, A. D.; Aldrich-Wright, J. R.; Greguric, I. D.; Pellegrini, P. A., *Inorg. Chem.*, 38 (1999) 5502

41. Tuite, E.; Lincolin, P.; Norden, B., *J. Am. Chem. Soc.*, 119 (1997) 239

42. Holmlin, R. E.; Stemp, E. D. A.; Barton, J. K., *Inorg. Chem.*, 37 (1998) 29

43. Naing, K.; Takahashi, M.; Taniguchi, M.; Yamagishi, A., *Inorg. Chem.*, 34 (1995) 350

44. Hiort, C.; Lincoln, P.; Norden, B., *J. Am. Chem. Soc.*, 115 (1993) 3448

45. Kim, H. K.; Lincoln, P.; Norden, B.; Tuite, E., *J. Chem. Soc. Chem. Commun.*, (1997) 2375

46. Tysoe, S. A.; Morgan, R. J.; Baker, A. D.; Strekas, T. C., *J. Phys. Chem.*, 97 (1993) 1707

47. Strekas, T. C.; Baker, A. D.; Zaltsman, L.; Wang, S., *J. Coord. Chem.*, 39 (1996) 281

48. Friedman, A. E.; Kumar, C. V.; Turro, N. J.; Barton, J. K., *Nucleic Acids Res.*, 19 (1991) 2595

49. Wan, K. X.; Shibue, T.; Gross, M. L., *J. Am. Chem. Soc.*, 122 (2000) 300

50. Wang, L.; Wu, J. Z.; Yang, G.; Zeng, T. X.; Yang, H. Y.; Ji, L. N., *J. Inorg. Biochem.*, 59 (1995) 174

51. Mahadevan, S.; Palaniandavar, M., *J. Inorg. Biochem.*, 59 (1995) 161

52. Eriksson, M.; Leijon, M.; Hiort, C.; Norden, B.; Graslund, A., *Biochemistry*, 33 (1994) 5031

53. Satyanaryana, S.; Dabrowiak, J. C.; Chaires, J. B., *Biochemistry*, 31 (1992) 9319

54. Hartshorn, R. M.; Barton, J. K., *J. Am. Chem. Soc.*, 114 (1992) 5919

55. Wu, J. Z.; Li, Lin.; Zeng, T. X, Ji, L. N., *Polyhedron*, 16 (1997) 103

56. Sigman, D. S.; Mazumder, A.; Perrin, D. M., *Chem. Rev.*, 93 (1993) 2295

57. Hudson, B. P.; Dupureur, C. M.; Barton, J. K., *J. Am. Chem. Soc.*, 117 (1995) 9379

58. Lincoln, P.; Broo, A.; Norden, B., *J. Am. Chem. Soc.*, 118 (1996) 2644

59. Tuite, E.; Lincoln, P.; Norden, B., *J. Am. Chem. Soc.*, 119 (1997) 239

60. Dupureur, C. M.; Barton, J. K., *J. Am. Chem. Soc.*, 116 (1994) 10286

61. Wu, J. Z.; Yang, G.; Chen, S.; Ji, L. N.; Zhou, J. Y.; Xu, Y., *Inorg. Chim. Acta.*, 283 (1998) 17

62. Marincola, F. C.; Casu, M.; Saba, G.; Lai, A.; Lincoln, P.; Norden, B., *Chem. Phys.*, 236 (1998) 301

63. Lincoln, P.; Norden, B., *J. Inorg. Biochem.*, 59 (1995) 156

64. Zhen, Q. X.; Ye, B. H.; Liu, J. G.; Zhang, Q. L.; Ji, L. N., *Inorg. Chim. Acta.*, 303 (2000) 141

65. Guerzo, A. D.; Demeunynck, M.; Lhomme, J.; Mesmaeker, A. K-D., *Inorg. Chem. Commun.*, 1 (1998) 339

66. Morgan, R. J.; Chatterjee, S.; Baker, A. D.; Strekas, T. C, *Inorg. Chem.*, 30 (1991) 2678

67. Baker, A. D.; Morgan, R. J.; Strekas, T. C., *J. Am. Chem. Soc.*, 113 (1991) 1411

68. Morgan, O.; Wang, S.; Bea, S. A.; Morgan, R. J.; Baker, A. D.; Strekas, T. C.; Engel, R., *J. Chem. Soc., Dalton Trans.*, (1997) 3773

69. Strekas, T. C.; Baker, A. D.; Morgan, O. H., *J. Coord. Chem.*, 34 (1995) 77

70. Mahadevan, S.; Palaniandavar, M., *J. Inorg. Biochem.*, 59 (1995) 161

71. Morgan, O., "Novel Uses of α-Diimine Ligands and their Ru(II) Metal Complexes." Ph.D dissertation, CUNY, 2001

72. Fanali, S.; Ossicini, L.; Foret, F.; Bocek, P.; *J. Microcol. Sep.*, 1 (1989) 190

73. Vogt, C.; Werner, G.; *J. Chromatogr.*, 686 (1994) 325

74. Okerberg, E. S.; Elshihabi, S.; Charmichael, P. T.; Woody, K. A.; Barckholtz, T. A.; Burke, J. A.; Bushey, M. M., *J. Microcol. Sep.*, 12 (2000) 391

75. See, M. M.; Elshihabi, S.; Burke, J. A.; Bushey, M. M., *J. Microcol. Sep.*, 7 (1995) 199

76. Shelton, C. M.; Seaver, K. E.; Wheeler, J. F.; Kang-Maguire, N. A. P., *Inorg. Chem.*, 36 (1997) 1532

77. Mytykh, O. V.; Martin, S. E.; Wheeler, J. F.; Kang-Maguire, N. A. P., *Inorg. Chim. Acta.*, 311 (2000) 143

78. Harris, J. E.; Desai, N.; Seaver, K. E.; Watson, R. T.; Kang-Maguire, N. A. P.; Wheeler, J. F., *J. Chromatogr.*, 919 (2001) 427

79. Watson, R. T.; Desai, N.; Wildsmith, J.; Wheeler, J. F.; Kang-Maguire, N. A. P., *Inorg. Chem.*, 38 (1999) 2683

80. Wren, S. A. C.; Rowe, R. C., *J. Chromatogr.*, 603 (1992) 235

81. Rundlett, K. L.; Armstrong, D. W., *J. Chromatogr.*, 721 (1996) 173

82. Lemesle-Lamache, V.; Taverna, M.; Wouessidjewe, D.; Duchene, D.; Ferrier, D., *J. Chromatogr.*, 735 (1996) 321

83. Penn, S. G.; Goodall, D. M., *J. Chromatogr.*, 636 (1993) 149

84. Sanger-van de Griend, C. E.; Groningsson, K.; Westerlund, D., *Chromatographia*, 42 (1996) 263

85. Gahm, K.; Stalcup, A. M., *Anal. Chem.*, 67 (1995) 19

86. Busch, M. H. A.; Kraak, J. C.; Poppe, H., *J. Chromatogr.*, 777 (1997) 329

87. McDonnell, P. A.; Caldwell, G. W.; Masucci, J. A., *Electrophoresis*, 19 (1998) 448

88. Busch, M. H. A.; Boelens, H. F. M.; Kraak, J. C.; Poppe, H.; Meekel, A. A. P.; Resmini, M., *J. Chromatogr.*, 744 (1996) 195

89. Kraak, J. C.; Busch, S.; Poppe, H., *J. Chromatogr.*, 608 (1992) 257

90. Erim, F. B.; Boelens, H. F. M.; Kraak, J. C., *Anal. Chim. Acta.*, 294 (1994) 155

91. Rundlett, K. L.; Armstrong, D. W., *Electrophoresis*, 18 (1997) 2194

92. Ohara, T.; Shibukawa, A.; Nakagawa, T., *Anal. Chem.*, 67 (1995) 3520

93. Lepecq, J. B., *J. Mol. Biol.*, 27 (1967) 87

94. Heegaard, N. H. H.; Robey, F. A., *Anal. Chem.*, 64 (1992) 2479

95. Lin, M.; Wu, N., *J. Liq. Chrom. & Rel. Technol.*, 22 (1999) 2167

96. Chu, Y. H.; Lees, W. J.; Stassionopoulos, A.; Walsh, C. T., *Biochemistry*, 33 (1994) 10616

97. Li, C.; Martin, L. M., *Anal. Biochem.*, 263 (1998) 72

98. Valtcheva, L.; Mohammad, J.; Pettersson, G.; Hjerten, S., *J. Chromatogr.*, 638 (1993) 263

99. Fanali, S.; Caponecchi, G.; Alurki, Z., *J. Micro. Sep.*, 9 (1997) 9

100. Desiderio, C.; Polcaro, C. M.; Podiglioni, P.; Fanali, S., *J. Chromatogr.*, 781 (1997) 503

101. Kilar, F.; Fanali, S., *Electrophoresis*, 16 (1995) 1510

102. Kilar, F., *Electrophoresis*, 17 (1996) 1950

103. Schmid, M. G.; Gubiltz, G.; Kilar, F., *Electrophoresis*, 19 (1998) 282

104. Amini, A.; Pettersson, C.; Westerlund, D., *Electrophoresis*, 18 (1997) 950

105. Amini, A.; Westerlund, D., *Anal. Chem.*, 70 (1998) 1425

106. Tanaka, Y.; Terabe, S., *Chromatographia*, 44 (1997) 119

107. Nelson, M. W.; Lee, C. S., *Anal. Chem.*, 68 (1996) 3265

108. Yang, L.; Harrata, A. K.; Lee, C. S., *J. Chromatogr.*, 780 (1997) 207

109. Nelson, M. W.; Tang, Q.; Harrata, A. K.; Lee, C. S., *J. Chromatogr.*, 749 (1996) 219

110. Wiedmer, S. K.; Jussila, M.; Riekkola, M-L., *Electrophoresis*, 19 (1998) 1711

111. Shen, T.; Wang, J.; Zhao, B., "Biochemistry", Education Plublishing Company, Shanghai, P. R. China, 1988

112. Haq, I.; Lincoln, P.; Suh, D.; Norden, B.; Chowdhry, B. Z.; Chaires, J. B., *J. Am. Chem. Soc.*, 117 (1995) 4788

113. Kalsbeck, W. A.; Thorp, H. H., *Inorg. Chem.*, 33 (1994) 3427

114. Friedman, R. A. G.; Manning, G. S., *Biopolymers*, 23 (1984) 2671

115. Kang-Maguire, N. A. P.; Wheeler, J. F., *Coordn. Chem. Rev.*, 211 (2001) 145

116. Martin, S. E.; Connatsar, M.; Kane-Magnuire, N. A. P.; Wheeler, J. F., *Anal. Chim. Acta.*, 445 (2001) 21

Part III

1. Tanaka, Y.; Terabe, S., *J. Chromatogr.*, 694 (1995) 277

2. Tanaka, Y.; Terabe, S., *Chromatographia*, 49 (1999) 489

3. Tanaka, Y.; Terabe, S., *Chromatographia*, 44 (1997) 119

4. Lorenzi, E. D.; Massolini, G.; Quaglia M.; et al., *Electrophoresis,* 20 (1999) 2739

5. Nelson, R. M.; Lee, C. S., *Anal. Chem.,* 68 (1996) 3265

6. Amini, A.; Pettersson, C.; Westerlund, D., *Electrophoresis,* 18 (1997) 950

7. Ward, T. J.; Dann III, C.; Brown, A. P., *Chirality,* 8 (1996) 77

8. Amini, A.; Paulsen-Sorman, U.; Westerlund, D., *Chromatographia,* 50 (1999) 497

9. Yang, L.; Harrata, A. K.; Lee, C. S., *J. Chromatogr.,* 780 (1997) 207

10. Nelson, M. W.; Tang, Q.; Harrata, A. K.; Lee, C. S., *J. Chromatogr.,* 749 (1996) 219

11. Wiedmer, S. K.; Jussila, M.; Riekkola, M-L., *Electrophoresis,* 19 (1998) 1711

12. Yang, L.; Harrata, A. K.; Lee, C. S., *Anal. Chem.,* 69 (1997) 1820

13. Koezuka, K.; Ozaki, H.; Matsubara, N.; Terabe, S., *J. Chromatogr.,* B 689 (1997) 3

14. Schulte, G.; Heitmeier, S.; Chankvetadze, B.; Blaschke, G., *J. Chromatogr.,* 800 (1998) 77

15. Javerfalk, E.; Amini, A.; Westerlund, D.; Andren, P. E., *J. Mass Spect.,* 33 (1998) 183

16. Otsuka. K.; Smith, C. J.; Grainger, J.; Barr, J. R.; Petterson, D. G.; Tanaka, Y.; Terabe, S., *J. Chromatogr.*, 817 (1998) 75

17. Tanaka, Y.; Kishimoto, Y.; Otsuka, K.; Terabe, S., *J. Chromatogr.*, 802 (1998) 83

18. Tanaka, Y.; Kishimoto, Y.; Otsuka, K.; Terabe. S., *Chromatography*, 19 (1998) 76

19. Fanali, S.; Desiderio, C.; Schulte, G; Heitmeier, S.; Strickmann, D.; Chankvetadze, B.; Blaschke, G., *J. Chromatogr.*, 800 (1998) 69

20. Fanali, S.; Caponecchi, G.; Alurki, Z., *J. Micro. Sep.*, 9 (1997) 9

21. Desiderio, C.; Polcaro, C. M.; Padiglioni, P.; Fanali, S., *J. Chromatogr.*, 781 (1997) 503

22. Kilar, F.; Fanali, S., *Electrophoresis*, 16 (1995) 1510

23. Kilar, F., *Electrophoresis*, 17 (1996) 1950

24. Schmid, M. G.; Gubitz, G.; Kilar, F., *Electrophoresis*, 19 (1998) 282

25. Amini, A.; Paulson-Sorman, U., *Electrophoresis*, 18 (1997) 1019

26. Hedeland, M.; Isakkson, R.; Pettersson, C., *J. Chromatogr.*, 807 (1998) 297

27. Heintz, J.; Hernandez, M.; Gomez, F. A., *J. Chromatogr.*, 840 (1999) 261

28. Mito, E.; Gomez, F. A., *Chromatographia*, 50 (1999) 689

29. Amini, A.; Westerlund, D., *Anal. Chem.*, 70 (1998) 1425

30. Amini, A.; Merclin, N.; Bastarni, S.; Westerlund, D., *Electrophoresis*, 20 (1999) 180

31. Chankvetadze, B.; Endresz, G.; Blaschke, G., *Electrophoresis*, 15 (1994) 804

32. Fanali, S.; Aturki, Z.; Desiderio, C.; Bossi, A.; Righetti, P. G., *Electrophoresis*, 9 (1998) 1742

33. Cherkaoui, S.; Veuthey. J-L., *J. Pharm. Biomed. Anal.*, 27 (2002) 615

34. Bednar, P.; Aturki, Z.; Stransky, Z.; Fanali, S., *Electrophoresis*, 22 (2001) 2129

35. Fanali, S.; Aturki, Z.; Desderio, C.; Righetti, P. G., *J. Chromatogr.*, 838 (1999) 223

36. Chankvetadze, B., *J. Chromatogr.*, 792 (1997) 269

37. Chankvetadze, B.; Endresz, G.; Blaschke, G., *Chem. Soc. Rev.*, (1996) 141

38. Vespalec, R.; Bocek, P., *Electrophoresis*, 20 (1999) 2579

39. Fanali, S., *J. Chromatogr.*, 792 (1997) 227

40. Gubitz, G.; Schmid, M. G., *J. Chromatogr.*, 792 (1997) 179

41. Vigh, G.; Sokolowski, A. D., *Electrophoresis*, 18 (1997) 2305

42. Vincent, J. B.; Kirby, D. M.; Nguyen, T. V.; Vigh, G., *Anal. Chem.*, 69 (1997) 4419

43. Cai, H.; Nguyen, D. M.; Vigh, G., *Anal. Chem.*, 70 (1998) 580

44. Vincent, J. B.; Sokolowski, A. D.; Nguyen, T. V.; Vigh, G., *Anal. Chem.*, 69 (1997) 4226

45. Williams, B. A.; Vigh, G., *J. Chromatogr.*, 777 (1997) 295

46. Hjerten, S., *J. Chromatogr.*, 347 (1985) 191